FOSSIL ENERGY

DOE/BC/15107-4
(OSTI ID: 791835)

ENHANCING THE EFFECTIVENESS OF CARBON DIOXIDE FLOODING BY MANAGING ASPHALTENE PRECIPITATION

Final Report
September 10, 1998-December 31, 2001

By:
Milind D. Deo

Date Published: February 2002

Work Performed Under Contract No. DE-AC26-98BC15107

University of Utah
Salt Lake City, Utah

National Energy Technology Laboratory
National Petroleum Technology Office
U.S. DEPARTMENT OF ENERGY
Tulsa, Oklahoma

DOE/BC/15107-4
Distribution Category UC-122

Enhancing the Effectiveness of Carbon Dioxide Flooding by Managing Asphaltene Precipitation

By
Milind D. Deo

February 2002

Work Performed Under DE-AC26-98BC15107

Prepared for
U.S. Department of Energy
Assistant Secretary for Fossil Energy

Dan Ferguson, Project Manager
National Petroleum Technology Office
P.O. Box 3628
Tulsa, OK 74101

Prepared by
Department of Chemical and Fuels Engineering
University of Utah
1471 Federal Way
Salt Lake City, UT 84112

Table of Contents

ABSTRACT xi

EXECUTIVE SUMMARY xiii

TABLE OF CONTENTS iii

LIST OF FIGURES v

LIST OF TABLES ix

1. INTRODUCTION 1

2. THERMODYNAMIC EXPERIMENTS 4

PURE COMPONENT EXPERIMENTS 4
CARBON DIOXIDE-OIL HIGH-PRESSURE EXPERIMENTS 6
The Experimental System 6
Carbon dioxide first contact with dead oil 8
Carbon dioxide first contact with live oil 9
Simulated multiple contact miscibility 9
True multiple contact miscibility 9
RESULTS 11
First Contact Experiments with Dead Oil 11
First Contact Experiments with Live Oil 14
Simulated Multiple Contact Experiments 20

3. ASPHALTENE CHARACTERIZATION 29

SAMPLES 29
CHROMATOGRAPHIC TECHNIQUES 29
Column Chromatography 29
High Temperature Gas Chromatography with Flame Ionization Detector (HT-GC-FID) 33
Gas Chromatography-Mass Spectrometry (GC-MS) 35
SPECTROSCOPIC TECHNIQUES 36
Fourier Transform Infrared Spectroscopy (FTIR) 36
Chemical Ionization 43
SURFACE TECHNIQUES OF CHARACTERIZATION 48
Scanning Electron Microscope (SEM) 48
TOF-SIMS 53
End-Group Effects 53
Maximum molecular weight 57
Observations regarding the asphaltene core 59

4. THERMODYNAMIC MODELING 63

PURE DENSE THERMODYNAMIC MODEL 63

HOMOGENEOUS MOLECULAR THERMODYNAMIC MODEL 65
RESULTS AND DISCUSSION 70
Pure Dense Phase Model Results *72*
Homogeneous Molecular Thermodynamic Model Results *74*
NOMENCLATURE 76

5. CORE FLOODING EXPERIMENTS 78

EXPERIMENTAL SYSTEM 78
EXPERIMENTAL PROCEDURE 79
EXPERIMENTAL RESULTS 80
A SIMULATED WELL-BORE FLASH EXPERIMENT 81
A COMPREHENSIVE COREFLOOD ON LIVE OIL 82

6. KINETIC MEASUREMENTS 85

PRELIMINARY APPROACH 85
Cooling Experiments *85*
Titration Experiments *87*
Modeling *88*
TITRATION KINETICS BASED ON TITRATION 94
ONSET MEASUREMENTS USING NEAR INFRARED SPECTROSCOPY 96
Introduction *96*
Experimental Procedure *98*
Summary *109*

7. COMPOSITIONAL MODELING 110

PURE-COMPONENT PRELIMINARY SIMULATIONS 110
SIMULATIONS WITH THE RANGELY CRUDE 111

8. SUMMARY AND CONCLUSIONS 118

9. ACKNOWLEDGEMENTS 120

10. REFERENCES 121

List of Figures

Figure 2-1 Ternary diagram of phenanthrene-hexane-toluene on the basis of weight percents of each component at 20°C. with ?=9.922 $(cal/cm^3)^{0.5}$, ? Hm=4300 cal/mole, Tm=373.15 K and T=293.15 K. (solid line : calculated result, ? : two-phase, precipitated and ? : single-phase, soluble) 4
Figure 2-2 Experimental system used to study solids precipitation with first and multiple contact experiments 7
Figure 2-3 Carbon Number distribution of the original crude oil 11
Figure 2-4 Saturates-aromatics-resins and asphaltenes distributions in the original oil 11
Figure 2-5 Precipitation amounts for first contact dead oil 12
Figure 2-6 Liquid fractions from dead oil experiments 14
Figure 2-7 Live oil molar composition 15
Figure 2-8 Precipitation amounts for first contact live oil experiments 16
Figure 2-9 Light ends extracted in gas phase 18
Figure 2-10 Asphaltenes in the liquid fractions from live oil experiments 19
Figure 2-11 Cumulative carbon number distribution of crudes from live oil experiments 19
Figure 2-12 Cumulative carbon number distribution of the light-cut added to the oil 20
Figure 2-13 Precipitation for simulated multiple contact 21
Figure 2-14 Asphaltenes in the liquid fractions for simulated multiple contact 21
Figure 2-15 True Multiple contact experimental procedure – a schematic 23
Figure 2-16 Comparison of CO2 induced precipitation for first and multiple contacts 24
Figure 2-17 Composition of gas phase from first contact 25
Figure 2-18 Comparison between liquid fraction from first contact and original oil 27
Figure 2-19 Comparison of liquid fractions between second and first contacts 27
Figure 2-20 Comparison of liquid fraction composition between third and second contacts 28
Figure 3-1 Fractionation of crude oil 30
Figure 3-2 Samples from column chromatography 32
Figure 3-3 HT-GC-FID chromatograms of precipitates and resins 34
Figure 3-4 FTIR spectra of the SARA fractions obtained using different solvents 39
Figure 3-5 FTIR - solids 42
Figure 3-6 Chemical Ionization – Precipitates from Rangely Oil 45
Figure 3-7 Chemical Ionization - Precipitates from Phillips oil 46
Figure 3-8 Chemical Ionization - CO_2 induced precipitates 47
Figure 3-9 Chemical Ionization – Resins from Rangely oil 48
Figure 3-10 SEM - Precipitates from Rangely oil 50
Figure 3-11 SEM – Precipitates from Phillips Oil 51
Figure 3-12 SEM - CO2 induced precipitates 52
Figure 3-13 TOF-SIMS – Asphaltenes from Rangely oil 54
Figure 3-14 TOF_SIMS – CO2 induced precipitates 58
Figure 3-15 Precipitate from Phillips oil 60
Figure 4-1 Calculation Flow Diagram for the Dense Phase Thermodynamic Model 65
Figure 4-2 Flow Diagram of homogeneous molecular thermodynamic model 69

Figure 4-3 Pure Dense Phase Model – Live Oil 73
Figure 4-4 Pure Dense Phase Model – Simulated Multiple Contact 73
Figure 4-5 Homogeneous Molecular Thermodynamic Model – Dead Oil 74
Figure 4-6 Homogeneous Molecular Thermodynamic Model – Live Oil 75
Figure 4-7 Homogeneous Molecular Thermodynamic Model – Simulated Multiple Contact Experiments 75
Figure 5-1 Experimental system used for the corefloods 79
Figure 5-2: Carbon number distributions of the oil samples collected as the flood progressed; analyses were performed using simulated distillation 80
Figure 5-3 Coreflood results from the live-oil experiment. Compositions of the oil samples were obtained using simulated distillation. The sample numbers indicate when they were collected. Higher numbers indicate later times. The CO2 breakthrough was at 15. 83
Figure 5-4 Plots of different carbon numbers in the samples as they eluted from the core with respect their original concentration in the oil. 84
Figure 6-1: Experimental system developed to determine composition induced precipitation 86
Figure 6-2: Temperature of the oil placed in a bath cooled at a predefined rate 87
Figure 6-3: Temperature of the Rangely oil as pentane is added at a rate of 1 ml/min 88
Figure 6-4: Effect of Emix and (d1 -do) on DT(t) (°C). (a) Effect of various values of (d1 -do) on DT(t) assuming Emix is zero, for curves from bottom to top (d1 -do) = 7.3, 7.5, 7.7, 7.9, (b) Effect of various values of Emix on DT(t) assuming (d1 -do) is zer 91
Figure 6-5: Difference in the experimental and curve fit of long time data identifying the temperature change due to the enthalpy of asphaltene precipitation 92
Figure 6-6: Solubility of asphaltene, Xeq, (solid line) and asphaltene, Xa, (dashed line), in solution assumed to be 4x10-8 as the solvent mole fraction, X1 is increased. Depending upon the amount of asphaltene in the oil, the point at which the solution is satur 93
Figure 6-7: Precipitation of asphaltenes as a function of time 95
Figure 6-8 Schematic diagram of the experimental system used. 98
Figure 6-9 Near-IR spectra at various times as oil is titrated with normal heptane. Spectra over the 1200 nm – 2400 nm range are shown 101
Figure 6-10 Near-IR absorbance at a wavelength of 1600nm for oil titration with heptane (Flow rate = 1mL/min) 101
Figure 6-11 Near-IR absorbance curves at 1600 nm when three different precipitants are employed 102
Figure 6-12 Asphaltene amounts versus n-alkane precipitant carbon number after 300 minutes of titration at 1mL/min. 102
Figure 6-13 Near-IR spectra at 1600 nm for titrations of oil-toluene mixtures with heptane. As more toluene is added, precipitation is delayed. 103
Figure 6-14 Plot indicating accelerated onset when additional n-heptane insoluble asphaltenes are dissolved in oil. 104
Figure 6-15 Effect of the initial dissolution of n-alkane-solids and polyaromatic compounds (weight percent) in the oil on the onset of asphaltene precipitation from the oil. 106

Figure 6-16 Asphaltene precipitation onset changes when combinations of n-alkane and polyaromatic solid compounds are used as additives. 106
Figure 6-17 Asphaltene precipitation onset from asphaltene-toluene mixtures with the addition of n-alkane solid or polyaromatic compounds 108
Figure 7-1 Oil and gas saturations for the Rangely crude oil system at 1900 psia 111
Figure 7-2 Individual component concentrations versus pore volumes of carbon dioxide injected - 1900 psia 112
Figure 7-3 Oil and gas saturations for the Rangely crude oil system at 3500 psia 112
Figure 7-4 Individual component concentrations versus pore volumes of carbon dioxide injected - 3500 psia 113
Figure 7-5 Oil and gas saturations for the Rangely crude oil system at 4000 psia 113
Figure 7-6 Individual component concentrations versus pore volumes of carbon dioxide injected - 4000 psia 114
Figure 7-7 Oil and gas saturations in the upper portion of the reservoir (top two layers) at 3500 psia 115
Figure 7-8 Compositions of all the components in the upper two layers at 3500 psia. Most of the components are recovered/drained prior to 1 PV injection with displacement resembling first-contact 115
Figure 7-9 Oil and gas saturations in the middle portion of the reservoir (middle layers) at 3500 psia. The saturation shocks travel slower than in the upper portion of the reservoir. 116
Figure 7-10 Compositions of all the components in the middle layers at 3500 psia. Most of the components are recovered/drained at about 1.5-2 PV injection with displacement resembling multiple-contact miscible 116
Figure 7-11 Figure 7-12 Oil and gas saturations in the bottom portion of the reservoir (bottom two layers) at 3500 psia. The saturation shocks travel the slowest. 117
Figure 7-13Compositions of all the components in the bottom two at 3500 psia. Most of the components are recovered/drained at about 2 PV injection with displacement resembling multiple-contact to immiscible 117

List of Tables

Table 2-1: Basic pure component properties in the solubility model 6
Table 2-2: Comparison of physical properties of phenanthrene appearing in different references 6
Table 2-3 Parameters of the true multiple contact experiment (mole%) 10
Table 2-4 Solid compositions determined from SARA analysis 12
Table 2-5 Wt% Composition of the gas phases while studying precipitation from dead oils 12
Table 2-6 Gas phase. z: compressibility factor, n: total number of moles 13
Table 2-7 Liquid fractions- Dead oil 14
Table 2-8 Gas composition – recombination 15
Table 2-9 Precipitates with live oil 15
Table 2-10 Wt % Compositions of the gas phases while studying precipitation from live oils 16
Table 2-11 gas Phase - Live oil 17
Table 2-12 Liquid Fractions - Live Oils 17
Table 2-13 C_{60}^{+} fraction for crudes - live oil 19
Table 2-14 Gas Compositions - Simulated Multiple Contact 21
Table 2-15 Gas Phase - Simulated Multiple Contact 22
Table 2-16 liquid fractions - Simulated Multiple Contact 22
Table 2-17 Precipitates SARA - True Multiple Contacts 25
Table 3-1 Sample Designations 29
Table 3-2 SARA distribution in CO_2 induced solids 30
Table 3-3 SARA distribution for different precipitant solvents 31
Table 3-4 Simulated distillation results of solid samples from the field and the laboratory (wt%) 33
Table 3-5 Peaks identified in the mass chromatograms 36
Table 3-6 Ratio of Intensity of alkane peaks 36
Table 3-7 Ratios of intensity of important peaks – FTIR 40
Table 3-8 Maximum molecular weight of ions 44
Table 3-9 Quantification of surface by SEM (wt%) 49
Table 3-10 Negative ions 60
Table 3-11 Positive ions CH_y^{+}/C_2^{+} 61
Table 3-12 Positive ions $C_2H_y^{+}/C_2^{+}$ 62
Table 3-13 Ions identified in TOF-SIMS spectra 62
Table 3-14 Important masses for different samples 62
Table 4-1 Composition and Properties of Rangely dead oil 70
Table 4-2 Composition and Properties of Rangely live oil 70
Table 4-3 Simulated multiple contact crude composition 71
Table 4-4 Interaction coefficients for dead oil 71
Table 4-5 Interaction coefficients for live oil 71
Table 4-6 Pure Dense Phase Model –Optimized Parameters 72
Table 4-7 Optimized parameters for different systems 74
Table 6-1:Rates of asphaltene precipitation with liquid solvents 94
Table 6-2 Solubility parameters and melting temperature of solids in this study 108

Abstract

This project was undertaken to understand fundamental aspects of carbon dioxide (CO_2) induced asphaltene precipitation. Oil and asphaltene samples from the Rangely field in Colorado were used for most of the project. The project consisted of pure component and high-pressure, thermodynamic experiments, thermodynamic modeling, kinetic experiments and modeling, targeted corefloods and compositional modeling.

Pure component thermodynamic experiments established that compositional changes to the solvent can bring about precipitation of polyaromatic compounds. These experiments were performed to establish parallels between solubility behavior of polyaromatic compounds in hydrocarbon solvents and asphaltenes in crude oils. A high-pressure, high-temperature pressure-volume-temperature apparatus in conjunction with a high-pressure core flooding system was used to study carbon dioxide induced precipitation from the Rangely crude oil. Rangely crude contains about 1% heptane insolubles. It was determined that first-contact precipitation, at different carbon dioxide concentrations was negligible. Core flooding experiments at field conditions revealed that precipitation did occur at the core exit. This essentially showed that the precipitation phenomenon in crudes that are likely CO_2-flood candidates is due to the multiple contact process and the associated compositional changes. Multiple contact experiments conducted to prove this hypothesis showed that multiple contact precipitation amounts were 3-5 times the first-contact precipitation values. The compositional changes (in the original crude) to cause widespread precipitation were established. Coreflooding experiments confirmed that due to the multiple contact process, three times as much precipitation was likely in CO_2 floods.

The solids were analyzed by a variety of methods; SARA fractionation, FTIR, chemical ionization – mass spectrometry, time of flight mass spectrometry, etc. A consistent picture of the nature of solids emerged from these analyses. Based on GC-MS analyses, a number of five ring aromatic compounds were identified among the polyaromatics. From their infrared spectra, it became evident that the polar groups in the asphaltene fractions are appreciably lower in intensity than those existing in the resins. It was also found that there were differences between CO_2 induced precipitates and paraffinic insoluble precipitates (asphaltenes); the former contained more polar functionalities and shorter substituted alkyl chains.

Two thermodynamic models were examined; dense solid-phase model and homogeneous thermodynamic model. The homogeneous thermodynamic model provided reasonable agreement with experimental data.

Titration experiments were used to study kinetics of precipitation. The fact that the asphaltenes are undersaturated in the oil was established using a variety of methods. Simple first-order kinetic constants for paraffinic solvents were determined. Onset of solid precipitation from oils was determined by identifying the minimum in Near-Infrared absorbance. Solvent induced precipitation typically causes asphaltene precipitation, but is also known to cause high-molecular weight waxes to come out of solution. The effects of

the addition of solid saturated and unsaturated compounds on the onset of solvent induced precipitation from a crude oil were examined. The solvent-induced precipitation was brought about using pentane, hexane and heptane. Based on limited solvent carbon number investigated (5-7), less solvent was required for precipitation onset as the carbon number of alkanes decreased. As the flow rate of the precipitant increased, the onset was delayed. Addition of solid n-alkanes, such as eicosane and tetracosane to the oil initially, accelerated the onset of precipitation. When solid polyaromatic compounds (naphthalene and phenanthrene) were dissolved in the oil, the precipitation more solvent was required to initiate onset. It was also shown that the crude oil was considerably undersaturated with respect to the asphaltenes and that initial dissolution of asphaltenes in the oil accelerated the precipitation.

Compositional simulations showed that different layers in layered reservoirs are subject to different compositional environments because of the CO_2 override. If multiple contact miscibility pressure required to bring about miscibility in one-dimensional system is used as an index, it was shown that the top layer undergoes first-contact like displacement, while the bottom layer immiscible-type displacement. The compositional changes in the middle layer are like in the multiple-contact miscibility, one-dimensional medium. The bottom and middle layer are thus more susceptible to the formation of precipitates than the top layer.

Executive Summary

Carbon dioxide flooding is the second most common enhanced oil recovery process (next only to steam flooding). Most oils that are candidates for carbon dioxide flooding are relatively light oils. Asphaltenes are a compound class in crude oils defined as solids precipitated on adding n-pentane or n-heptane to the crude oil. Most of the oils in carbon dioxide flooding applications have relatively low asphaltene content, initially in the parent oil. However, asphaltene precipitation is one of the most serious production problems in the technological implementation of carbon dioxide flooding. The objective of this project was to understand why this was the case and to explore possibilities of preventing the problem. Carbon dioxide flood at Rangely, Colorado, operated by Chevron Oil Company is the field example being used in the project.

In previous work on carbon dioxide induced precipitation, there was considerable disagreement on the concentration range over which precipitation was likely. The previous thermodynamic experiments were also performed over a range of phase behaviors. In some single experiments, single-phase, liquid-vapor and liquid-liquid regions were traversed and it was difficult to decipher the effect of phase behavior on precipitation. Also, most previous work emphasized the so-called single-contact studies, wherein carbon dioxide and oil in certain ratio and at a specific temperature and pressure are mixed and precipitation observed/measured. It is well known that carbon dioxide is most effective in recovering crude oil when it induces multiple contact miscibility. The compositional changes during the multiple contact process and the precipitation tendency of the crude were not formally linked, even though it was observed that there is greater tendency for the multiple contact mixture to form precipitates. One of the primary goals of this project was to study the link between generation of miscibility and formation of precipitates. Both high-pressure thermodynamic experiments and high-pressure core floods were targeted to understand this phenomenon. The hypothesis was proven through a number of thermodynamic experiments further validated through specialized high-pressure corefloods.

A new high-temperature, high-pressure experimental system was assembled to study thermodynamics of precipitation and to perform core floods. Initial precipitation experiments revealed that first-contact precipitation is negligible with the Rangely crude oil. An experiment with a crude containing ten times as much asphaltenes (as the Rangely oil) also showed only a small quantity of first-contact precipitation. These experiments revealed that first-contact data might be irrelevant to what is happening in the field and that compositional changes during the flood and precipitation possibilities from these mixtures were more important. The core flood experiment showed that multiple contact miscibility was being developed. There was no evidence of precipitation in the core or in the production equipment (back pressure regulator, separator, etc.). The kinetic experiments showed that the particles were smaller than a typical pore (about 10-15 Angstroms in size) to cause serious formation damage. However, the particles had the potential of getting separated under centrifugal forces to plug pumps and associated equipment.

One other goal of this project was to gain as much insight about the nature of solids formed from different solvents and from different processes. A variety of analytical methods for liquid and solid analysis were developed. It was conclusively shown that the solids deposited in the field were quite different from the solids obtained in the laboratory using the same oil solvent systems. This basically showed that the processes underway in the field leading to precipitation were somewhat different from processes underlying the laboratory experiments. The fundamental nature of these solids was established through a variety of sophisticated analytical measurements, which would make it easier to develop treatment options.

Examination of thermodynamic models showed that the current models were very system specific and were not easily extendable to other applications. A new thermodynamic framework was required to predict solids precipitation from oils. Once the exact conditions of precipitation were established, one of the project aims was to find an appropriate thermodynamic model to explain the data. Homogeneous thermodynamic model that provided a reasonable match with the data was developed.

Compositional model (with thermodynamic input from the thermodynamic model) were performed to study the mechanisms of displacement in the field. This study showed that measurement of thermodynamic data and determination of minimum miscibility pressures was valuable; however, these data will need to be complemented by compositional simulations in the precise geometry of the reservoir. The results of these compositional measurements would have to be interpreted in the context of compositional variations in the reservoir and whether these variations make precipitation likely in those specific portions of the reservoir.

Kinetics of carbon dioxide induced precipitation have never been measured. These measurements are fairly common in the study of crystallization from inorganic mixtures. Using techniques specially developed at the University of Utah to study Lithium Bromide crystallization to examine asphaltene precipitation was also one the project goals. These experiments showed that it might be possible to use calorimetric methods to study kinetics; however, the temperature changes were small and data interpretation was difficult. Hence the focus was shifted to using Near Infrared spectroscopy to measure the onset of precipitation and thus some kinetic information. It was determined that the onset was faster when the n-alkane carbon number of the precipitant decreased resulting ultimately in higher amounts of asphaltenes precipitated. Addition of toluene delayed precipitation and also showed that the oil was undersaturated with respect to the asphaltenes. When phenanthrene and naphthalene were initially mixed with the oil, the onset of solid deposition was delayed. With the addition of eicosane and tetracosane, the onset of solid precipitation was accelerated. Addition of separated asphaltenes to the oil, however, accelerated the precipitation onset. When mixtures of polar and nonpolar solids were added, the precipitation was governed by the nonpolar compound additive. These observations were true for the reprecipitation of dissolved/dispersed asphaltenes as well. The measurements show that the complex phenomenon of dissolved asphaltene precipitation is controlled to a significant extent by simple solubility rules.

Here are the most important findings from this project:

?? Carbon dioxide-induced asphaltene precipitation can occur at carbon dioxide compositions of 20% and above.

?? First-contact precipitation amounts for low asphaltic crude oils are in the same range as heptane insolubles from the same oil.

?? Multiple-contact precipitation amounts are three times as much as first-contact amounts due to the enrichment of the original oil with intermediates. Corefloods confirmed that most of the precipitation in carbon dioxide floods is associated with the generation of multiple-contact miscibility.

?? Precipitation in producing wells will therefore be highest when the "multiple-contact" front breakthrough, which is followed closely by the carbon dioxide front.

?? No additional precipitation was observed in simulated wellbore experiments, where the multiple-contact mixture was flashed.

?? Homogeneous thermodynamic models are useful in matching the thermodynamic data, even under multiple-contact conditions.

?? Kinetic experiments showed that addition of simple polyaromatic compounds delays precipitation. These experiments also showed that co-precipitation of wax was likely with asphaltene precipitation, but significant co-precipitation of asphaltenes with wax was unlikely.

?? Compositional simulations showed that, even though multiple-contact displacement may be occurring , overall, in the reservoir, different portions of the reservoir may experience different compositional environments. This would be true even in homogeneous reservoirs, where carbon dioxide override and thus gravity drainage is possible.

1. Introduction

Asphaltene precipitation is known to occur during carbon dioxide floods, particularly in producing wells. Precipitation of solids for the most part is detrimental to flooding operations. This fundamental project was about understanding the thermodynamic issues regarding precipitation and characterizing the solids formed in as much detail as was possible.

Solids precipitation in reservoirs may be catastrophic if it causes irreversible plugging. In some cases, the solids may coat the rock surfaces possibly altering reservoir flow properties, without bringing about catastrophic permeability reduction. Asphaltenes are a compound class determined by performing standard solubility tests. They are defined usually as either pentane or heptane insolubles in the parent oil. When the oil is contacted, however, with carbon dioxide, the composition of the precipitate may differ significantly from the composition of asphaltene determined from the standard test. The precipitation of solids from a complex mixture of hydrocarbons depends on the overall composition of the mixture, and on temperature and pressure. Other kinetic factors may also be important apart from these thermodynamic effects. If the composition of the parent oil is continually changing (as may be the case in carbon dioxide flooding) trying to determine when precipitation might occur and the amount and composition of the precipitate is an added challenge. In order to comprehend this phenomenon, one has to move away from the traditional asphaltene in resin type models and basically look at the oil as a mixture of hundreds of hydrocarbons. Under certain conditions of temperature and pressure, and overall composition of the carbon dioxide-oil mixture, some of the compounds in the oil will come out of solution. When some of the lighter oil components are depleted, the class of compounds that precipitate changes and shifts basically to a set of lighter compounds.

The project's focus was on the miscible CO_2 flood operated by Chevron U. S. A. in the Rangely field, Rio Blanco County, northwestern Colorado. The flood is considered to be one of the most successful applications of the CO_2 miscible flooding technology. The tertiary project was initially designed for a 1:1 WAG (water alternating gas) injection of a 30% HCPV (hydrocarbon pore volume) of CO_2 in approximately 20 equal cycles (Brock and Bryan, 1990). Several papers describing flood updates and WAG optimization strategies have been published since the start of the flood (Masoner and Wackowski, 1994). Asphaltene precipitation has been considered one of the most pressing problems in the field. In the extensive laboratory evaluation undertaken to evaluate the flood (Graue and Zana, 1981), asphaltene precipitation was observed at gas concentrations of 25-44 mol% (depending on the gas composition) in reservoir oil. Apart from asphaltene precipitation, an unequal CO_2 utilization (with some zones needing considerably higher amounts of CO_2 than some other zones to effect similar oil recoveries) has been cited as an important project concern. Harvey and Iakovakis (1991) provided a comprehensive performance review of the flood; the problems faced and technology solutions attempted. One of the more serious field problems was reduced fluid production from CO_2 breakthrough wells and resultant reduced injection rates. This reduced processing rate was attributed to increased reservoir pressure that was due to reduced fluid production.

However, this could also partially be due to precipitation and overall compositional variations that are also responsible for the pour point increases in produced crudes. It was also observed that asphaltenes appeared in the well soon after CO_2 breakthrough and that deposits were found in pumps, tubing, wellheads and workover equipment. Thus, handling asphaltene precipitation was considered one of the challenges facing the unit.

A lot more attention has been paid in the industry to asphaltene precipitation without the presence of CO_2. Hirschberg et al. (1984) were among the first to study the influence of temperature and pressure on asphaltene precipitation during natural depletion. They proposed a simple thermodynamic model to explain the data. They deduced that asphaltene precipitation may particularly be expected in light crudes that are highly undersaturated with respect to gas. Burke et al. (1990) also reported extensive data for asphaltene precipitation from live crudes and crudes mixed with hydrocarbon solvents. Mansoori and his research group at the University of Illinois at Chicago have performed extensive work on asphaltene deposition predictive models using concepts from continuous thermodynamics (Kawanaka, et al., 1991).

The most comprehensive organic deposition studies from oils during CO_2 flooding were reported by Monger and Trujillo (1991) and Monger and Fu (1987). Additional data for forward and swept-zone multiple contacts was also provided by Bryant and Monger (1988). Monger's experiments showed a clear correlation between the original asphaltene content (measured as pentane insolubles) and the *total* organic deposition (which included other higher molecular compounds such as waxes, etc.) from the oils. The experimental system used was a variable volume circulating cell wherein the overall CO_2 concentration increased throughout a run. Thus even though the deposition data provided an index of the precipitation tendency from a given oil, it was difficult to associate the quantitative organic deposition to a definite overall composition. It was observed that the asphaltene content of the precipitate was significantly higher than the parent oil and that the precipitate contained fractions other than asphaltenes. For instance, saturates made up about 25% of the precipitates on the average. It should be noted however, that the compound class fractionations of the precipitates cannot be viewed in the same context as that of the parent oil. For example, chemically, the asphaltenes from the precipitate could not be expected to be identical compositionally to the asphaltenes from the parent oil. One can not undertake asphaltene balances, for example to estimate the amount of asphaltenes from the parent oil left in the precipitate. This concept was clearly illustrated by Deo and co-workers (Deo and Hanson, 1993; Deo et al, 1993; Deo and Hanson, 1994) by using asphaltene data from parent oils and from precipitates resulting from the oil supercritical extraction by propane. One of the interesting features of Monger's experiments was that a high asphaltene crude (Huntington Beach) displayed low precipitation tendency. One of the explanations for this was that this crude had a large fraction of resins that held the asphaltenes in suspension. In an earlier study, Monger and Fu (1987) reported that the precipitation peaked at the minimum miscibility pressure and showed a slight decline afterwards. As temperature increased, precipitation also increased, but not as significantly as with pressure. Bryant and Monger (1988) found large amounts of tar like organic deposits (as

much as 20 wt% of the stock tank oil hydrocarbon) in their forward multiple contact experiment and no precipitation in their swept-zone (backward contact) experiments.

Monger and co-workers observed precipitation for mixtures containing well over 60 CO_2 mole percent. Others (Graue and Zana, 1981; Novosad and Costain, 1990) have observed precipitation at 20-40 mole % CO_2 concentration. There was a need to identify the exact composition range over which precipitation is likely for oils containing varying levels of asphaltenes. As the project progressed it was evident that there was a strong relationship between carbon dioxide phase behavior with the crude oil and precipitation. For example, it was clear that establishing first-contact precipitation tendencies was not sufficient or even relevant in understanding precipitation in the field. Compositions or the phases generated at various phases of the CO_2 flood were important in determining the precipitation tendencies.

There is no question that asphaltene precipitation is common in producing wells and that this precipitation causes loss of producibility. Even though there have been a number of asphaltene/organic deposition studies there are still questions concerning the wellbore conditions that *lead* to precipitation. Most of the asphaltene precipitation experiments and models have dealt with equilibrium issues. There are no known studies on precipitation kinetics; supersaturating required for precipitation, nucleation of molecules, surface precipitation effects, etc.

The report is organized into seven additional sections:

?? Single and multiple contact experiments with the Rangely crude oil
   Pure component experiments and modeling is described first.
   In this section, all the thermodynamic experiments are described. This section includes results on the analyses of the gas and liquid phases.
?? Solids characterization.
   Comprehensive characterization on all of the solids formed during experiments and collected in the field is in this section.
?? Thermodynamic modeling
   Thermodynamic models that match the experimental data have been developed and discussed.
?? Kinetic experiments and modeling
   A variety of kinetic experiments are described here along with appropriate models.
?? Corefloods
   Several coreflooding experiments and results are described. A special coreflood was conducted to simulate the wellbore conditions, where the multiple contact mixture was "flashed" at wellbore pressure – keeping the temperature constant. This experiment and results are described in this section.
?? Compositional simulations
   Compositional simulations using lumped representation of the Rangely crude oil are discussed.
?? Summary of results and conclusions

2. Thermodynamic Experiments

This section consists of a report on pure component experiments which were performed to show that precipitation of polar compounds can be initiated by compositional changes in the nature of the solvents, and a report on the high-pressure, carbon dioxide-oil thermodynamic experiments.

Pure Component Experiments

A liquid mixture containing varying amounts of toluene and phenanthrene were mixed with a mixture containing hexane and small amounts of phenanthrene to simulate the precipitation of asphaltenes. The solid-liquid equilibrium was completely mapped for this system and is shown in Figure 2-1.

Use of a solid-liquid equilibrium model was investigated to describe the results. When the solvent does not enter the solid phase, the fugacity of the solid solute remains that of pure solid, so the condition of equality of partial fugacities at equilibrium becomes (Walas, 1985)

$$\hat{f}_{2(soloid)} \; ? \; f_{2(solid)} \; ? \; ?_2 x_2 f_{2(subcooled\_liquid)}$$

Which means that

$$x_2 \; ? \; \frac{f_{2s}}{?_2 f_{2(scl)}},$$

where, x_2 is the mol fraction of the solute in the solution and $f_{2(scl)}$ represents the fugacity of the pure solid solute in a subcooled liquid state below its melting point.

The general solubility equation for x_2 is given by:

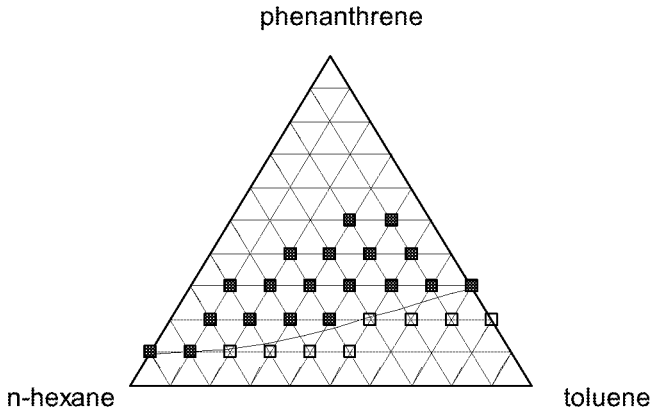

Figure 2-1 Ternary diagram of phenanthrene-hexane-toluene on the basis of weight percents of each component at 20°C. with ?=9.922 (cal/cm^3)$^{0.5}$, ? Hm=4300 cal/mole, Tm=373.15 K and T=293.15 K. (solid line : calculated result, ? : two-phase, precipitated and ? : single-phase, soluble)

$$x_2 = \frac{1}{\gamma_2}\exp\left[\frac{\Delta H_{tp}}{R}\left(\frac{1}{T_{tp}} - \frac{1}{T}\right) - \frac{\Delta Cp}{R}\ln\frac{T_{tp}}{T} + \frac{T_{tp}}{T} - 1\right]\left(1 - \frac{\Delta V}{RT}(P - P_{tp})\right)$$

In the above equation, the subscript *tp* designates the triple point.

This form of the equation applies when the heat capacity difference is relatively insensitive to temperature.

When the pressure and heat capacity differences are neglected,

$$x_2 = \frac{1}{\gamma_2}\exp\left[\frac{\Delta H_{tp}}{R}\left(\frac{1}{T_{tp}} - \frac{1}{T}\right)\right] = \frac{1}{\gamma_2}\exp\left[\frac{\Delta S_{tp}}{R}(1 - \frac{T_{tp}}{T})\right]$$

where $\Delta S_{tp} = \Delta H_{tp} / T_{tp}$ is the entropy of fusion at the triple point.

Since triple-point temperatures usually are very close to melting points the solubility equation is often written in terms of properties at this better known property.

$$x_2 = \frac{1}{\gamma_2}\exp\left[\frac{\Delta H_m}{R}\left(\frac{1}{T_m} - \frac{1}{T}\right)\right] = \frac{1}{\gamma_2}\exp\left[\frac{\Delta S_m}{R}(1 - \frac{T_m}{T})\right]$$

where the subscript m identifies conditions at the atmospheric melting point.

The above equation is used with of the Scatchard-Hildebrand equation for the activity coefficient of the solute which requires only properties of pure components.

$$\gamma_2 = \exp\left[\frac{\Delta S_m}{R}(1 - \frac{T_m}{T}) - \frac{V_2\phi_1^2(\delta_1 - \delta_2)^2}{RT}\right],$$

where,

$$\phi_1 = \frac{V_1 x_1}{V_1 x_1 + V_2 x_2}$$

The equations below are used for the calculation of the phenanthrene solubility in toluene and hexane mixture.

$$x_2 = \exp\left[\frac{\Delta H_m}{R}\left(\frac{1}{T} - \frac{1}{T_m}\right) - \frac{V_2}{RT}\left(\frac{\delta_1 - \delta_2}{1 + \frac{V_2 x_2}{V_1(1 - x_2)}}\right)^2\right]$$

Mean solubility parameter is given by:

$$\bar{\delta} = \frac{\sum x_i V_i \delta_i}{\sum x_i V_i}$$

$$x_2 = \exp\left[\frac{\Delta H_m}{R}\left(\frac{1}{T} - \frac{1}{T_m}\right) - \frac{V_2}{RT}\left(\frac{\delta_1 - \bar{\delta}}{1 + \frac{V_2 x_2}{V_1(1 - x_2)}}\right)^2\right]$$

There were significant differences in literature values of various parameters required. Basic pure component properties are shown in Table 2-1. Variations in properties of phenanthrene important in determining solid-liquid equilibria are shown in Table 2-2.

Solubilities calculated using various combinations are compared to experimental results. The comparison shows that a melting point of 373.15 K, a solubility parameter of 9.922 and a heat of fusion of 4300 cal/mol are the phenanthrene properties that provide a good match between the experimental data and the solubility model predictions.

Table 2-1: Basic pure component properties in the solubility model

	Molecular weight (g / mol)	?, solubility parameter (cal / cm^3)$^{0.5}$	V, molar volume (cm^3 /mol)
Phenanthrene	178.23	9.922	158
Hexane	86.18	7.27	131.51
Toluene	92.14	8.93	106.84

Table 2-2: Comparison of physical properties of phenanthrene appearing in different references

Reference	Heat of fusion (cal/mol)	Melting temperature (^{o}C)	Solubility parameter (cal/cm^3)$^{0.5}$
Prausnitz, et al.		100	9.922
Perry's Handbook	4455		
Gordon and Scott	4300	96.3	9.8*
Barton - CRC			9.775**
David Lide - CRC	3921	99.24	

*estimated

** Hilderbrand solubility parameter

The experiments thus provided a check on phenanthrene properties and showed that polyaromatic compounds precipitate according to simple solubility rules.

Carbon dioxide-Oil High-Pressure Experiments

Martha Parra Ramirez performed this work. More details appear in her Ph. D. dissertation (Parra, 2002).

The Experimental System

Experiments were carried out in high-pressure, high-temperature equipment illustrated in Figure 2-2. The system was designed for temperatures up to 300 ^{o}F and pressures up to 5,000 psi permitting the experiments to be run at reservoir conditions. The system was mercury free.

Placing the equipment in an insulated wooden box regulated the temperature to about 2^0F. This box uses a heater, circulating fan, thermocouple, and a thermostat to regulate temperature. Temperature is held within two degrees of the set point. A coaxial heating cable is used to regulate the temperature of the pump that is placed outside of the box.

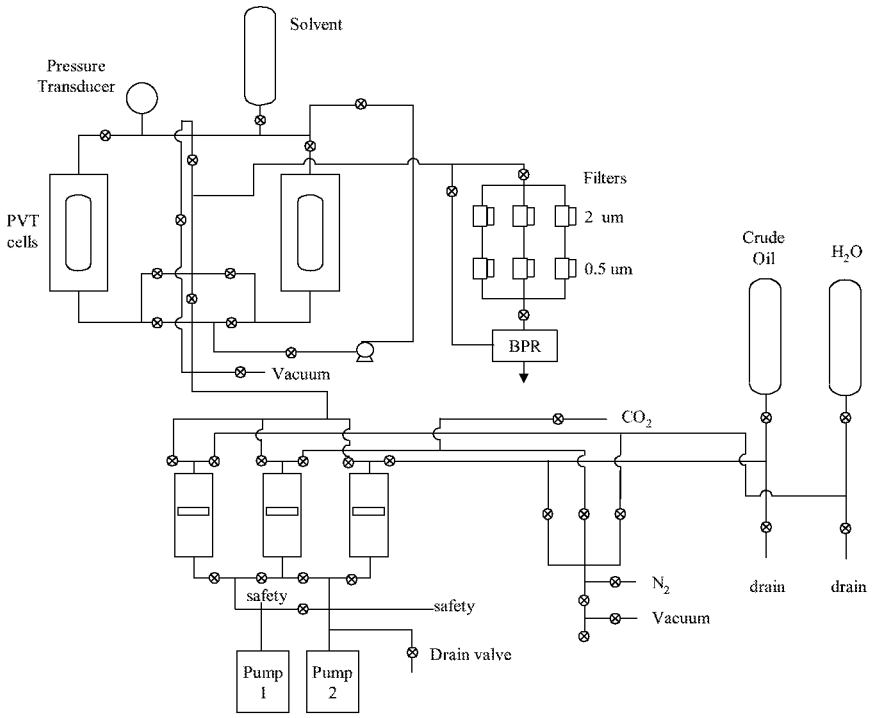

Figure 2-2 Experimental system used to study solids precipitation with first and multiple contact experiments

The fluid displacement system comprises of three moveable piston vessels (MPV) and two positive-displacement pumps to transfer fluids to the PVT cell. The positive displacement pumps allow careful control of flow rate (0-30 cc/min), and volume during displacement. The pistons in the MPVs are controlled by the displacement of oil from the positive displacement pumps.

The piston vessels are filled with water, gas or crude oil from a low-pressure input by pushing the piston down with nitrogen at low pressure, then evacuating the vessel to draw in the corresponding fluid. Carbon dioxide is filled by vacuuming the vessel and lowering the piston while it is connected to a liquid CO_2 tank equipped with a siphon

tube. The outlets of the vessels are connected to a manifold, which provides a very flexible fluid displacement configuration. The PVT cells have glass windows on either side, which are useful in visualizing the experiment. The cells are connected to a circulating pump, allowing equilibration of the fluids. The tubing in and out of the cells is versatile and permits filling and emptying of the cells from top or bottom, and moving fluids from one cell to the other. The outlet from the PVT cells is connected to a set of three parallel, high-pressure, in-line filters; each line has two filters with pore sizes of 2 and 0.5 microns for trapping precipitates for quantitative analyses of the solid phases. A bypass line is provided for experimental cases when filters are not required. The system pressure is maintained with a special back-pressure regulator (BPR). Commercially designed and built BPRs have serious problems maintaining back-pressure when high-pressure carbon dioxide is the displacement fluid. The BPR employed in all the studies was specially designed and fabricated by Chevron, Inc. and was donated to the University of Utah.

The fluid from the PVT cells is displaced into two interconnected cylinders equipped with a pressure indicator. The sample is received in the first cylinder, and the gas fraction is moved to the second cylinder. The separation procedure, along with pressure and compositional measurements permits quantitative analyses of the gas and the liquid samples collected.

Four, different types of thermodynamic experiments were performed, each of which has a definite protocol. All of the experiments were performed by contacting a sample with high-pressure carbon dioxide. The experiments differed in the nature of the sample used and are classified accordingly. The experiments are: carbon dioxide first contact with dead oil, carbon dioxide first contact with live oil, simulated multiple contact miscibility experiments, and true multiple contact miscibility evaluations. Procedures are described below; in all the experiments, the procedure of filling for water, CO_2 and crude oil into the MPVs is common.

Carbon dioxide first contact with dead oil

Dead oil is the oil without any dissolved gas. The volumes of CO_2 and dead oil are calculated by considering the total volume of the PVT cell, a shrinkage factor, molecular weight and densities of the CO_2 and crude oil. The equipment is heated at the desired temperature, 160 ^{o}F for several hours before transferring the fluids from the piston vessels to the PVT cell. The PVT is evacuated before filling it. The volume of crude oil is transferred from the piston vessel to the PVT cell. The volume recorded corresponds to the amount of hydraulic oil moved from the pump to the piston vessel and it's corroborated by visual observation of the volume in the PVT cell.

The CO_2 piston vessel is pressurized to the system pressure, usually 3,000 psia, and then this vessel is opened to the PVT cell. The pressure of the cell is continually monitored with a pressure transducer installed at the top of the PVT cell. The transducer signal is sent to a computer by making use of a real-time data acquisition and control system. OPTO 22, an industrial-grade data acquisition system was used for this purpose. More CO_2 is pumped into the cell until the set pressure is obtained. The CO_2 piston vessel is

closed, and the valves from the PVT cell to the recirculating pump are opened. Crude oil and CO_2 are completely mixed using the heated, high-pressure recirculating pump attached to the PVT cell to attain thermodynamic equilibrium.

Carbonated brine (2%KCL) is used to displace this mixture of crude oil and CO_2 through the sampling system. The BPR is set at the system pressure (same as the PVT cell pressure), and the water is pressurized to this value inside the piston vessel. The mixture is displaced through the filter battery, into the sampling system by gradually filling the PVT cell with carbonated water. Pressure in the appropriate sampling cylinders is recorded and the sample cylinders are removed for sample analyses. CO_2 is passed through the filters in an attempt to remove occluded crude oil and water from the filters

Carbon dioxide first contact with live oil

The only difference between carbon dioxide first contact experiments with the dead oil and the live oil is in the preparation of the live oil. Properties of the live oil are calculated using Winprop-CMG software by providing the compositions of the dead oil, the gases used, and natural gas.. Gas oil ratio (GOR), the proportion in which the oil and gas are mixed to make the live oil is also given. GOR in all the live oil experiments was maintained at 155 scf/stb, since this value was reflected in most field measurements.

Even though, field gas was collected for use in the experiments, it was procedurally difficult to load this into the PVT cells. Significantly more gas was also required than was available through several field samples. Hence the gas used in all the live experiments was prepared in the laboratory. An attempt was made to match the gas composition from the field. This required mixing propane and natural gas in definite proportion. Once the gas in the PVT cell is at the desired pressure, an appropriate MPV is evacuated and filled with CO_2. Subsequently, the dead oil is added to the PVT cell, and the mixture of gas and dead oil is recirculated overnight, while the system is heated to the desired temperature. CO_2 is added according to the procedure in section 3.2.1 and the mixture of CO_2 and live oil is recirculated and equilibrated. Afterwards, the mixture is displaced using the procedure mentioned in section 3.2.1.

Simulated multiple contact miscibility

To simulate the process of enrichment of the gas phase through extraction of the light and intermediate fractions of the oil, a light-intermediate cut from the Rangely crude oil (up to C15) was obtained by ASTM distillation procedure.

This light cut is mixed with the live oil, and then with CO_2, creating an artificial enrichment similar to the one experienced by the crude oil in the reservoir. Winprop-CMG software is used to calculate properties of the mixture of light cut and live oil to guide the experiments with respect to volume and pressure changes on mixing. The molar proportion of light cut to live oil is determined to be 1 to 2, according to some results obtained on the enrichment of crude oil in a coreflooding experiments.

True multiple contact miscibility

True multiple contact miscibility is achieved by vaporizing gas drive mechanism (forward contacts) in which the gas phase is getting enriched through extraction of the

light and intermediate fractions of oil (Figure 3.2). The overall composition of the oil-CO_2 mixture for the first contact was 76 mole% CO_2 and 24 mole% dead oil. This mixture is equilibrated in one of the PVT cells at a pressure below the bubble point of this mixture. Most of the vapor phase from this mixture is transferred isobarically to the second PVT cell which already contains fresh crude essential for the second contact. The remaining mixture in the first PVT cell is displaced through the high pressure filters into the fluid sampling system. The vapor phase from the second contact is displaced in a similar fashion into a third-contact PVT cell (the first PVT cell was prepared to be the third contact cell, once all the sample was displaced from it). Prior to this displacement, this PVT cell also was charged with the necessary crude oil. The remainder of the sample from the second contact was displaced through a separate line of filters into the fluid sampling system. Third contact yielded miscibility. Solid, liquid and gas sampling procedures were repeated for the third contact.

In the first PVT cell (first contact), 76 mole% CO_2 was mixed with 24% oil. A two-phase mixture resulted from this contact at 1475 psia and 160^0F. Upper phase occupied 70% by volume of the cell (total volume of 77 cc). From this cell, 90 vol% of the upper phase was mixed with fresh crude in the second contact to produce a total of 77 cc. 45% of the cell after this contact contained the gas phase. 90% by volume of this cell was displaced into the third contact cell, once again to produce a total of 77 cc. Complete miscibility was obtained in the third contact cell at 1400 psia. The molar concentrations of CO_2 and crude oil in the first and in subsequent contacts are shown in Table 3.1.

Table 2-3 Parameters of the true multiple contact experiment (mole%)

Contact	CO2	Oil
First	76	24
Second	67	33
Third	54	46

RESULTS

The C_5-C_{60} carbon number distribution of the original crude oil is shown in Figure 2-3. The oil contained 3.75 wt% C_{60}^{+}. The gravity of the oil was about 34 ?API. Thus,

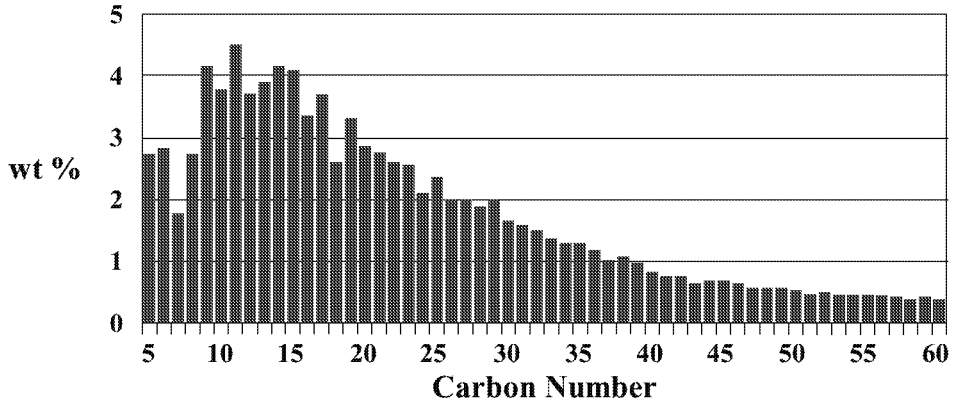

Figure 2-3 Carbon Number distribution of the original crude oil

Rangely oil is a light crude oil. The SARA (Saturates Aromatic, Resins and Asphaltenes) fractionation of the crude is shown in Figure 2-4. The asphaltene fraction of the oil as determined as pentane insolubles was found to be 2.8 wt% and the heptane insolubles were also determined as 1.4 wt%. The temperature in all the experiments was maintained at 160 ?F.

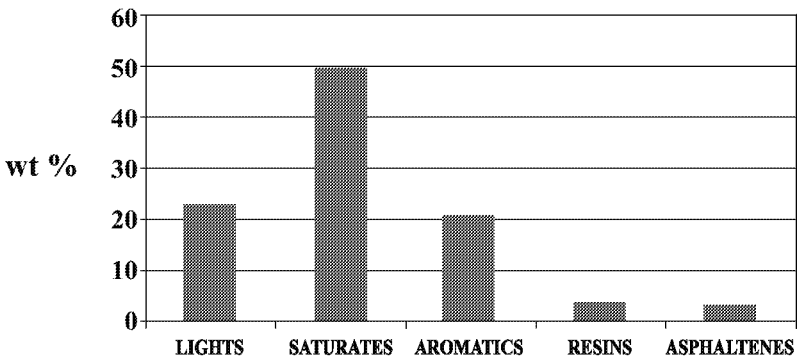

Figure 2-4 Saturates-aromatics-resins and asphaltenes distributions in the original oil

First Contact Experiments with Dead Oil

First contact experiments with carbon dioxide were performed by charging the PVT cell with crude oil and CO_2 mixtures in different molar proportions according to the method described. The mixtures were displaced above the bubble point through online, high-

pressure filters at constant pressure. The amounts of precipitates at various CO_2 concentrations are shown in Figure 2-5. The solids were collected from the filters

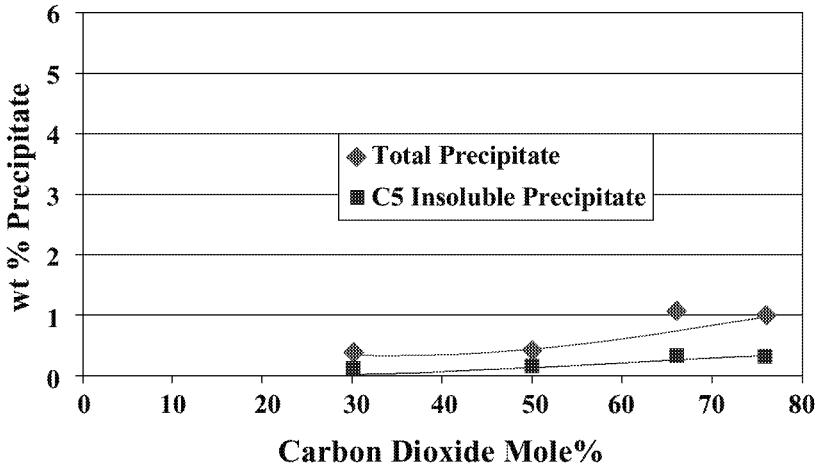

Figure 2-5 Precipitation amounts for first contact dead oil

and from the PVT cells. About 70% of the solids were from the filters. Based on these results, the precipitation onset is between 20-30 mole% of CO_2, which is consistent with the findings by Graue and Zana (1981). Precipitate amounts are less than 1% even at CO_2 concentrations of 76 mole%. The solids compositions determined from SARA analysis are shown in Table 2-4.

Table 2-4 Solid compositions determined from SARA analysis

Compound Class	Mole % CO_2		
	30	50	66
Saturates	45.24	38.92	45.35
Aromatics	22.20	16.09	20.12
Resins	7.01	7.86	6.70
Asphaltenes	23.49	34.2	27.36

The sum of pentane insolubles (asphaltenes) and resins were between 30 and 40% showing that saturates and aromatics constitute a significant portion of solids.

The C_5 insolubles in the precipitates are shown in Figure 2-5 and display the same trend as for the total precipitate. Table 2-5 presents the composition of gas phases obtained from the experiments.

Table 2-5 Wt% Composition of the gas phases while studying precipitation from dead oils

	Mole % CO_2		
Components	30	50	66
Air	7.59	4.29	0.74
CO_2	89.07	90.11	95.37

C_3	0.23	0.65	1.44
C_4	1.54	2.02	0.89
C_5	1.25	1.89	1.05
C_6	0.32	1.04	0.52

From the data of this Table, it can be observed that the sum of C_3 - C_6 components is 3.34, 5.6, and 3.9 % in experiments with 30, 50, and 66% CO_2 respectively. The composition data in Table 2-5 needs to be reduced to the actual concentration using pressures recorded in the sampling systems.
Table 2-6 provides data on the gas pressures in the sampling cylinders, the calculated values of the compressibility factor (z), the total number of moles of gas (n), and the weight fraction of C_3-C_6 extracted in the gas with respect to the crude.

Table 2-6 Gas phase. z: compressibility factor, n: total number of moles

Mole % CO_2	30	50	66
$P_{(500\ cc)}$, psia	142	143	290
$P_{(1000\ cc)}$, psia	65	59	135
Z	1.0045	1.1150	1.0055
N	0.1449	0.1316	0.3056
C_3-C_6 %	0.33	0.52	1.04

It can be observed that the concentrations of the C_3-C_6 fraction extracted in the gas phase increases with the concentration of CO_2. Therefore at higher CO2 concentrations, there is additional extraction of light hydrocarbons, and the miscibility increases as the concentration of CO_2 increases. From the data of precipitation, the precipitated solids increase with the concentration of CO_2.

The compound class analysis of these liquids is presented in Table 2-7.

Table 2-7 Liquid fractions- Dead oil

Compound Class	Mole % CO_2		
	30	50	66
Lights	17.79	18.75	17.51
Saturates	56.51	52.77	58.41
Aromatics	17.5	16.50	15.16
Resins	2.01	2.13	2.09
Asphaltenes	3.69	3.36	2.4

Concentrations of pentane insolubles in the liquid fraction after the thermodynamic experiments decrease with increase in the CO_2 concentration used in the experiment. The values are higher than the ones in the original crude due to the loss of heavier components in the precipitate and loss of some of the lighter components to the gas phase. Figure 2-6 shows the SARA fractions in these liquid samples and in the original oil. In this graph, the light fraction was not considered, and the data were normalized using only saturates, aromatics, resins and asphaltenes. The proportion of saturates increases as more CO_2 was in contact with the dead oil, while the aromatics were reduced.

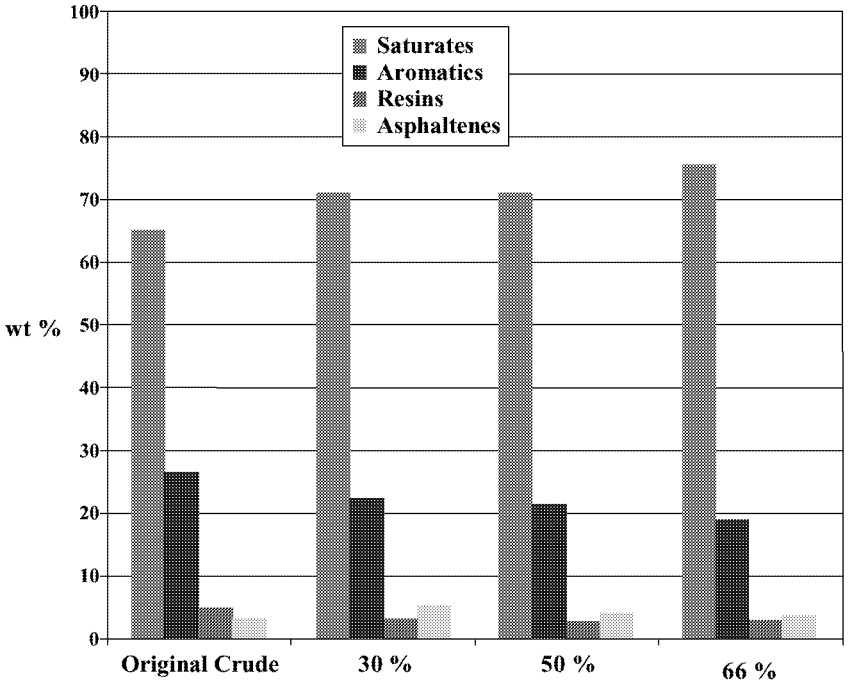

Figure 2-6 Liquid fractions from dead oil experiments

First Contact Experiments with Live Oil

In the live oil experiments, the gas oil ratio (GOR) was kept constant at 155 scf/stb. The composition of the gas to be used in the recombination process to obtain the live oil is shown in Table 2-8. Recombination calculation is performed at the gas oil ratio (GOR) given, 155 scf/stb, pressure of 3000 psi and 160 °F. The composition of the live oil is

shown in Figure 2-7. Concentrations of CO_2 (mole fractions) are reported with respect to dead oil instead of live oil.

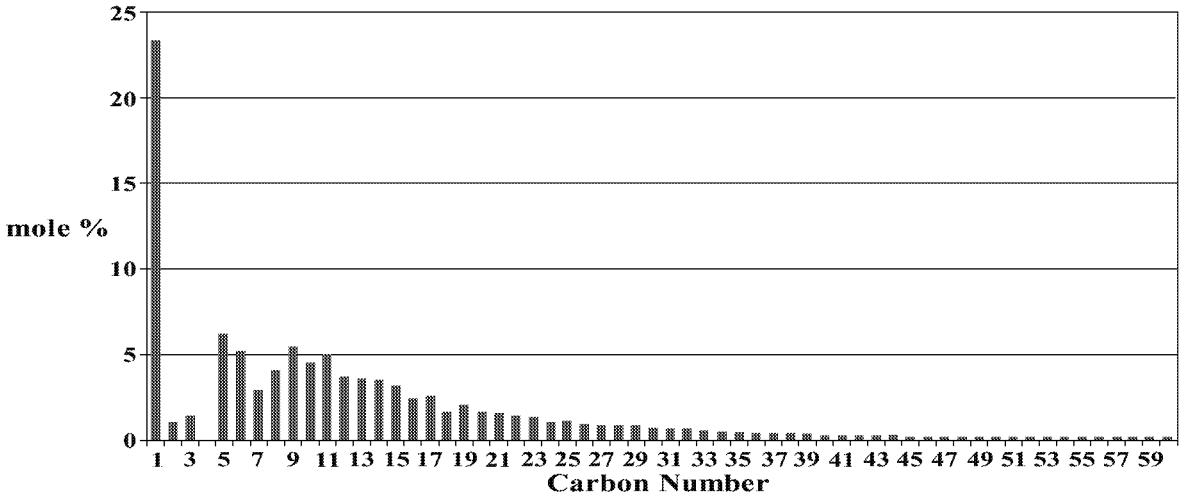

Figure 2-7 Live oil molar composition

Table 2-8 Gas composition – recombination

Component	Mole %
Methane	91.1
Ethane	3.7
Propane	5.2

Amounts of precipitates at different CO_2 concentrations are shown in Figure 2-8. The precipitate amounts compared with equivalent dead oil experiments are 3 to 4 times higher. These results confirm that the precipitation starts between 20-30 mole % CO_2 (Graue and Zana, 1981). The maximum amount of precipitate is about 4%. Table 2-9 shows the solids compositions determined from the SARA analysis.

Table 2-9 Precipitates with live oil

Compound	Mole % CO_2					
Class	0	11	28	38	55	66
Saturates	60.42	44.61	36.26	38.65	37.82	38.67
Aromatics	20.09	18.40	19.84	20.98	21.00	18.32
Resins	5.66	4.50	6.16	7.18	7.11	7.97
Asphaltenes	8.83	16.65	34.09	30.27	33.60	35.01

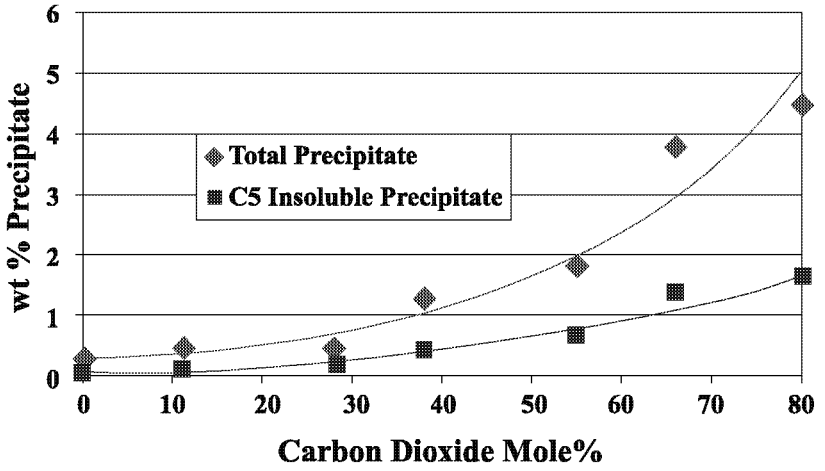

Figure 2-8 Precipitation amounts for first contact live oil experiments

The precipitation in the blank experiment (0 mole% CO_2) is 0.22 wt% of the original oil. From the SARA analysis of this precipitate, the concentration of asphaltenes (defined as pentane insolubles) is only 8.83 wt% of the precipitate, which means that the precipitate obtained in the filters, in this experiment, must correspond mainly to occluded oil. From this value, it can be estimated that the amount of occluded oil in the precipitates is low. Precipitate from the experiment with 11 mole% CO_2 is small (0.45 wt% of the original oil), its asphaltene content is higher than for the blank experiment, but low compared with other precipitates. From the SARA results of precipitates obtained from thermodynamic experiments, it can be concluded that when a significant amount of precipitation occurs, (28 mole% CO_2) the quality of the precipitates is similar. The data also show that CO_2 induced precipitates contain about 35 wt% of asphaltenes (defined as pentane insolubles); the sum of asphaltenes and resins in the precipitates goes up to 43 wt%. It is observed that at 80 mole% CO_2, the CO_2 induced precipitate is 4.45 wt% while the pentane insolubles in the precipitate are only 1.58%.

Table 2-10 presents the composition of the gas phase obtained from live oil experiments. Hydrocarbons as heavy as heptane are extracted in live oil experiments at high concentrations of CO_2; this is an indication of better extraction into the gas phase in these experiments.

Table 2-10 Wt % Compositions of the gas phases while studying precipitation from live oils

	CO_2 mole%						
Components	0%	11%	28%	38%	55%	66%	80%
Air	1.63	4.89		2.45	4.22	1.32	1.25
CO_2		70.22	81.53	62.43	78.04	71.45	86.38
C1	60.87	18.96	10.13	26.77	8.85	6.34	7.6
C2	19.99	0.39	0.21	0.55	0.18	0.13	0.16
C3	6.79	0.94	2.96	1.6	2.13	2.26	0.49
C4	5	0.68	1.93	2.09	1.43	1.78	1.2
C5	3.08	1.06	2.23	2.31	1.83	3.94	1.23
C6	2.64	2.86	1.01	1.8	1.99	7.05	0.99
C7					1.33	5.73	0.7

Table 2-11 gives the pressures of the sampling systems, compressibility factors, total number of moles of gas, and fraction of $C_3 - C_7$ extracted in the gas with respect to the crude, obtained using the same procedure described in an earlier section.

Table 2-11 gas Phase - Live oil

	0%	11%	28%	38%	55%	66%	80%
$P_{500\ cc}$, psia	90	280	170	223	270	390	465
$P_{1000\ cc}$, psia	36	120	76	100	130	190	220
Z	1.141304	1.072072	1.034239	1.03621	0.989529	0.984665	1.012784
N	0.079754	0.267292	0.1702	0.224911	0.298958	0.439683	0.508577
C_3-C_7 extracted	0.43	0.77	0.89	0.95	2.61	2.75	2.93

From the data in these tables, concentration of $C_3 - C_7$ extracted in the gas phase increases with concentration of CO_2 in the experiment. Figure 2-9 compares extraction of light ends from the crude oil in the gas stream for experiments with dead oil and live oil. Extraction is much higher for live oil, especially after 40 mole% CO_2. In this range, extraction with live oil results in at least three times more C_3-C_7 fraction than for dead oil. There is greater miscibility with live oil than with dead oil, therefore more extraction of light ends, and more precipitation (see Figure 2-9). Liquid fractions after experiments were analyzed by compound class and these results are presented in Table 2-12.

Table 2-12 Liquid Fractions - Live Oils

Compound class	Mole % CO_2					
	0%	11%	28%	38%	55%	66%
Lights	8.54	5.81	19.27	18.13	28.22	29.5
Saturates	61.47	61.01	48.82	54.72	46.53	46.86
Aromatics	17.54	22.25	17.49	17.11	14.75	16.79
Resins	2.11	2.98	2.50	2.26	3.13	3.42
Asphaltenes	3.11	3.01	3.29	2.25	2.04	1.05

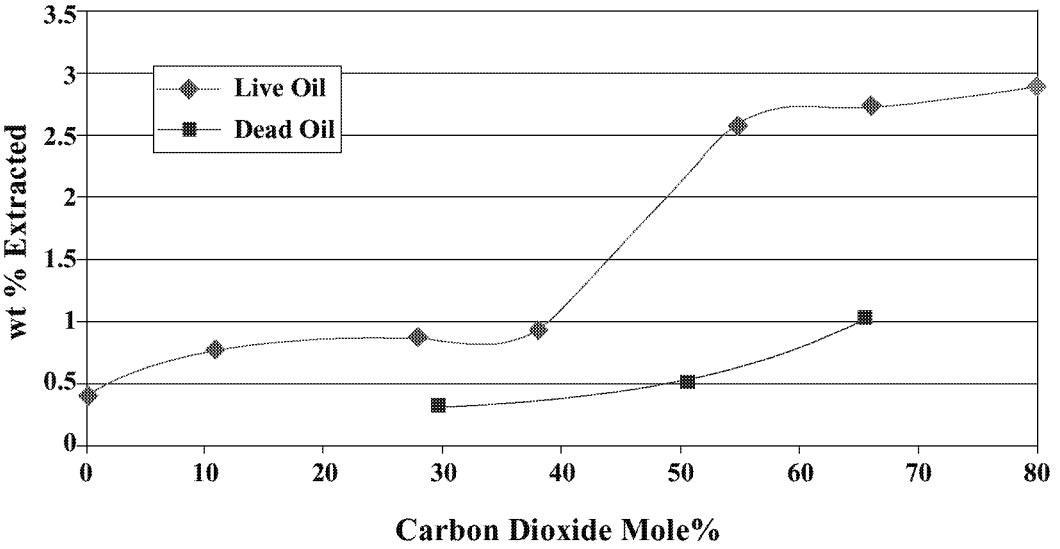

Figure 2-9 Light ends extracted in gas phase

Asphaltenes (defined as pentane insolubles) in the liquid fraction after the precipitation experiment are shown in Figure 2-10 . At lower CO_2 concentrations, the asphaltene amounts are comparable to those from the original crude oil; however, at higher CO_2 concentrations lower amounts of asphaltenes are obtained. The crude oil at the time of the test has lost some of the heavier components and some of the lighter components to the flashed gas phase. The relative importance of these two competing effects determines the asphaltenes content of the oil from which CO_2 induced precipitation has already occurred.

Figure 2-11 presents the cumulative carbon number distribution from GC-FID of the original crude, and liquid fractions obtained from experiments with 38% CO_2, 55% CO_2, and 66% CO_2 concentrations. The compositions of liquid fractions after CO_2 thermodynamic experiments appear to be close to each other when concentrations of CO_2 in the experiments were 38%, 55% and 66%. However, there are important differences in the heavy components C_{60}^+ as presented in Table 2-13. C_{60}^+ fraction, the heaviest portion of the crude oil, reduces from 9.33 wt% in the original crude to 2.36 wt% when the concentration of CO_2 in the precipitation experiment was 66 mole%.

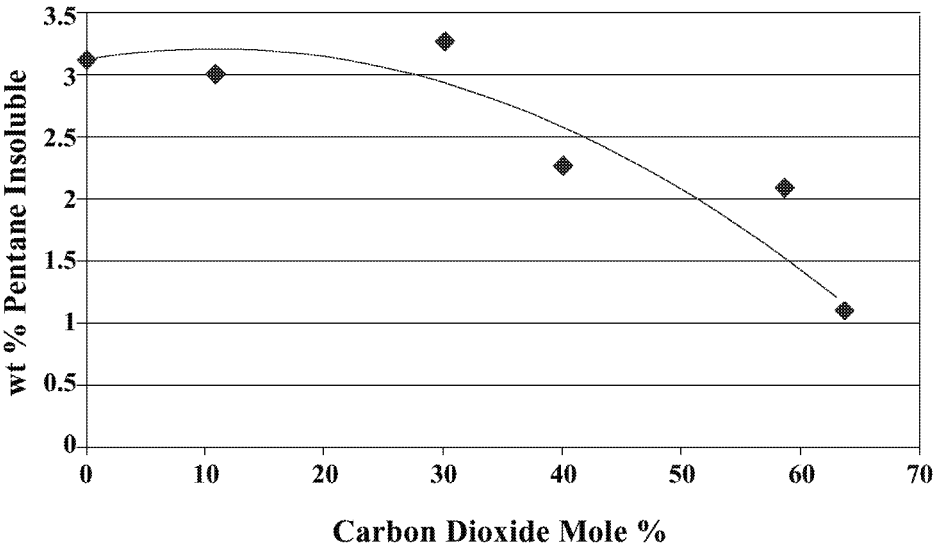

Figure 2-10 Asphaltenes in the liquid fractions from live oil experiments

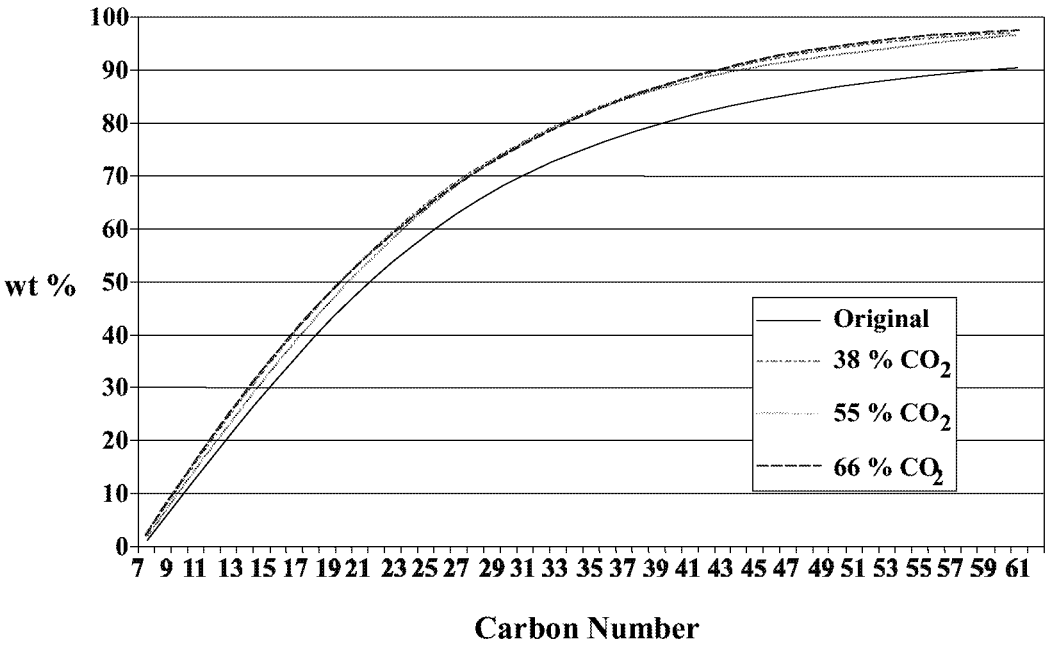

Figure 2-11 Cumulative carbon number distribution of crudes from live oil experiments

Table 2-13 C_{60}^{+} fraction for crudes - live oil

Crudes	C_{60}+
Original crude	9.33
38%	2.42
55%	3.16
66%	2.36

Simulated Multiple Contact Experiments

In the carbon dioxide multiple contact process, the oil just before attainment of miscibility is enriched with intermediates (Orr 1981). In order to simulate this effect without undertaking true multiple contact tests, a light cut from the crude oil itself was added to the oil. For this experiment, an ASTM D-2886 distillation column was first used to generate a C_{15}- fraction from the Rangely crude. The Rangely oil was distilled to an upper boiling point of 520^0F. The cumulative carbon number distribution for this distillation cut is shown in Figure 2-12, about 84% of the cut is below C_{15}. The fraction added to the oil to simulate multiple-contact composition amounted to 30% (molar) with respect to the live oil and 48% with respect to the dead oil. The precipitation with the addition of the light-intermediate fraction to the oil is also plotted in Figure 2-13. With the addition of the "light – intermediate" fraction, amount of precipitate is approximately twice the amount for equivalent CO_2 concentration without the cut (compared to the live oil precipitates). This suggests that multiple-contact mixtures are likely to yield twice the amount of precipitate expected through first-contact experiments. With the addition of the light-cut, the precipitation is also more sensitive to CO_2 concentrations and increases more rapidly as CO_2 concentration goes up.

The concentrations of pentane insolubles in the precipitates are 27.49%, 43.77%, and 42.62% for experiments with 25, 48, and 68 mole% CO_2 respectively. **Figure 2-14** includes total precipitate and precipitates expressed as asphaltenes (pentane insolubles). These CO_2 induced precipitates contain more pentane insolubles than the precipitates from the dead or live oils, indicating that the solids are heavier. **Table 2-14** presents the gas compositions of the flashed gas phase obtained from simulated multiple contact experiments.

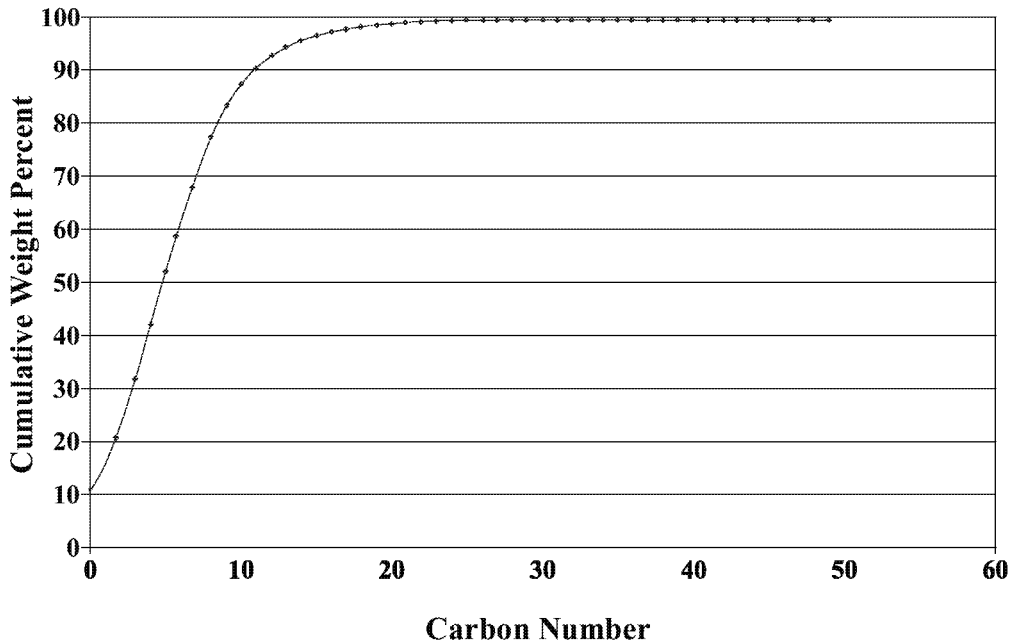

Figure 2-12 Cumulative carbon number distribution of the light-cut added to the oil

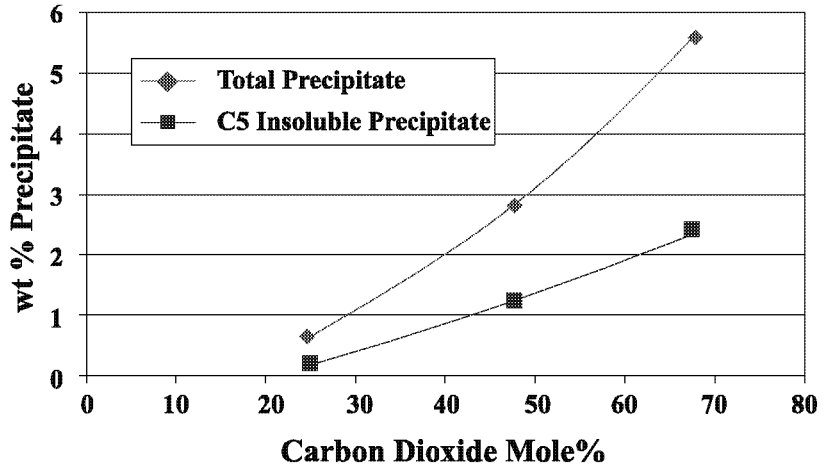

Figure 2-13 Precipitation for simulated multiple contact

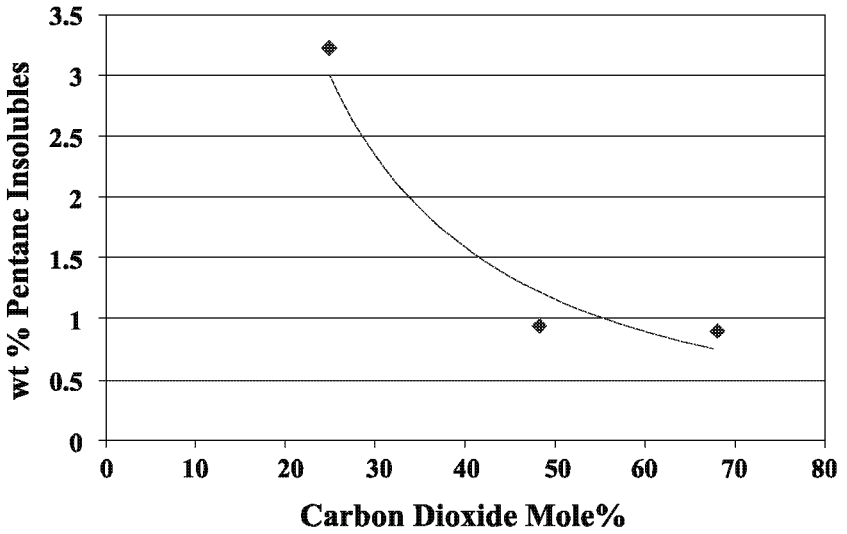

Figure 2-14 Asphaltenes in the liquid fractions for simulated multiple contact

Table 2-14 Gas Compositions - Simulated Multiple Contact

Component	Mole % CO_2		
	25%	48%	68%
Air	2.94	3.9	1.2
CO_2	79.10	75.43	75.61
C_1	13.84	11.78	13.55
C_2	0.28	0.24	0.28
C_3	0.96	1.21	1.19
C_4	0.74	1.38	1.78
C_5	1.02	2.80	2.94
C_6	1.13	3.26	3.45

Table 2-15 gives pressures in the sampling cylinders, compressibility factors, total number of moles of gas, and fraction of C_3-C_7 extracted in the gas respect to the crude according to calculations explained before.

Table 2-15 Gas Phase - Simulated Multiple Contact

	25%	48%	68%
$P_{(500\ cc)}$, psia	230	273	395
$P_{(1000\ cc)}$, psia	90	118	188
Z	1.1904	1.0764	0.9870
N	0.202855	0.26567	0.42692
C_3-C_7 extracted	0.51	1.53	2.16

From Table 2-14 and Table 2-15, concentration of C_3-C_7 extracted in the gas phase increases with CO_2 concentration, and it is intermediate between extraction for dead oil and live oil, closer to values for live oil. Liquid fractions obtained after CO_2 induced precipitation in simulated multiple contact experiments were analyzed by compound classes (Table 2-16).

Table 2-16 liquid fractions - Simulated Multiple Contact

	25%	48%	68%
Lights	22.59	26.93	40.53
S	51.44	47.73	39.48
A	16.31	13.59	12.64
R	2.24	1.63	2.09
A	3.20	0.97	0.88

Pentane insolubles in the liquid fractions are reduced even more than in the case of live oil experiments. **Figure 2-14** presents these results. Thus, simulated multiple contact experiments lead to the precipitation of heavier solids, reducing the "heavy-polar" fraction in the oils left behind.

True Multiple Contact Experiments

The procedure for true forward multiple contact experiments is described in the previous chapter. In the first PVT cell (first contact), 76 mole% CO_2 was mixed with 24% oil. A two-phase mixture resulted from this contact at 1475 psia and 160^0F. Upper phase occupied 70% by volume of the cell (total volume of 77 cc). From this cell, 90 vol% of the upper phase was mixed with fresh crude in the second contact to produce a total of 77 cc. 45% of the cell after this contact contained the gas phase. 90% by volume of this cell was displaced into the third contact cell, once again to produce a total of 77 cc. Complete miscibility was obtained in the third contact cell at 1400 psia (Figure 2-15).

The amounts of precipitates with multiple contacts are compared to the first contact amounts in Figure 2-16. The multiple contact experiments were performed with dead oils, instead of the live oil used in simulated multiple contact experiments. The multiple

contact precipitate amounts are about two to three times the first contact precipitate amounts for the same CO_2 concentrations.

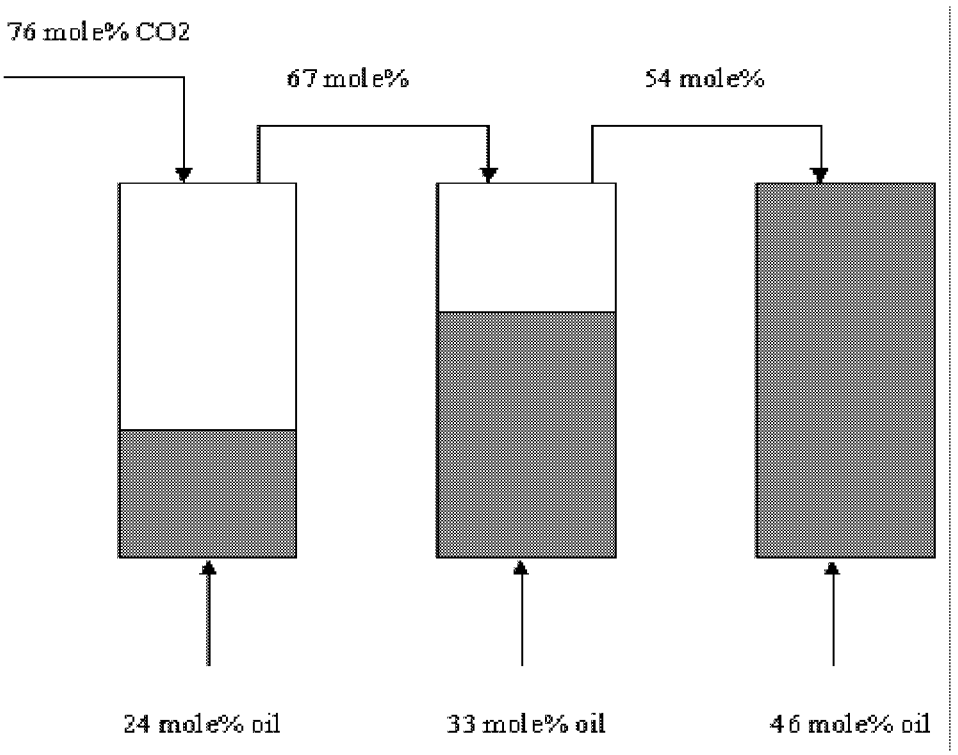

Figure 2-15 True Multiple contact experimental procedure – a schematic

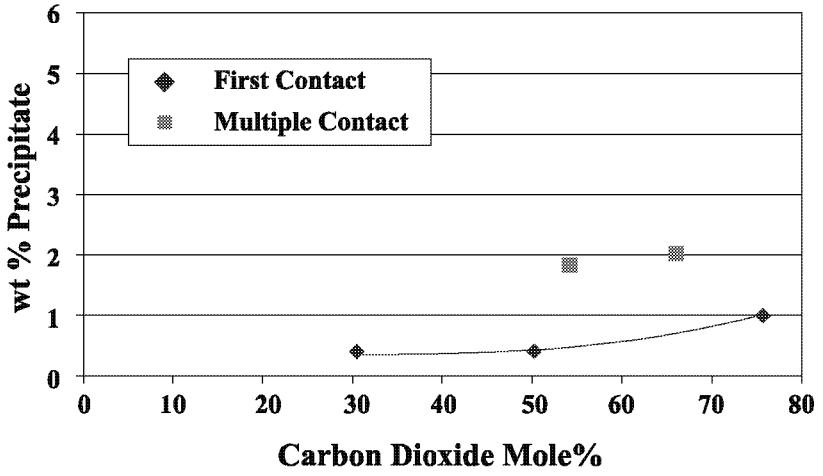

Figure 2-16 Comparison of CO2 induced precipitation for first and multiple contacts

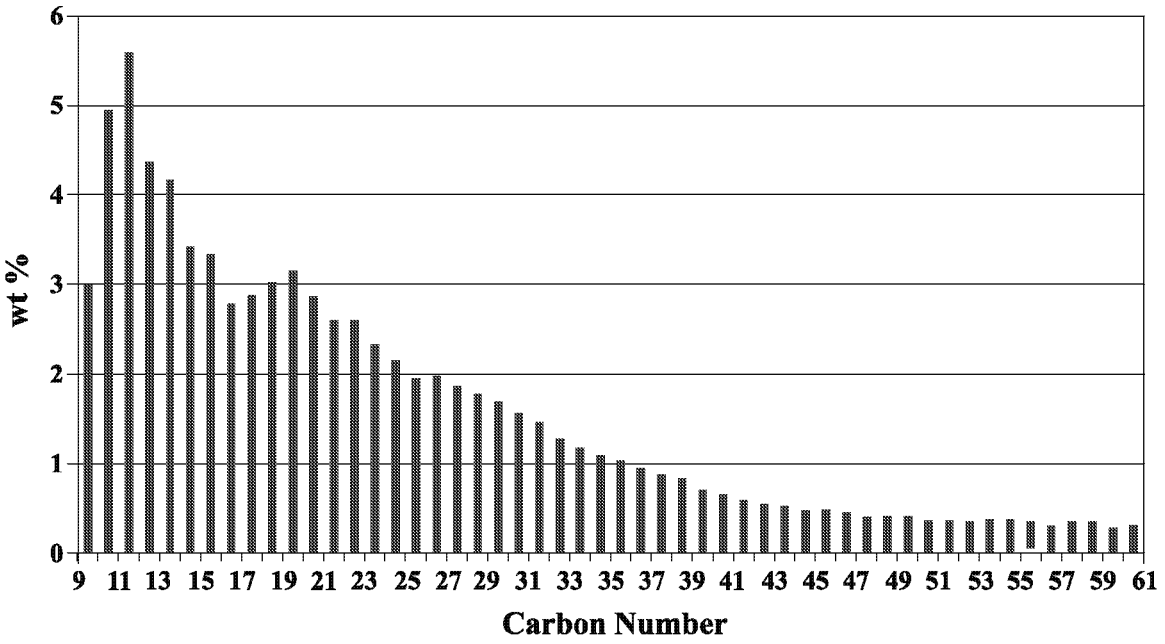

Figure 2-17 Composition of gas phase from first contact

First contact experiments with live oils gave three to four times more precipitation than first contact experiments with dead oils. Therefore true multiple contact experiments with live oils would be expected to yield six to eight times more precipitation than first contact experiments.

Precipitates from the three contacts were analyzed by SARA and the composition of these fractions are shown in Table 2-17. Pentane insolubles in the precipitates are about 35% of the precipitate, and resins are about 7%.

Table 2-17 Precipitates SARA - True Multiple Contacts

Compound class	Contact		
	1st	2nd	3th
Saturates	37.12	39.67	36.98
Aromatics	16.40	18.15	20.03
Resins	7.81	6.93	7.76
Asphaltenes	36.77	33.17	32.7

Gas phases for first and second contacts were analyzed and the concentrations of CO_2 were 93.2 and 90.2 wt%, respectively. CO_2 concentrations decrease from first to second contact. Thus, more hydrocarbons are extracted into the gas phase as contacts advance.

Table 2-17 presents the composition of gas phase (HT-GC-FID) from first contact without CO_2. From these data, the enrichment of intermediate components in the gas phase can be observed. This composition shows how hydrocarbons are distributed in the gas phase, where 93.2 wt% is CO_2 and the difference is the hydrocarbons extracted from the crude oil. It is also observed that 60 wt% of the oil extracted is constituted of hydrocarbons with carbon number up to C_{31}.

Figure 2-18, Figure 2-19 and Figure 2-20 show the cumulative compositions of the liquid fractions after CO_2 precipitation. In Figure 2-18, the original crude is compared with the liquid fraction obtained from first contact; during first contact, there are a slight enrichment of intermediate components and a reduction of C60+ fraction. In Figure 2-19, first and second contact liquid fractions are compared; light and intermediate components are enriched and heavy components are reduced. In Figure 2-20, second and third contacts are compared; in the third contact the concentrations in all the range are lower than in second contact.

Thermodynamic experiments with Rangely oil were performed at different conditions with CO_2. About 20-25% CO_2 molar concentration is necessary to induce measurable precipitation in crude oils containing originally low quantities of asphaltenes. Live oils yielded significantly higher amounts of precipitates than equivalent dead oils. A hypothesis that multiple contact mixtures yielded significantly higher amounts of precipitates was conclusively proven based on results from simulated multiple contact (addition of an intermediate cut) and true multiple contact experiments.

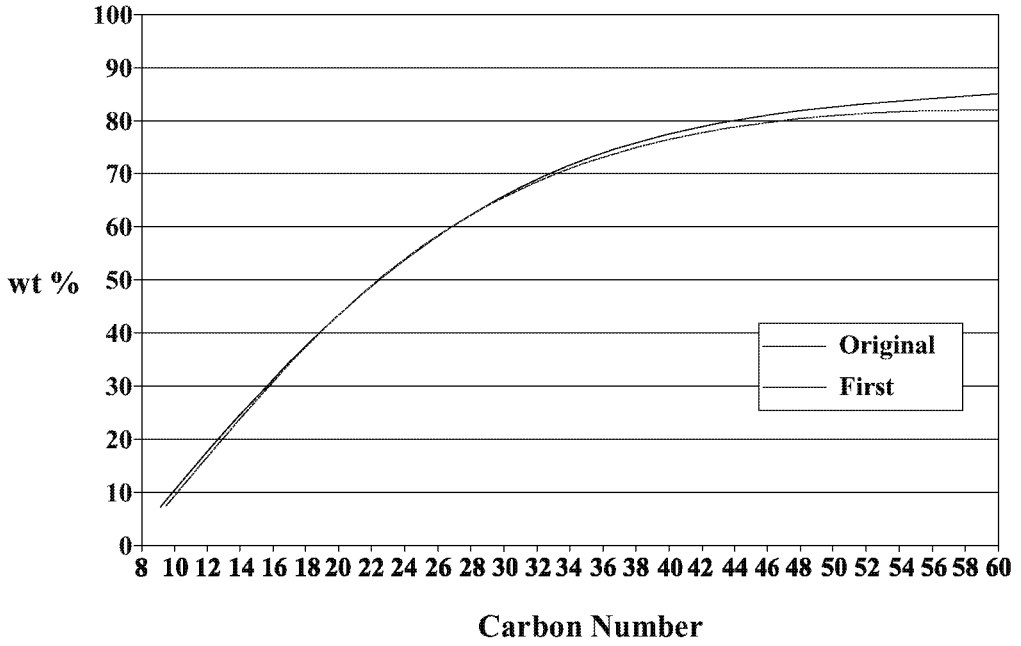

Figure 2-18 Comparison between liquid fraction from first contact and original oil

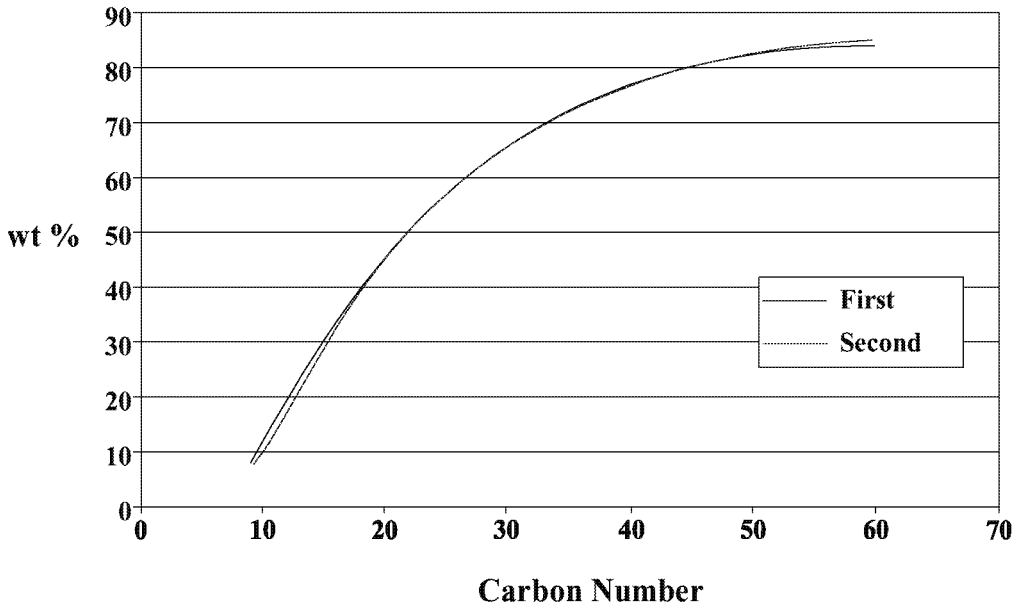

Figure 2-19 Comparison of liquid fractions between second and first contacts

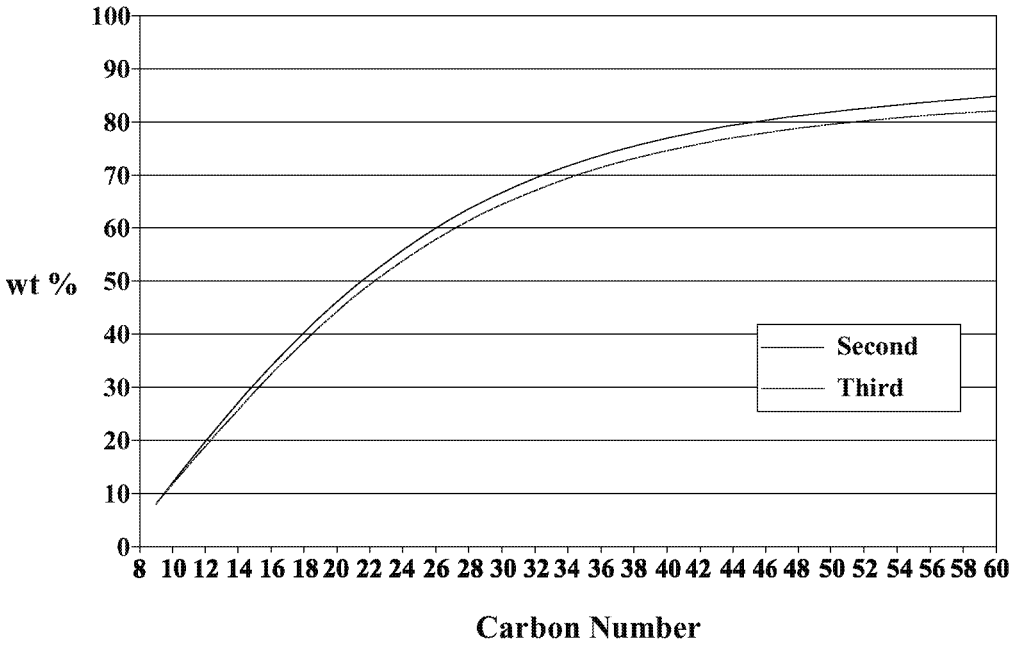

Figure 2-20 Comparison of liquid fraction composition between third and second contacts

3. Asphaltene Characterization

Martha Parra Ramirez performed this work. More details appear in her Ph. D. dissertation (Parra, 2002).

Samples

Sample designations are given in Table 3-1.

Table 3-1 Sample Designations

Sample	Description
Field	Precipitate obtained from the field in Rangely
RO-lab	Precipitate from thermodynamic experiment with Rangely oil (30% mole CO_2)
C_5-sol-field	Pentane soluble from field sample
C_5-field	Pentane insoluble from field sample
Ph-lab	Precipitate from thermodynamic experiment with Phillips oil (30% mole CO_2)
RO-C_5 asph	Pentane insoluble in Rangely Oil
RO-C_6 asph	Hexane insoluble in Rangely Oil
RO-C_7 asph	Heptane insoluble in Rangely Oil
C_5-sol-field	Pentane soluble portion of field sample
Ph-C_5-asph	Pentane insoluble in Phillips Oil
Ph-C_6-asph	Hexane insoluble in Phillips Oil
Ph-C_7-asph	Heptane insoluble in Phillips Oil
Rangely	Rangely crude oil
Resins	Resins form Rangely
RO-Cn-X	Compound classes from Rangely after solid removal with Cn
Ph-Cn-X	Compound classes from Phillips after solid removal with Cn

X=S= saturates, A= aromatics, R= resins; n= 5,6,7

Chromatographic Techniques

Column Chromatography

Fractionation of crude oils into compound classes is shown in Figure 3-1. This fractionation method combines asphaltene precipitation and column chromatographic separation into compound classes such as saturates, aromatics and resins.

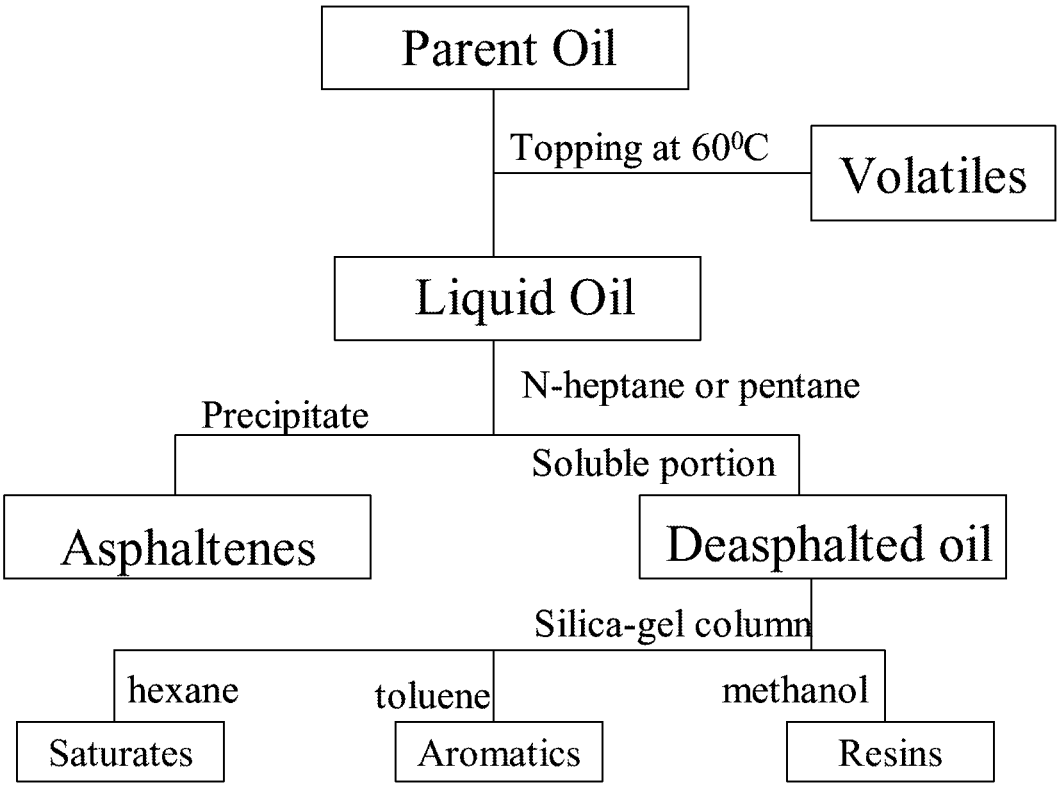

Figure 3-1 Fractionation of crude oil

This method was used to analyze liquids and precipitates. Collection of precipitates from the high-pressure thermodynamic experiments was described in an earlier section. Solid samples from the field (Rangely were also include in the analysis). Table 3-2 shows weight % of saturates, aromatics, resins and asphaltenes in the field sample and in the solids deposited on one of the filters.

Table 3-2 SARA distribution in CO_2 induced solids

Fraction	Field	RO-lab
Saturates	12.71	32.14
Aromatics	9.96	13.42
Resins	2.67	4.61
Asphaltenes (C_5 insolubles)	74.12	47.83

The analysis reveals that the solids are not all asphaltenes. The laboratory sample contains significantly higher percentage of saturates. The asphaltenes in the field solid sample in comparison to the laboratory sample are much higher. The exact process by which the field sample was deposited was not known. The laboratory sample (RO-lab) possibly includes occluded oil. Conditions at which the solids are formed in the field and in the laboratory may be vastly different. Once the solids are formed in the field, they may have been subjected to other solvent treatments. Xylene is often used to treat solids. Residual xylene in the wellbore may have dissolved the saturate portion of the precipitate

making it more aromatic/polar. It is also unclear what role "weathering" plays on the composition of the precipitated solids. Thus, there are a variety of reasons why the solids from the field differ in composition from the solids obtained in the laboratory.

Column chromatography was also used to characterize Rangely crude oil and Phillips crude oil. Figure 3-2 shows this characterization and provides names of the different samples. Asphaltenes were precipitated from the crude using three different paraffinic solvents; pentane, hexane, and heptane. The procedure for obtaining saturates, aromatics and resins from the deasphalted crude oil was identical, once asphaltenes were separated. The distributions of lights, saturates, aromatics, resins, and asphaltenes (C_5, C_6, C_7 insolubles) are provided in Table 3-3 for the two oils.

Table 3-3 SARA distribution for different precipitant solvents

	Lights	Saturates	Aromatics	Resins	Asphaltenes
RO-C_5	22.88	53.54	18.93	2.20	2.45
RO-C_6	22.88	52.14	20.38	2.66	1.94
RO-C_7	22.88	54.19	19.36	2.17	1.40
Ph-C_5	20.51	38.40	25.04	4.16	11.89
Ph-C_6	20.51	38.50	25.41	4.24	11.34
Ph-C_7	20.51	42.64	27.35	4.39	5.11

RO – Rangely Oil; Ph – Phillips Oil
C5,C6,C7: precipitating agents

As the carbon number of the paraffinic solvent increases, there is a decrease in the amount precipitated. In the case of the Rangely crude oil, 26% more precipitate is obtained when pentane is the solvent instead of hexane. There are 75% more pentane insolubles compared to heptane insolubles. For the Phillips crude oil, these numbers are 5% and 133% respectively.

It is well known that as the carbon number of the paraffinic solvent decreases, amounts of solids precipitated increase. This increase is more significant for "asphaltic" crudes such as the Phillips crude oil. From Table 3-3 it is clear that the amounts of resins remain relatively constant. The increase in asphaltene content, in the case of Rangely oil comes about at the expense of the aromatic fraction, while in the case of the Phillips crude, it is achieved at the expense of both the saturate and the aromatic fraction. It is clear that a compound classified as saturates or aromatics in one solubility test becomes part of the "asphaltene" class in another test.

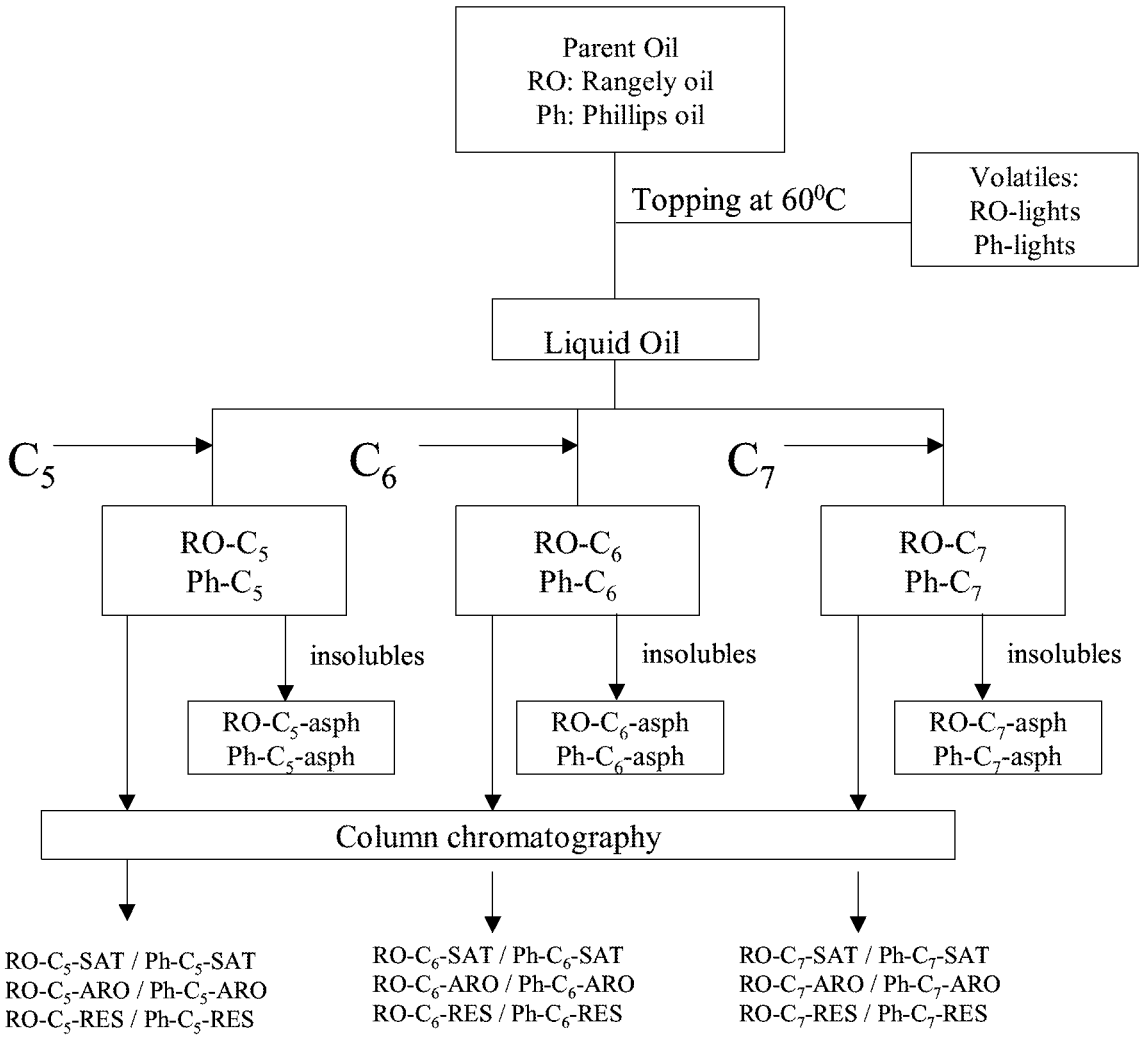

Figure 3-2 Samples from column chromatography

High Temperature Gas Chromatography with Flame Ionization Detector (HT-GC-FID)

HT-GC-FID chromatograms were determined with a Hewlett – Packard Model 5860 Series II gas chromatograph. The initial temperature was 70°C, and the rate of temperature increase was 10°C per minute until the temperature reached 450°C, and was kept constant for eleven minutes. The peaks were analyzed by the well-known technique of simulated distillation. The entire field sample (field), pentane insolubles from this sample (C_5-Field), pentane soluble portion of the field precipitate (C_5-Sol-Field) and a precipitate from a thermodynamic experiment (RO-lab) were analyzed. The corresponding chromatograms are shown in Figure 3-3. Table 3-4 shows fractions eluted and non-eluted, and the cumulative fraction up to C_{40} from the eluted fractions for different samples.

Table 3-4 Simulated distillation results of solid samples from the field and the laboratory (wt%)

Sample	Eluted fraction	Non-eluted fraction	C_{40} -
Field	28.91	71.09	25.44
C_5-Field	4.47	95.53	0
C_5-Sol-Field	93.54	6.46	83.55
RO-lab	71.73	28.27	61.11
Resins	14.13	85.87	9.97

It is expected that the compounds that elute from the field sample would be in the pentane soluble portion of the same. This is confirmed by observing the chromatograms. Most of the peaks observed in part a are also seen in part b. The pentane insoluble chromatogram (part d) is impossible to decipher since most of the sample does not elute,

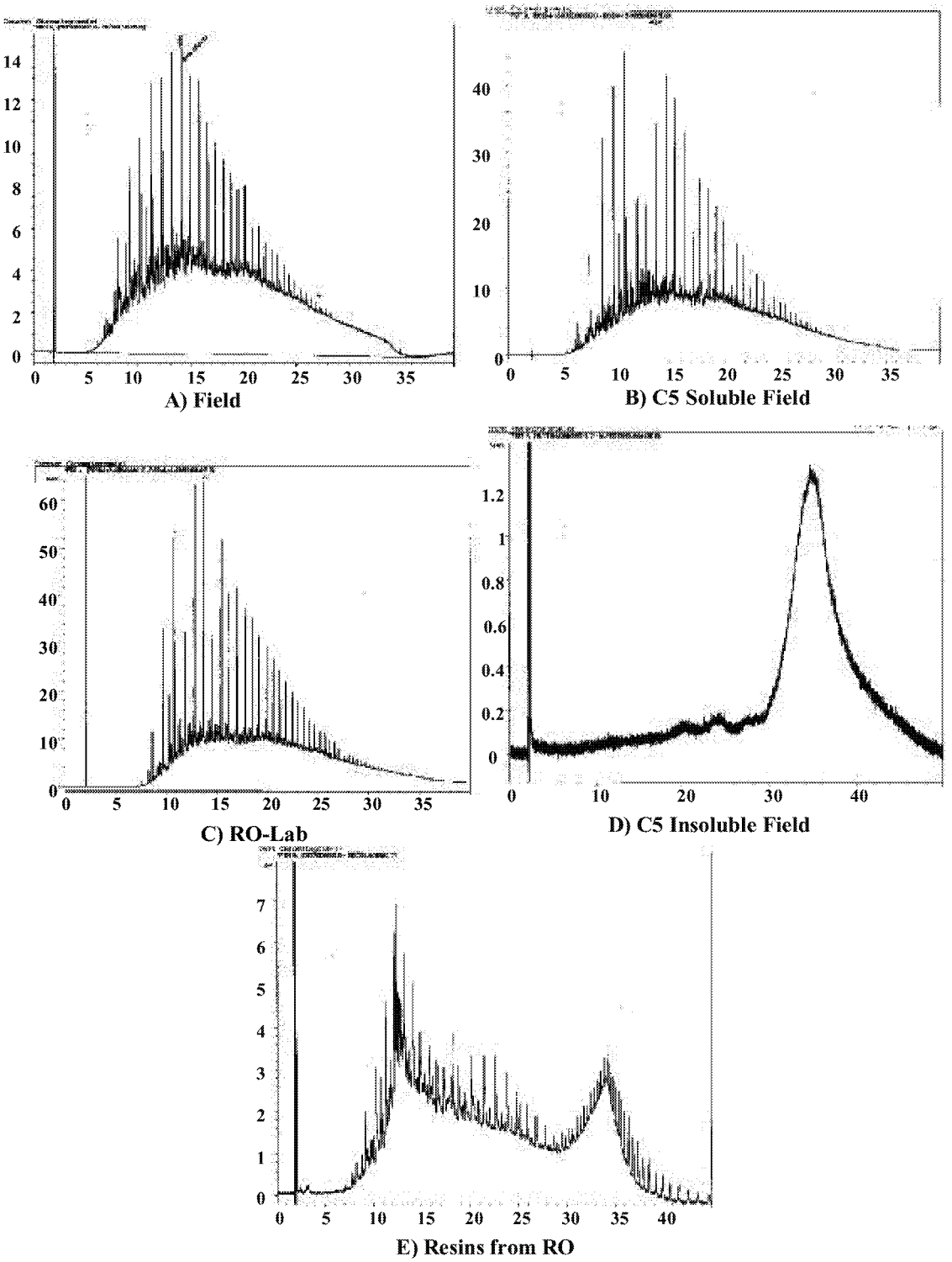

Figure 3-3 HT-GC-FID chromatograms of precipitates and resins

and constitutes 74.12% of the whole field sample. RO-lab precipitate has a chromatogram (part c) similar to the ones for the field precipitate (part a) and the pentane soluble in the field precipitate (part b); 47.83% of the RO-lab sample is pentane insoluble. Eluted fractions of samples field and RO-lab consist of 88 wt% and 85 wt% of C_{40}^- respectively.

Chromatogram of the resin fraction is shown in part e. Some peaks corresponding possibly to lighter polyaromatic compounds are observed. However, only about 14% of the sample elutes from the column. It is evident that lighter aromatic compounds (low boiling) get into the resin fraction when the SARA separation is performed. The eluted fraction of resins consists of 70% C40-, indicating that it is heavier than the equivalent whole samples.

Gas Chromatography-Mass Spectrometry (GC-MS)

Mass spectral data were obtained using a HP-5980A chromatograph equipped with a quadrupole mass spectrometer. The following samples were analyzed:

- ?? Rangely crude oil and its fractions: saturates, aromatics and resins.
- ?? Field solids
- ?? C_5-Field
- ?? C_5-Sol-Field

Table 3-5 gives a list of compounds identified in these fractions. Compounds up to about C_{42} elute from the column and are identified. Saturate chains are easily identified in the crude and are present in low proportions in the aromatics and resin fractions.

It was possible to identify aromatics and polyaromatic compounds from the aromatic fraction while from the resins fraction it was difficult, if not impossible to identify compounds except a few saturate chains and a few aromatic compounds. Among the aromatics, benzenes, naphthalenes, dibenzothiophenes and phenanthrenes, are identified. Most of the components identified in a crude sample after the CO_2 experiment are the same as the ones in the original crude, but after the experiment there are changes in the intensity.

Table 3-5 Peaks identified in the mass chromatograms

Ions	Compounds
57	Alkanes up to C_{42}
113,183	Isoprenoids ($C_{13} - C_{25}$)
69	Alkylcyclopentane ($C_{13} - C_{30}$)
83	Alkylcyclohexane ($C_{13} - C_{30}$)
97	Alkylated methyl cyclic ($C_{11} - C_{34}$)
109,123,193	Bicyclic terpanes ($C_{21}H_{38}$, $C_{22}H_{40}$, $C_{23}H_{42}$, $C_{24}H_{44}$)
191,163	Hopanes ($C_{27}H_{46}$, $C_{29}H_{50}$, $C_{30}H_{52}$)
191	Tetracyclic terpanes ($C_{24}H_{42}$, $C_{26}H_{46}$, $C_{27}H_{48}$)
217	Steranes (C_{27} - C_{22})
91	Monoaromatics ($C_{12} - C_{39}$)
105	Alkylated toluene (alkyl chain: $C_{13} - C_{33}$)
128,142,156,170	Naphthalene and metyl naphthalenes (C_{10}, C_{11}, C_{12}, C_{13})
148,162,176	Benzothiophenes (C_9, C_{10}, C_{11})
184,198,212	Dibenzothiophenes (C_{12}, C_{13}, C_{14})
178,192,206,228,242,256	Phenanthrene (C_{14} - C_{19})
191,206,220,234	Alkylated methyl phenanthrene
248	Methyl benzonaphthothiophene
228,242,56,270	Chrysene (C_{18}H12, $C_{19}H_{14}$, $C_{20}H_{16}$, $C_{21}H_{18}$)
252	Benzopyrene

Table 3-6 shows the ratios of pristane/$C_{17}H_{36}$, Phytane/$C_{18}H_{38}$, Pr/Ph and ratios of normal hydrocarbons. The first three ratios do not change significantly, indicating that there is no fractionation of these hydrocarbons. According to Hwang (1998) the hydrocarbons at these molecular sizes are miscible with CO_2 under reservoir conditions. The fractionation of heavy hydrocarbons would be related to change in the ratios C_{30}/C_{16} and C_{25}/C_{16} (Hwang, 1998); the oil after the CO_2 experiment is enriched with high carbon number paraffins as indicated by higher values of these ratios.

Table 3-6 Ratio of Intensity of alkane peaks

	Pr/C17	Ph/C18	Pr/Ph	C_{30}/C_{16}	C_{25}/C_{16}
Original crude	.58	.61	.98	.43	.56
CO_2 expt crude	.58	.63	.93	.51	.75

Spectroscopic Techniques

Fourier Transform Infrared Spectroscopy (FTIR)

FTIR spectra were obtained using a Perkin Elmer FTIR Model 100 equipped with a model spectrum II data processing system with a spectral range from 4000 to 400 cm^{-1}. FTIR was used to analyze the SARA fractions from Rangely oil and Phillips oil, and solids from Rangely field (field) and from the CO_2 induced precipitation thermodynamic experiment (laboratory).

Saturate fractions of Rangely oil were obtained after precipitation of the insoluble portions in pentane, hexane or heptane, by column chromatography. The spectra of the saturate fractions consisted of absorption bands arising from methyl and methylene group stretching (3000-2800 cm^{-1}) and bending (1463 and 1377 cm^{-1}) vibrations (Wilt,1998). The three fractions had the similar features (see Figure 3-4 part a).

Aromatic fractions also have similar features among them. The spectra show that close to the methyl and methylene group stretching, there is another band at 3000 – 3100 cm^{-1} that appears as a hump; this band can be assigned to the CH of the aromatic ring. 1454 cm^{-1} and 1377 cm^{-1} are also important peaks in these spectra that correspond to methyl and methylene bending vibrations. The broad peak at 1602 cm^{-1} can be assigned to the aromatic C=C stretch and the peaks at 870, 811 and 748 cm^{-1} can be assigned as the out-of-plane bending modes of 1, 2 and 4 adjacent hydrogens respectively (Andersen, 1997). There are also other bands, such as 1704 cm^{-1} that can be assigned to carbonyl group, and 1033 cm^{-1} that can be assigned either to C-O or C-S bands that occur at the same position. (see Figure 3-4 part b). Part c presents the spectra of the resins that have very strong bands corresponding to methyl and methylene groups stretching and bending vibrations at 3000 to 2800 cm^{-1}, and 1455 and 1377 cm^{-1}. These peaks for resins are stronger than in the case of aromatics, and are more intense for RO-C5-R compared with the other two. The ratio CH2/C=C (Table 3-7) for resins goes from 3.3 to 4.4 and for aromatics is about 1.3.

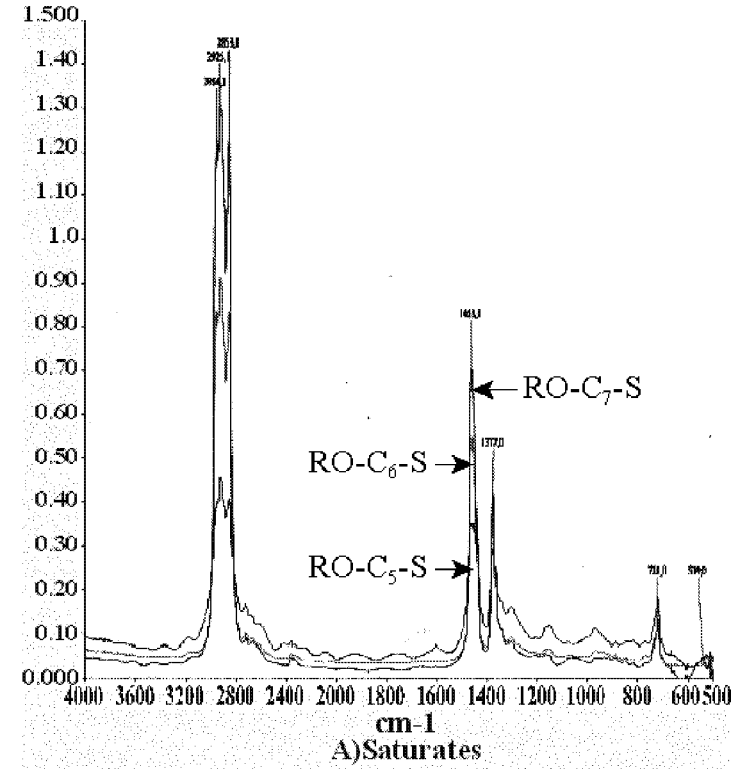

A)Saturates

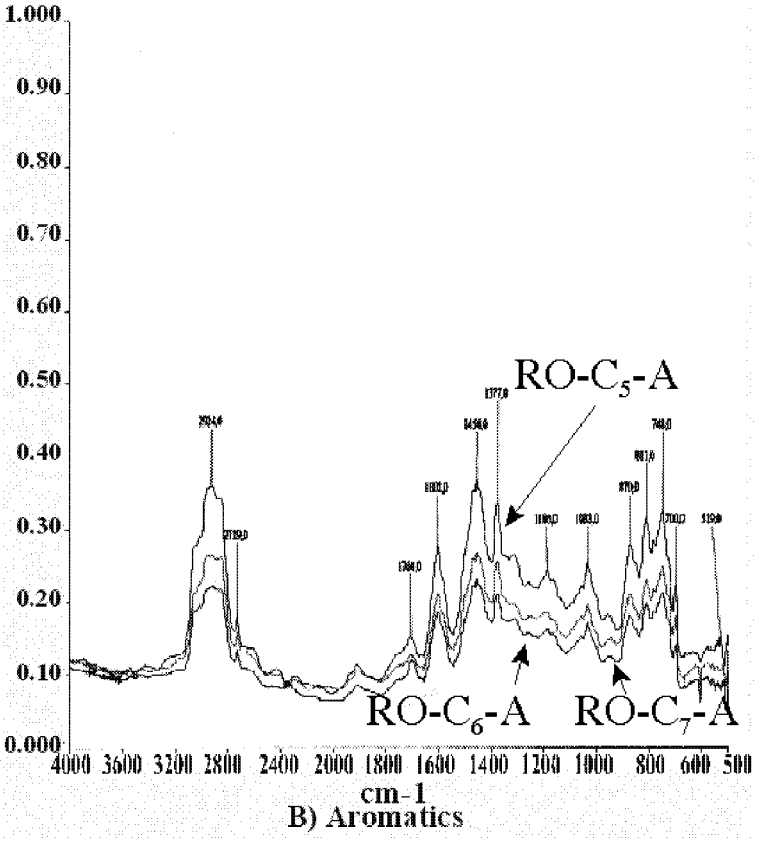

B) Aromatics

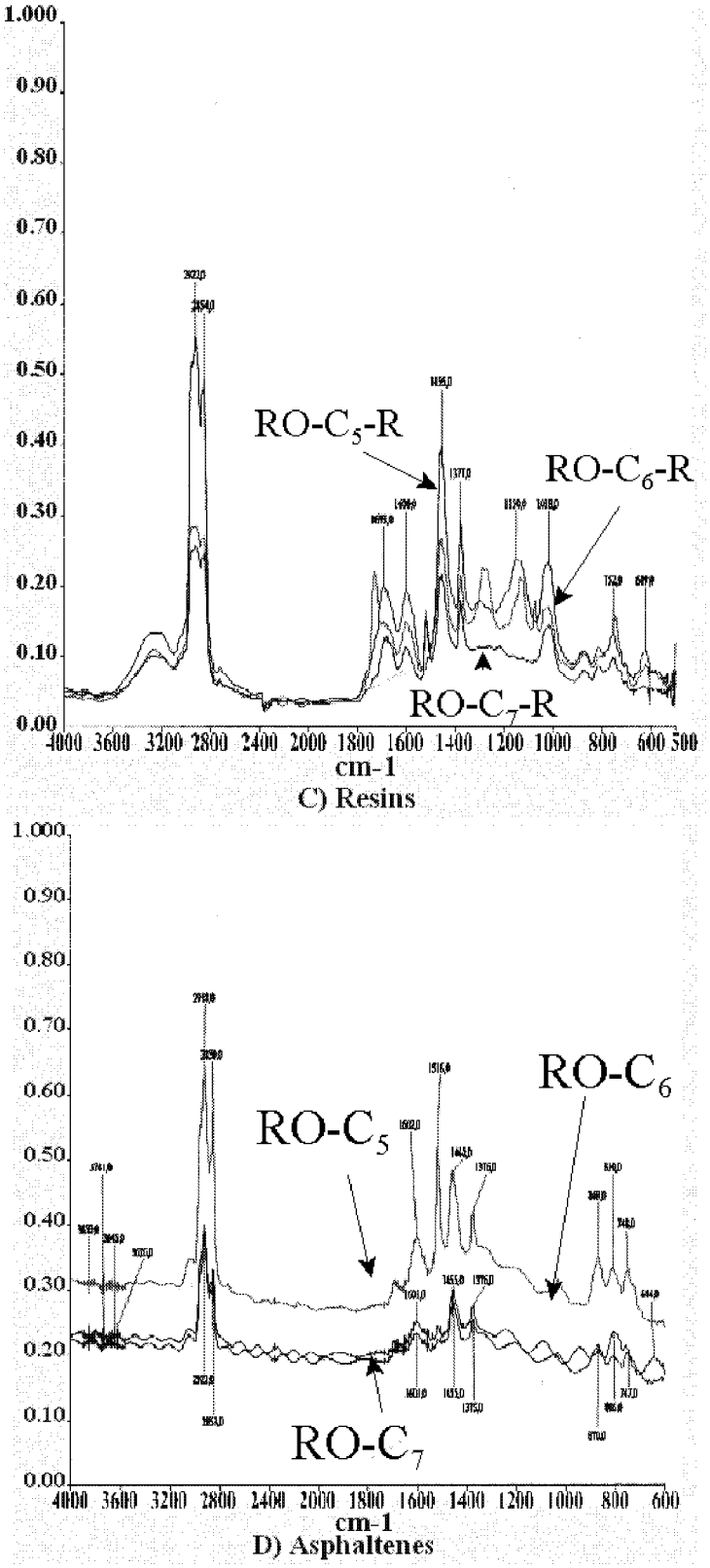

Figure 3-4 FTIR spectra of the SARA fractions obtained using different solvents

Table 3-7 Ratios of intensity of important peaks – FTIR

Samples	CH_2/CH_3	$CH_2/C{=}C$	$C{=}C/C{=}O$
RO-C_5-ARO	~1	1.345	2.94
RO-C_6-ARO	~1	1.324	3.03
RO-C_7-ARO	~1	1.23	3.00
RO-C_5-RES	1.069	4.429	0.931
RO-C_6-RES	1.0	3.346	1.0
RO-C_7-RES	1.022	3.788	0.765
RO-C_5-ASPH	1.39	3.12	2.76
RO-C_6-ASPH	1.426	3.35	5.5
RO-C_7-ASPH	1.526	3.73	4.5
Field	1.095	3.83	1.081
RO-laboratory	1.205	10.11	1.083

Resin spectra also display intense bands at 1693 cm^{-1} and 1018 cm^{-1} that correspond to carbonyl and ether or esters stretching vibrations. A broad absorbance band between 3100 and 3550 cm^{-1} can be assigned to NH and OH stretching, representing the polar nature of the resins. Several peaks in the range between 1050 cm^{-1} and 1350 cm^{-1} are present especially in the resins obtained when the solids are extracted with pentane and hexane; these peaks suggest the presence of various functional groups, corroborating also the polar nature of these samples.

The methyl, methylene and functional groups found on the resins must have attachments to aromatic cores. The presence of aromatics are shown on the peaks at 1600 cm^{-1} and the series of peaks at 870 cm^{-1}, 811 cm^{-1} and 752 cm^{-1}, that correspond to the C=C stretching and the out of plane bending modes. There is also a smooth hump at about 3100 cm^{-1}which is assigned to the CH in the aromatic ring. The relative intensity of the peak at 1600 cm^{-1} to the one at 1693 cm^{-1} is about 1 for the resins, while for aromatics is about 3 (Table 3-7). As expected, the presence of the carbonyl functional group it is much higher in resins than in aromatics. The FTIR technique permits comprehensive characterization of resin fractions because of the presence of functional groups, including oxygen functionalities.

FTIR spectra of asphaltene fractions (insolubles in heptane, hexane, and pentane) show that various functional groups (1693 cm^{-1} and 1018 cm^{-1}), corresponding to polar compounds appear in less intensity than in the resin fractions. The relative intensity of the peak at 1600 cm^{-1} to the one at 1693 cm^{-1} is about 4. This clearly indicates that oxygen functionalities in the resins are quantitatively stronger than in the asphaltenes.

Responses to methyl and methylene groups in comparison to the aromatic C=C is similar among asphaltenes precipitates (3000 – 2800 cm^{-1}, 1462 cm^{-1} and 1376 cm^{-1}). The 1032 cm^{-1} peak is present at about the same intensity in the pentane and heptane insoluble precipitates, and in lower proportion in the hexane insoluble portion. The distinct aromatic bands (3000-3100 cm^{-1}, 1602 cm^{-1}, 869 cm^{-1}, 810 cm^{-1}, and 748 cm^{-1}) are

present in all these fractions (see part d). The bands at 3000 –3100 cm^{-1} form clear peaks in the asphaltene fraction, while for the resins there is only a smooth hump. Aromatics out of plane peaks in the asphaltenes (869 cm^{-1}, 810 cm^{-1} and 748 cm^{-1}) are more intense than in the resins. In Figure 3-5, IR spectrum of the asphaltenes from the Phillips crude is shown. This crude has a higher amount of asphaltenes (11.34% pentane insoluble) compared to the Rangely oil (2.45% pentane insoluble). However, the spectra appear similar to the ones for Rangely oil. There are no important differences among the precipitates from Philips oil obtained with the three different solvents. Pentane insolubles in Phillips oil show higher intensity in peaks related to saturated groups than the other two precipitates. This observation is common for both oils in spite of significant differences in their asphaltene fractions (Figure 3-5 part a). The intensities of the peaks due to the presence of methyl and methylene groups are higher for the precipitates from Rangely oil than for the ones from Phillips oil. The ratio of intensities at 2920 cm^{-1} (-CH_2-) and 1600 cm^{-1} (aromatic) for Rangely oil is 5.2 while the ratio for Phillips oil is 3.6.

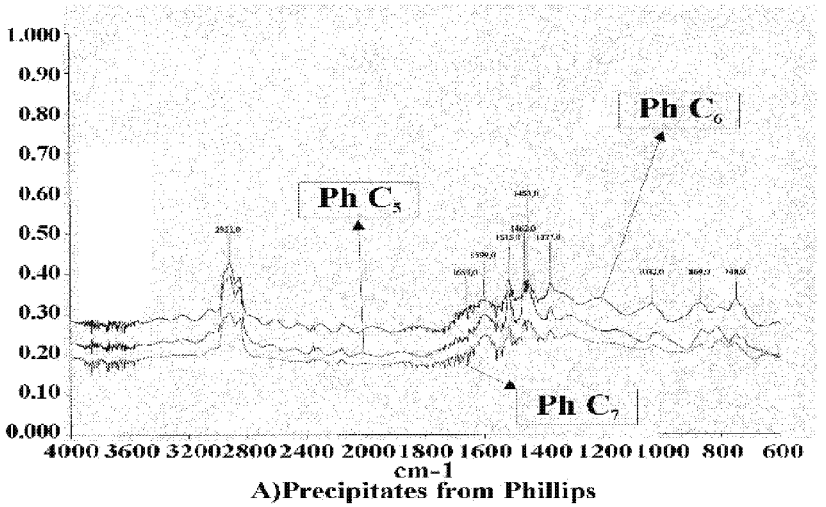

A)Precipitates from Phillips

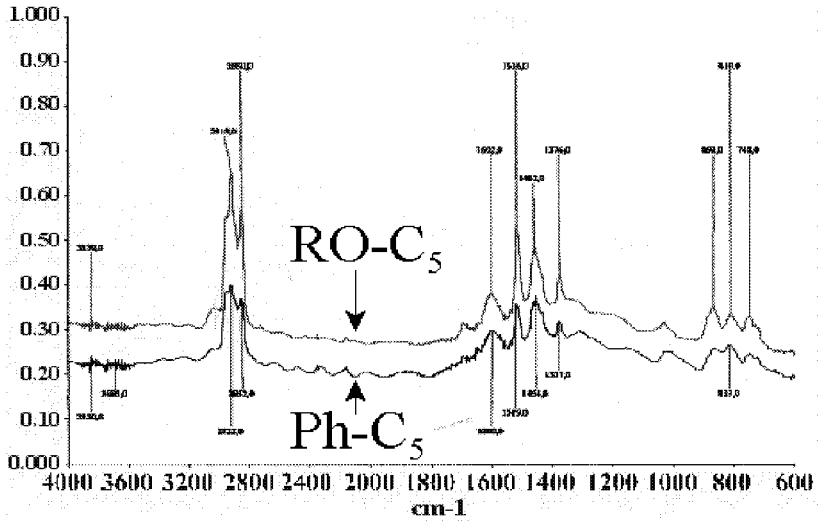

B) C5 Insolubles Phillips vs RO

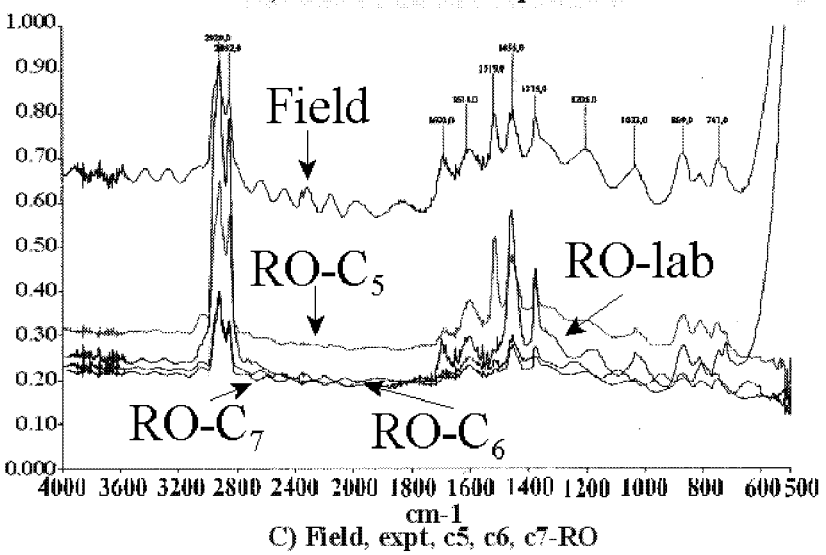

C) Field, expt, c5, c6, c7-RO

Figure 3-5 FTIR - solids

Figure 3-5 part b shows a great similarity between the spectra of pentane insolubles from the two crude oils. The most important feature is the apparent higher content of alkyl chains in the Rangely oil precipitate.

Figure 3-5 part c shows different precipitates obtained from the Rangely oil by different procedures: precipitate from a well in Rangely oil Field, precipitate from CO_2 experiment in the laboratory with 30 mole % CO_2, and paraffin (C_5, C_6, C_7) insolubles in Rangely oil. The presence of methyl and methylene groups is common in all the precipitates. The intensity of these groups is higher for the precipitate from CO_2 experiment possibly due to the presence of occluded oil. Table 3-7 presents CH_2/CH_3 intensity ratio for the different precipitates. These ratios indicate shorter substituted alkyl chains for CO_2 induced precipitates (RO-lab: 1.2 and field: 1.1) compared with paraffinic insolubles in the same oil (from 1.4 to 1.5). Peaks at 1693 cm^{-1} and 1033 cm^{-1} are higher for CO_2 induced precipitates than for paraffinic insoluble precipitates. The relative intensity of peaks at 1600 cm^{-1} and 1693 cm^{-1} for the CO_2 induced precipitates is close to 1, while that for the paraffin insoluble precipitates is about 4. Therefore, the presence of oxygen functionalities is quantitatively higher in the CO_2 induced precipitates. Both CO_2 induced precipitates and pentane insoluble precipitate have similar intensities of the aromatic peak at 1600 cm^{-1}.

From the IR spectra, it can be concluded that the functional groups of solids obtained by using different paraffinic solvents and by CO_2 induced precipitation are very similar. This observation is true in general for significantly different crude oils. Resins from different fractions and from different oils also exhibit remarkably similar features. All of the evidence points to aromatic compounds with a considerable number of alkyl groups, some carbonyl groups and other oxygen functionalities. The main differences are the distributions of the different chemical groups. This is in agreement with a study by Christy (1989) that affirms that apart from the absolute quantities for the various functional groups, all the spectra show similar structural features for kerogen, asphaltenes (described as heptane insolubles) and resins.

Chemical structures of asphaltenes and resins are complex and similar. However, from their IR spectra, it becomes evident that the polar groups in the asphaltene fractions are appreciably lower in intensity than those existing in the resins. It was also found that there are differences between CO_2 induced precipitates and paraffinic insoluble precipitates; the former contained more polar functionalities and shorter substituted alkyl chains.

Chemical Ionization

Chemical Ionization is a soft ionization method in mass spectrometry used to obtain molecular weights of thermally stable volatile compounds. The ion source in this technique is maintained at high pressure with isobutene at 150 eV, and the spectrum shows quasimolecular ions with little fragmentation. This technique requires small quantities (of the order of picograms) of samples. Chemical ionization analyses were performed on insolubles from parafinic solvents of Rangely oil and Phillips oil (Figure 3-6 and Figure 3-7), pentane insolubles of the field sample, and precipitates from thermodynamic experiments (Figure 3-8) and resins from Rangely crude oil (Figure 3-9),

Precipitates were analyzed in a range from 50 to 3000 amu. Table 3-8 presents maximum molecular weights of the ions found in the different samples. The maximum mass increases with the increase of the carbon number of the solvent utilized for the extraction. The maximum ion fragments found on the CO_2 induced precipitates (C_5-field and RO-lab) and heptane insolubles are between 630 and 681 amu. An important peak among the precipitates from Rangely oil using paraffinic solvents is phenanthrene (178).

Table 3-8 Maximum molecular weight of ions

Sample	Molecular weight
RO-C5	399
RO-C6	500.8
RO-C7	647.3
Ph-C5	510.4
Ph-C6	662.6
C5-field	630
RO-lab	680.8

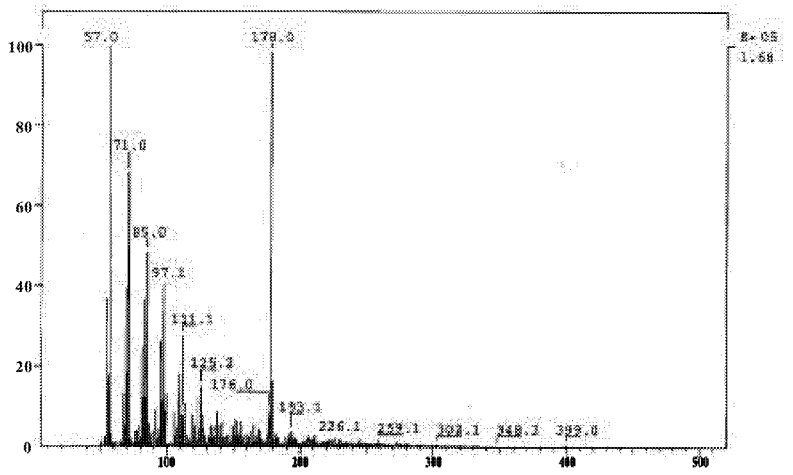

A) RO-C_5

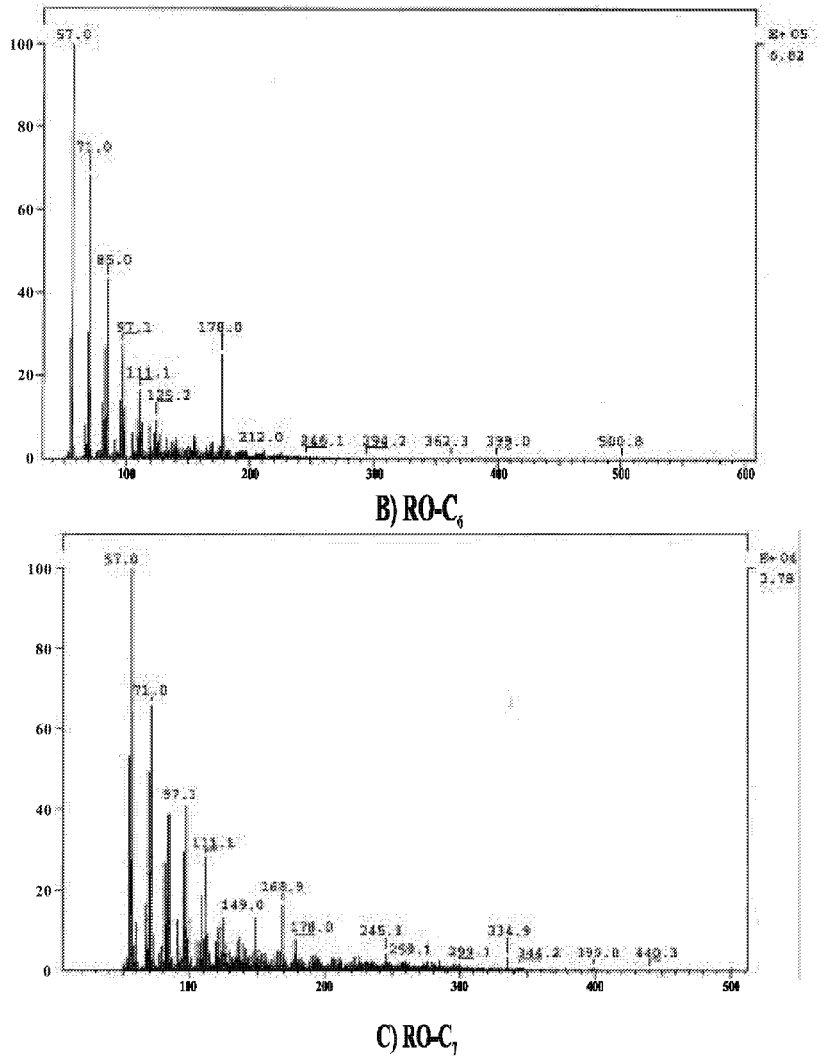

Figure 3-6 Chemical Ionization – Precipitates from Rangely Oil

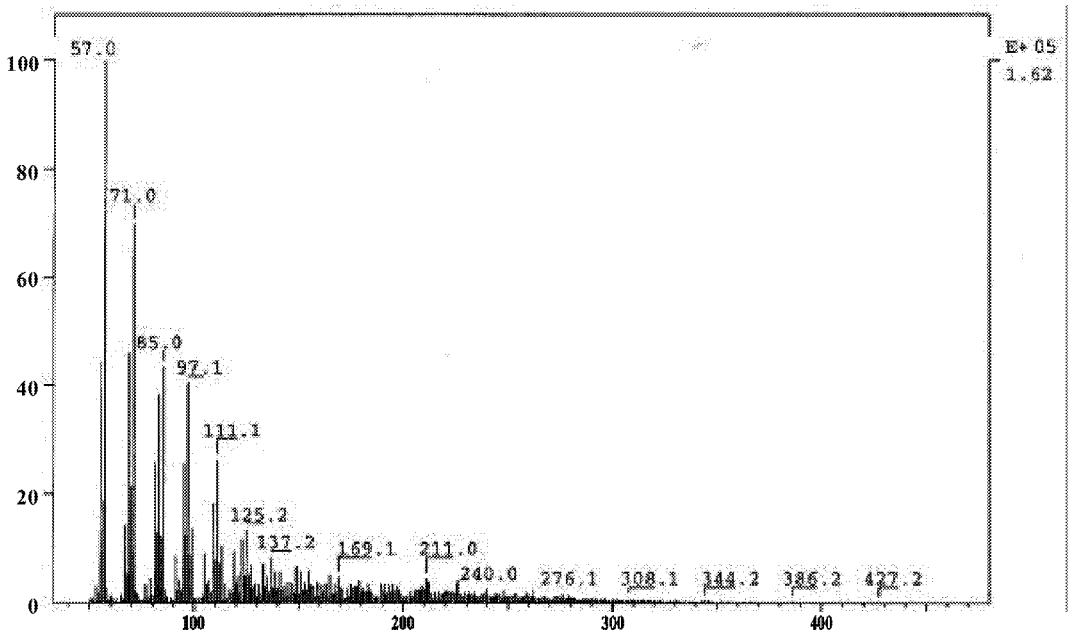

A) PH-C_s

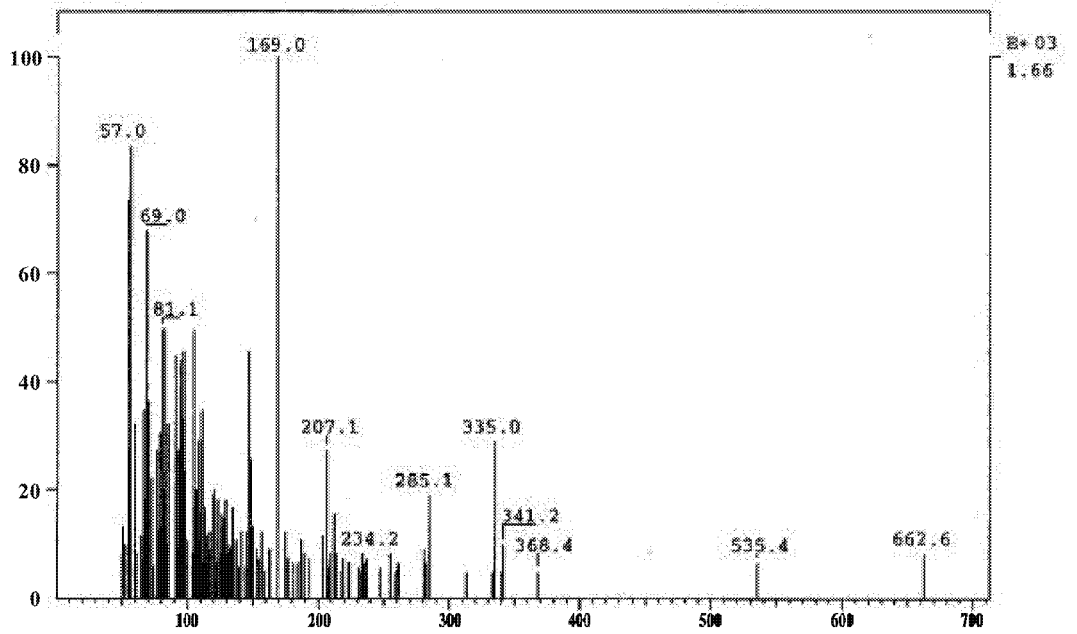

B) PH-C_s

Figure 3-7 Chemical Ionization - Precipitates from Phillips oil

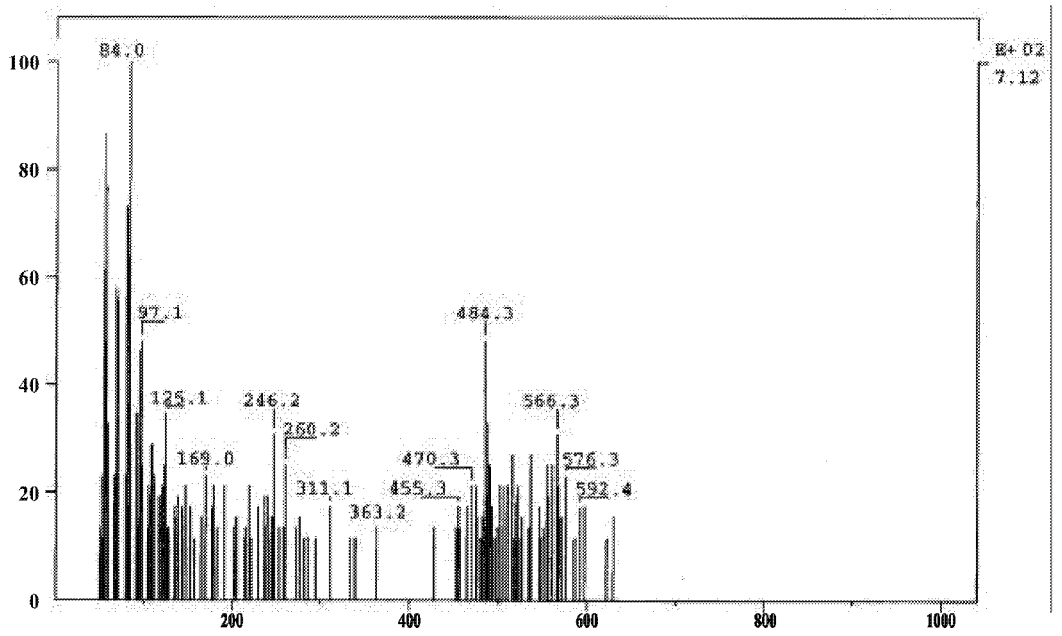

Field

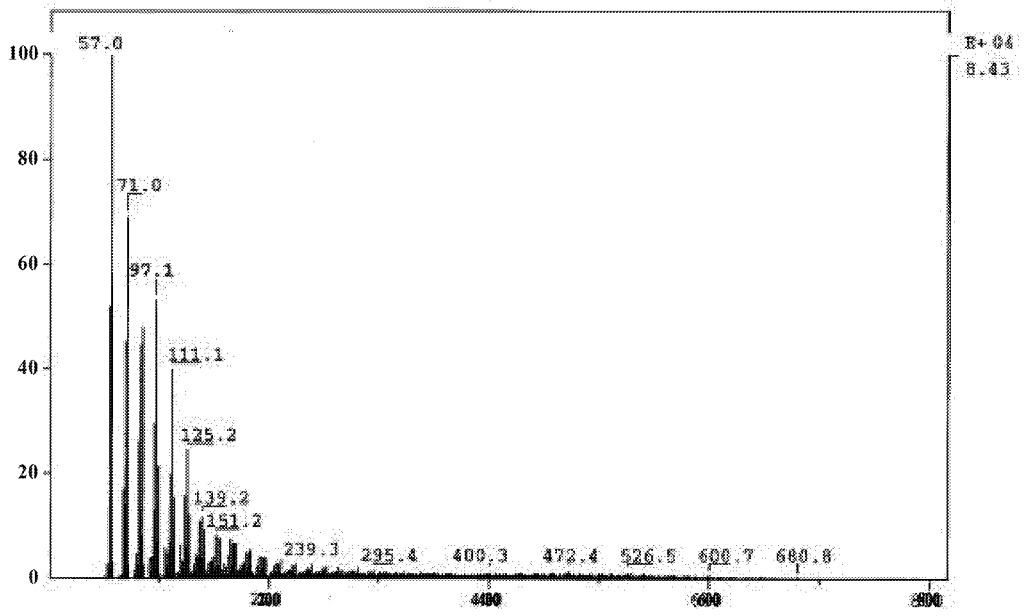

C) Laboratory

Figure 3-8 Chemical Ionization - CO_2 induced precipitates

According to chemical ionization spectra, molecular weights of CO_2 induced precipitates and asphaltenes are below 1000 amu. From Figure 3-6, Figure 3-7, and Figure 3-8 it is important to recognize the high intensity of alkyl ions (57, 85) among the ion fragments.

For the resins, masses from 60 to 1000 amu were examined, and the fragments go from 200 to 850 amu, with a mean molecular weight of about 600 amu. (Figure 3-9).

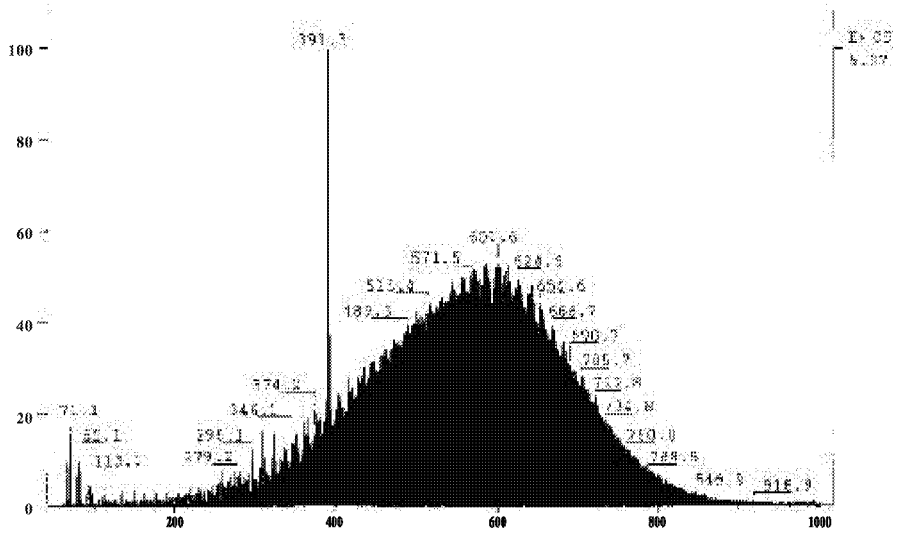

Figure 3-9 Chemical Ionization – Resins from Rangely oil

Surface Techniques of Characterization

Samples of precipitates obtained from Rangely oil and Phillips oil were analyzed for chemical characterization and morphology using x-ray photoelectron spectroscopy (XPS), Time of flight Secondary Ion Mass Spectroscopy (TOF-SIMS), and Scanning Electron Microscopy (SEM). This section discusses the analytical methods used and presents characterization results.

Scanning Electron Microscope (SEM)

Micrographs of the asphaltenes extracted from Rangely oil and Phillips oil by using different solvents pentane, hexane and heptane are shown (Figure 3-10 and Figure 3-11). Precipitates generated in the CO_2 - thermodynamic experiments with the Rangely crude oil, solids from the field and pentane insolubles from the field were also analyzed (Figure 3-12).

The micrographs were obtained with a Hitachi S-3000N Scanning Electron Microscope/EDAX. The surface composition was determined with an energy-dispersive X-ray (EDAX) spectrometer. The samples were mounted by means of a double sided tape and they were gold sputter coated for two minutes at high vacuum. Samples extracted by using solvents were obtained from filtration with a 2-micron filter paper; CO_2 induced precipitate from thermodynamic experiments was generated at high pressure in line filters (2 microns), and field precipitate was a sample obtained from precipitate accumulated in submersible pumps in the Rangely field. The field sample was ground with a mortar. The morphology of all the samples is irregular, and the fractions are amorphous. The C_5-field sample has smaller particles than the field sample

suggesting lesser agglomeration. This must be related to the fact that this is just the pentane insoluble in the field, and it does not include saturates, aromatics from the field sample. The sample that looked the most agglomerated of all the samples is the one from the thermodynamic experiment (RO-lab). This is an expected result because this sample is not washed with solvent. When this sample was analyzed by SARA, the results showed that only 45% of it is pentane insoluble, indicating that it has saturates, naphtenaromatics and resins that can contribute to its appearance like one chunk of solid instead of particles. The EDAX spectra showed that all the surfaces of the solids analyzed consisted mainly of carbon, some gold from the coating, and some oxygen and sulfur. Table 3-9 shows these results, the data were normalized to only carbon, oxygen and sulfur. This technique does not identify hydrogen.

Table 3-9 Quantification of surface by SEM (wt%)

Element	C	O	S
RO-C_5	95.89	2.98	1.13
RO-C_6	93.75	4.64	1.61
RO-C_7	93.71	2.14	4.14
RO-lab	94.26	2.60	3.14
C_5-field	90.61	4.78	4.61
Field	91.83	3.49	4.68

From these data, it can be concluded that when asphaltenes are obtained by precipitation with paraffinic solvents, as the carbon number increases, the concentration of sulfur increases and concentration of carbon decreases. Comparing the CO_2 induced precipitates obtained from the field (field) and the precipitates obtained from thermodynamic experiments the great difference is in the concentration of carbon, the experimental sample having the higher number. This is in agreement with the higher concentration of saturates in experimental samples (32.14 %), compared with field sample (12.71 %). The ratio S/O for both samples is close (1.21 for laboratory and 1.34 for field).

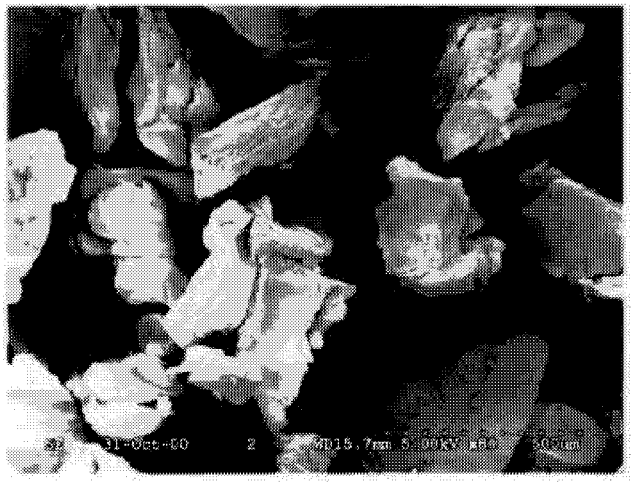

A) RO-C_5

A) RO-C6

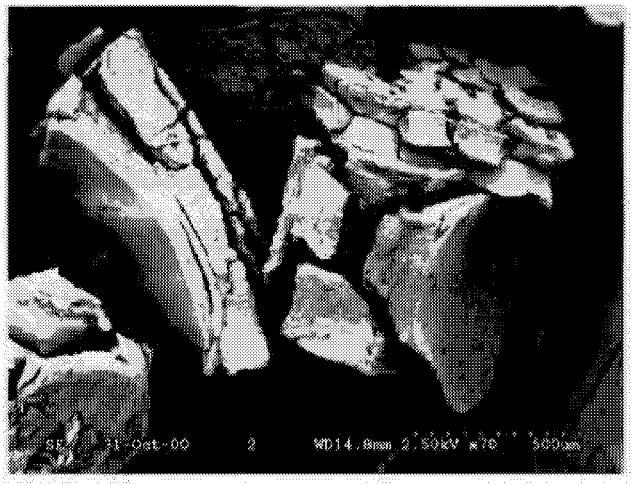

A) RO-C_7

Figure 3-10 SEM - Precipitates from Rangely oil

A) PH-C_5

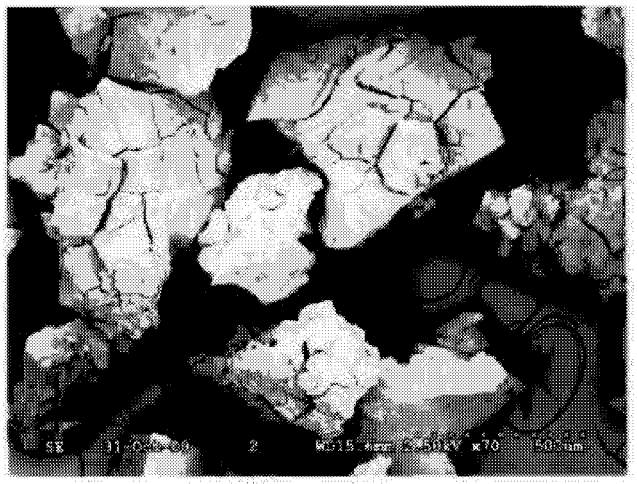

A) PH-C_6

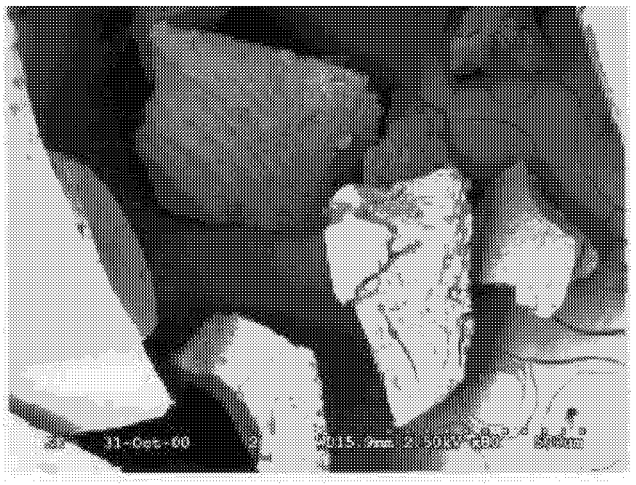

A) PH-C_7

Figure 3-11 SEM – Precipitates from Phillips Oil

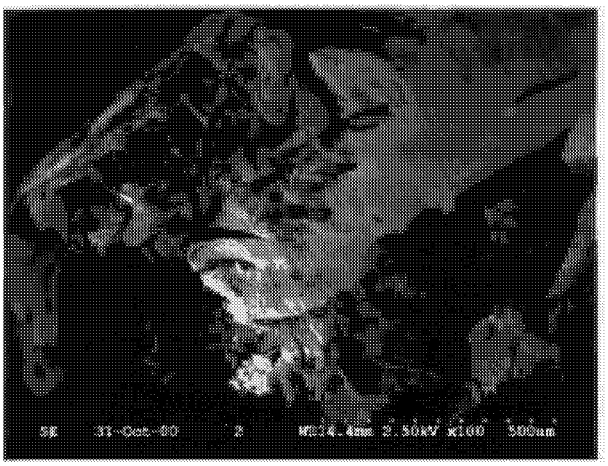

A) Laboratory

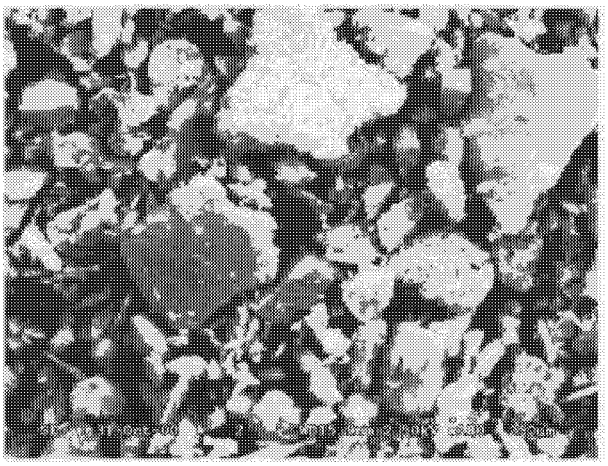

A) C_5-Field

A) Field

Figure 3-12 SEM - CO2 induced precipitates

TOF-SIMS

Samples were prepared by using a very dilute solution of the solid sample in carbon disulfide. A few drops of this solution were placed on silver mica substrates and after solvent evaporation, a film of sample was left on the surface. The SIMS spectra were recorded with Cameca TOF-SIMS 1V equipment using Ga^+ ions (25 Kev) with an electrical current of 3pA for positive ions and 20 pA for negative ions. The total ion dose after recording the positive and negative SIMS spectra was less than $1.2x10^{10}$ ions/cm^2 and $7.5x10^{10}$ ions/cm^2 respectively. The area analyzed in all cases was 500x500 ?m^2 with acquisition time of 10 minutes.

Asphaltenes (pentane and heptane insolubles) and CO_2 induced precipitates from Rangely oil and a CO_2 induced precipitate from Phillips oil were analyzed using TOF-SIMS. Their spectra are in Figure 3-13, Figure 3-14 and Figure 3-15.

The dense nature of the TOF-SIMS spectra required their interpretation to be considered in three areas: end-group effects, maximum molecular weight, and observations about the asphaltene core.

End-Group Effects

End groups are the molecular forms attached to the asphaltene cores. These are quite stable, which is the reason for their highest abundance on the total ion count. The most prominent fragment ions are below a mass of 100, and especially below 50; the more

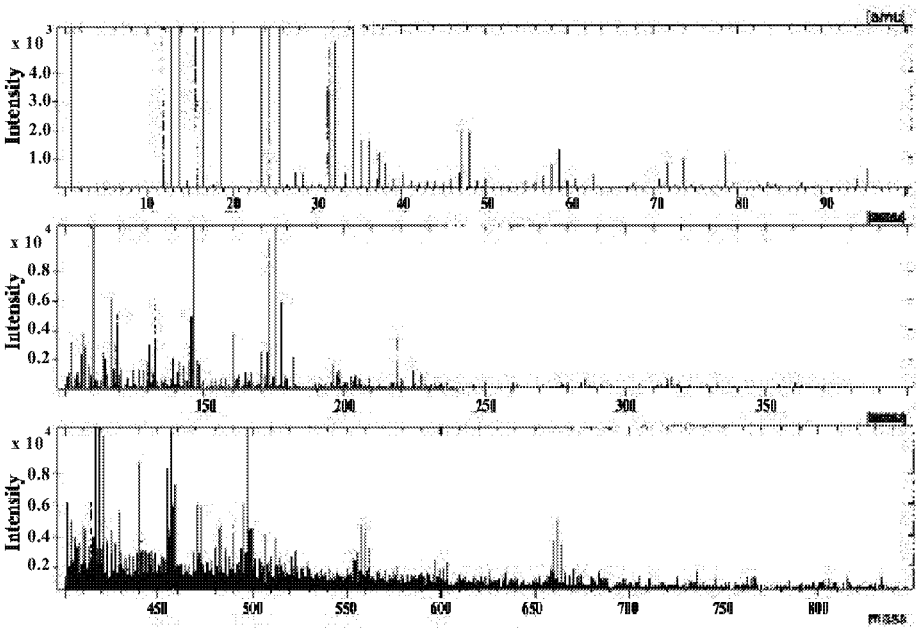

A)C_5-RO Neg.

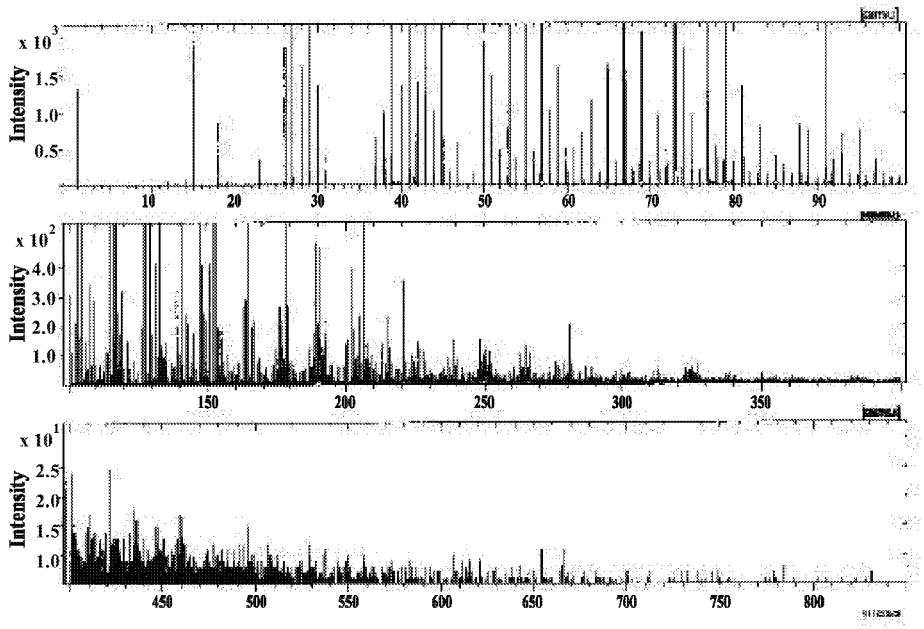

B)C_5-RO Pos.

Figure 3-13 TOF-SIMS – Asphaltenes from Rangely oil

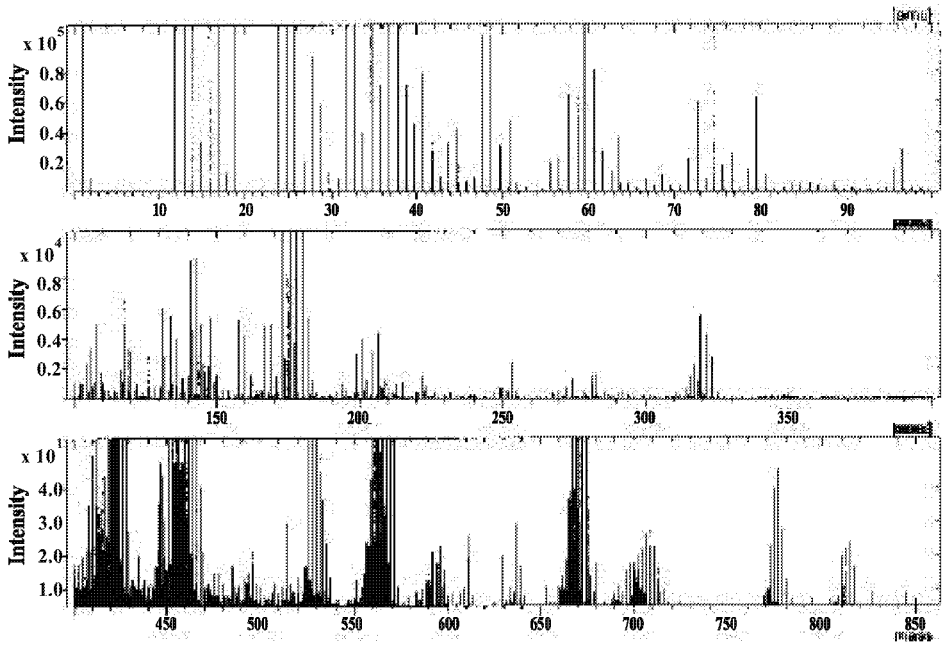

C)C_7-RO Neg.

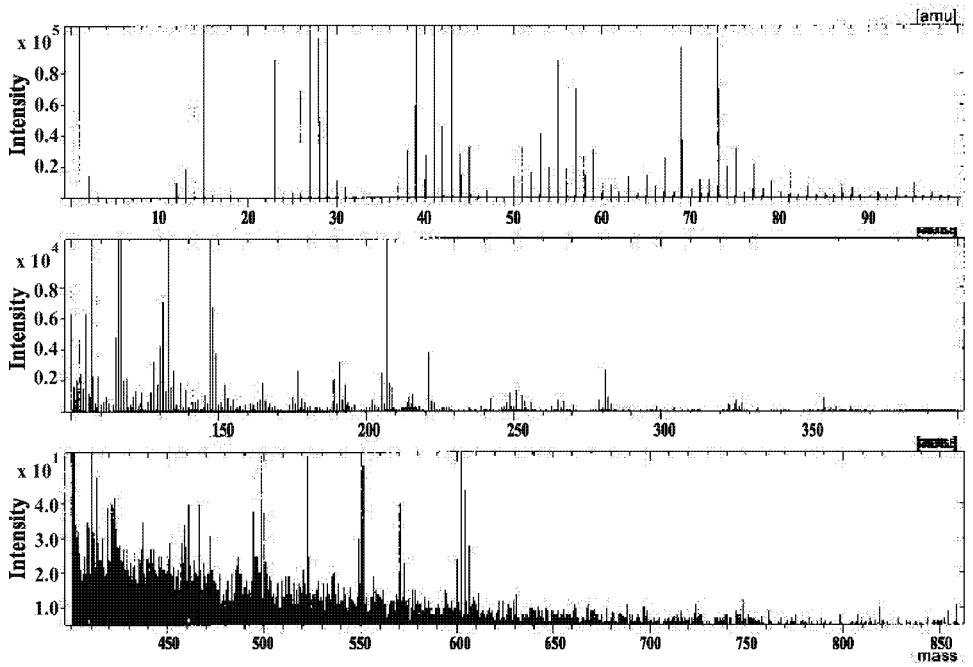

D) C_7-RO Pos.

Figure 3-13 continued

prominent of these ions are the CHx and C_2Hx where x is the number of hydrogens. Table 3-10 presents the intensity of these ions for the different samples. The data on these masses must be related to their aromatic and/or aliphatic nature. In a study of

carbon black surfaces using SIMS, the C_2^-, C_2H^-, and CH_x^+ signals were considered sensitive to the amount of aromatic carbon, aromatic C-H groups and aliphatic C-H groups respectively; when the C_2H^-/C_2^- ratio increases, the ratio of aromatic hydrogen to aromatic carbon increases (Darmstadt, H et al. 1996 Fuel). The ions found in the different samples are analyzed using this concept. The relative intensities of some characteristic negative secondary ions (intensity of C_2^- peak) are presented in Table 3-10. According to Table 3-10 the C_2H^-/C_2^- ratio doesn't change much for the different samples except for the C_5 field sample, which is 1.25 times the other values. This result would mean that the aromatic system of C_5 field precipitate is smaller. This is not conclusive because it could be that there is an aliphatic contribution to the C_2H^- peak, and the difference with other samples is not that great. The CH_y^+/C_2^+ ratios can be related to the fraction of different aliphatic groups (Table 3-11). The ratio CH_3^+/C_2^+ was more intense than the CH^+/C_2^+ ratio and the CH_2^+/C_2^+ ratio. The ratio of CH_3^+/C_2^+ and the ratio of the sum of the three CH_y^+ peaks with respect to the C_2^+ peak increased in the order: C_5 field <field < C_7 nro < Phillips < C_5 ro. Low concentration of aliphatic C-H groups in the C_5 field (? CH_y^+/C_2^+ 20 times less than field) is in agreement with the origin of this sample, pentane precipitate from field, or field without saturates, aromatics, and resins. ? CH_y^+/C_2^+ for C_7-RO is 2 times less than C_5-RO, so there are more aliphatics in C_5-RO.It must be remembered that pentane precipitate from a crude oil is larger than heptane precipitate, so part of this difference is due to aliphatic C-H. The order in intensity for the different samples with respect to the $C_2H_y^+/C_2^+$ ratios and its sum (

Table 3-12) was more or less the same. The most pronounced peaks among these were when y=3-5, which meant that $C_2H_3^+$, $C_2H_4^+$, and $C_2H_5^+$ peaks are due to strongly aliphatic C-H groups.

Maximum molecular weight

The intensity in either positive or negative ion spectra falls rapidly for m/z values higher than about 320. The maximum molecular weight found for the different samples based on the spectra is about 815. In the chemical ionization method, masses up to about 700 were observed. Thus, TOF-SIMS and FIMS consistently suggest that the asphaltene molecular weights are below 1000. Groenzin and Mullins (2000) studied the molecular size and structure of asphaltenes (from various sources using fluorescence depolarization measurements). They reported mean molecular weights of about 750 amu, in complete agreement with the results obtained in this study. Miller et al. (1998) used laser desorption mass spectrometry to analyze Mayan asphaltenes, finding a molecular weight distribution from about 300 to 600 amu with an average molecular weight of about 400. Asphaltene molecular weight values of several thousand amu must be due to the high aggregation of asphaltenes in solution, which usually means that the values reported do not correspond to individual molecules (Andersen & Speight, 1993).

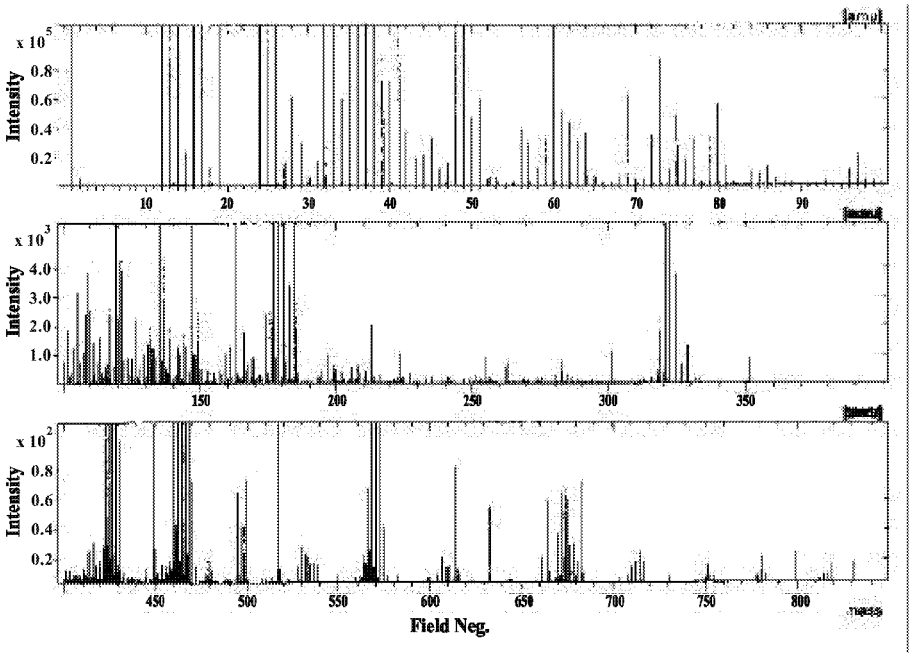

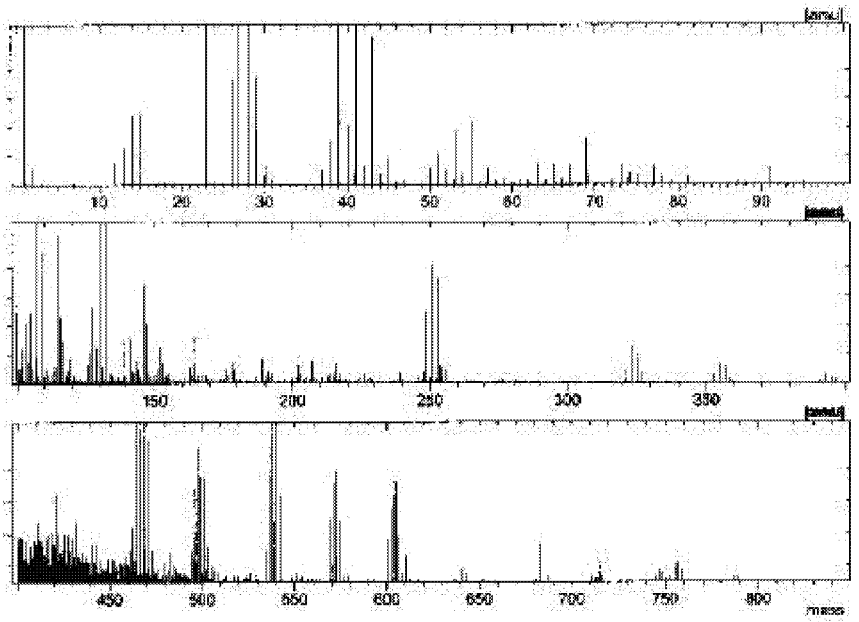

Figure 3-14 TOF_SIMS – CO2 induced precipitates

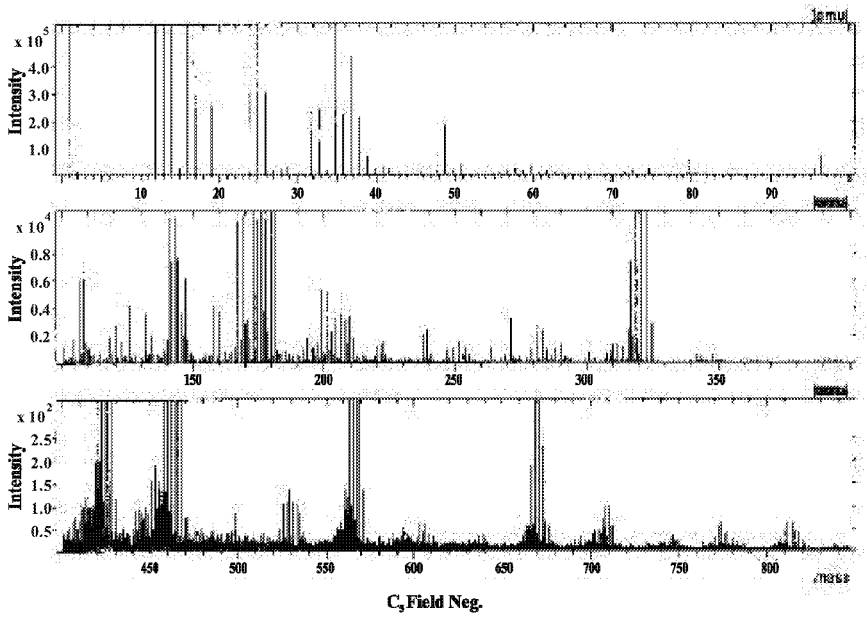

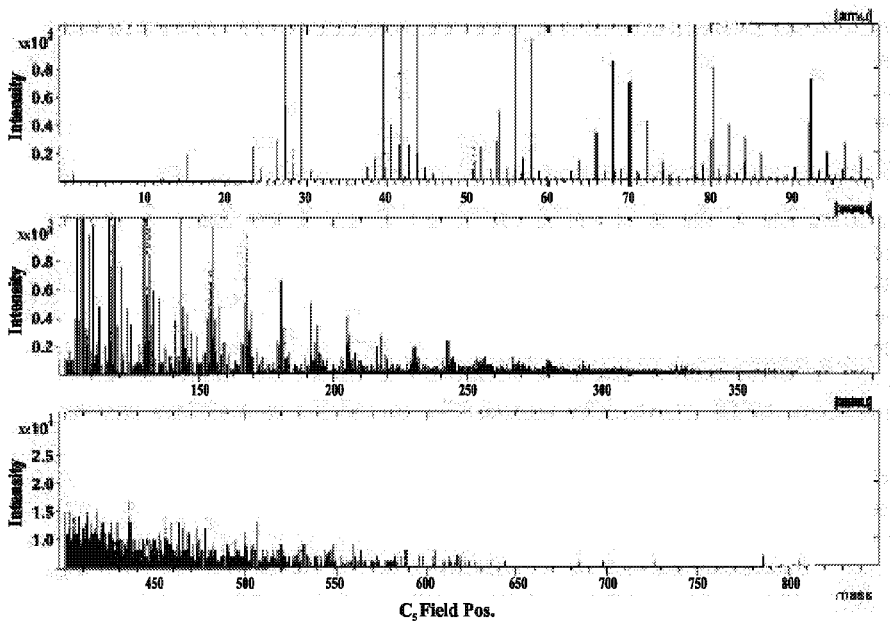

Figure 3-14 **continued**

Observations regarding the asphaltene core

Molecular weights of aromatic ring systems from 3 to 10 rings were calculated, and any of the following fragments were added to the base aromatic system: one or more methyl or alkyl groups, thiophenic, pyrrolic, pyridinic or furanic moeities, or oxygenated functional groups. Various combinations of the above fractions with different aromatic base structures were proposed and molecular weight tables of different possible compounds were constructed (Parra-Ramirez, 2002). Molecular ions from these possible compounds could then be compared to the molecular ions obtained through TOF-SIMS. This exercise is performed and the results are tabulated in Table 3-14. The table shows the possible structure (number of aromatic rings, alkyl and methyl groups, and functional group) for an identified peak. As can be seen from the Table, most compounds, even with complex structures have only 5-7 rings, a finding that is consistent with the observations of Miller(1998) & Groenzin and Mullins(2000). Another notable fact is that the spectral signature does not change significantly when asphaltenes obtained from different solvents and from different processes are analyzed. It is even more remarkable to note that there are more similarities between asphaltenes of two completely different oils than there are differences. For example, all samples had peaks at about 110, 145, 175, 320, 425, 460, 530, 565, 670, and 710 (Negative ion spectra – Figure 3-13, Figure 3-14 and Figure 3-15). Important masses in all the samples are summarized in Table 3-14. Asphaltene molecules could have two aromatic core systems in each molecule, with several benzene rings in each one to obtain a total molecular weight of about 800. SEM-EDAX and XPS analyses report the presence of sulphur and oxygen. Therefore thiophenic and carbonyl moieties in the molecules are taking into account the presence of these elements.

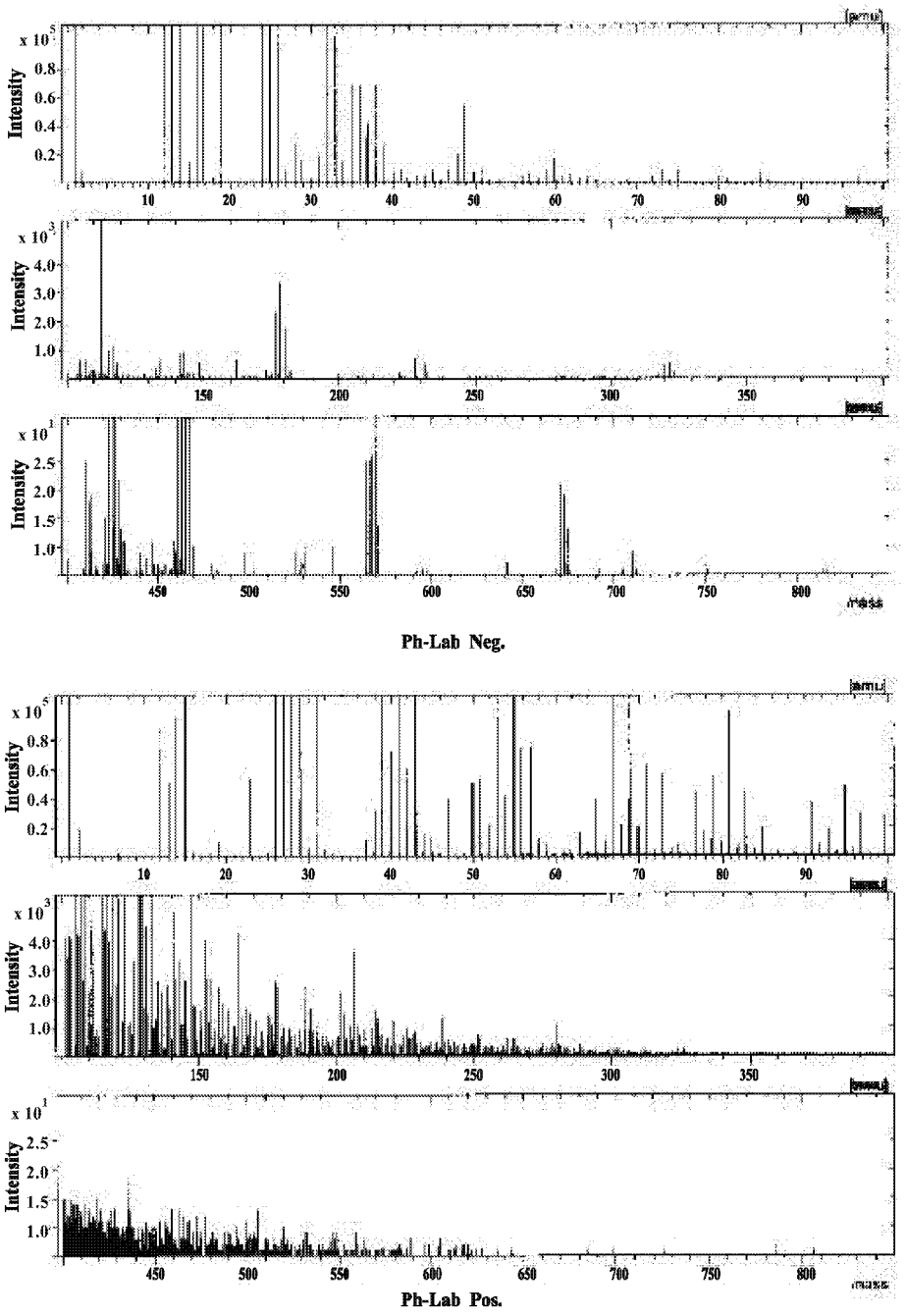

Figure 3-15 Precipitate from Phillips oil

Table 3-10 Negative ions

	C_2H^-/C_2^-	$C_2H_2^-/C_2^-$	CH_2^-/C_2^-	CH^-/C_2^-	C^-/C_2^-	C^-/CH_2^-	CH^-/CH_2^-
C_7-RO	2.86	0.28	0.54	3.65	1.15	2.13	6.74
C_5-RO	2.68	0.20	0.41	3.03	1.11	2.71	7.43

C_5-field	3.43	0.09	1.06	6.01	1.42	1.34	5.65
Phillips	2.72	0.08	1.10	7.32	1.84	1.68	6.68
Field	2.64	0.19	0.28	2.49	0.90	3.20	8.80

Table 3-11 Positive ions CH_y^+/C_2^+

	CH^+/C_2^+	CH_2^+/C_2^+	CH_3^+/C_2^+	?
C_7-RO	14.81	55.91	142.17	212.89
C_5-RO	2.6	4.83	457.30	464.73
C_5-field		0.33	3.26	3.59
Phillips	53.79	114.66	259.92	428.37
Field	9.64	22.49	38.84	70.97

Table 3-12 Positive ions $C_2H_y^+/C_2^+$

	C_2H^+/C_2^+	$C_2H_2^+/C_2^+$	$C_2H_3^+/C_2^+$	$C_2H_4^+/C_2^+$	$C_2H_5^+/C_2^+$	$C_2H_6^+/C_2^+$	?
C_7-RO	2.53	67.23	421.48	351.51	265.06	10.07	1117.88
C_5-RO	5.27	463.63	2000	227.27	2854.54	272.73	5823.44
C_5-field	0	5.50	38.65	4.23	48.84	1.48	98.7
Phillips	5.42	157.8	1183.99	179.04	767.50	17.32	2311.07
Field	2.05	27.93	113.69	71.75	46.16	6.93	268.51

Table 3-13 Ions identified in TOF-SIMS spectra

Mass	Alkyl groups	Methyl groups	Moiety	aromatic Rings
97	1	1	-	1*
105	1	1	-	1
141	1	-	-	2
178	-	-	-	3
205	2	-	-	3
254	1	-	Pyrrolic	4
279	2	-	-	5
319	3	-	-	5
321	1	-	Thiophenic	5
350	3	-	Thiophenic	5
364	4	-	Thiophenic, C=O	5
390	4	-	Thiophenic, C=O	5
420	3	-	Pyridinic	6
424	-	1	Thiophenic	7
426	4	-	Thiophenic, C=O	7
454	3	1	Thiophenic, C=O	6
466	3	-	Thiophenic, pyridinic C=O	6
565	3	-	Thiophenic, furanic	8

?? cyclic, not aromatic

Table 3-14 Important masses for different samples

Sample	Mass (m/z)
C_5-field	110, 145, 175, 200, 250, 320, 425, 460, 530, 565, 605, 670, 710, 748, 770, 815
Field	110, 120, 135, 145, 175, 200, 250, 320, 425, 460, 530, 565, 605, 670, 710, 748, 780, 815
C_7-RO	110, 145, 175, 200, 280, 320, 425, 460, 530, 565, 595, 670, 710, 775, 815
C_5-RO	110, 145, 175, 200, 320, 425, 455,465, 500, 560, 600, 670, 765
Ph	110, 145, 175, 250, 320, 425, 460, 530, 565, 595, 670, 710, 748

4. Thermodynamic Modeling

Martha Parra Ramirez performed this work with the help of Duan Schici. Results and discussion are excerpted from her Ph. D. dissertation. More details appear in her Ph. D. dissertation (Parra, 2002).

In this work, two molecular thermodynamic models of asphaltene precipitation are used. The first approach is due to Hirschberg et al. (1984) and Burke et al. (1990). Asphaltenes are considered as mono-dispersed polymeric molecules dissolved in the crude oil in this model. The other model used was proposed by Nghiem et al. (1993), and the precipitated asphaltenes were modeled as pure dense phase. In this model the heaviest component was split into two components: a non-precipitating component and a precipitating component.

It is important to accurately characterize and describe the mechanisms involved in asphaltene flocculation and precipitation for the development of realistic theoretical models. Asphaltene molecules are surrounded by resins that act as peptizing agents; that is, the resins maintain the asphaltenes in a colloidal dispersion (as opposed to a solution). The resins are typically composed of a highly polar end group, which often contains heteroatoms such as oxygen, sulphur and nitrogen, as well as long, non-polar paraffinic groups. The resins are attracted to the asphaltene micelles through their end group. This attraction is a result of hydrogen bonding through the heteroatoms and dipole-dipole interactions arising from the high polarities of the resin and asphaltene molecules. The paraffinic component of the resin molecule acts as a tail making the transition to the relatively non-polar bulk of the oil where individual molecules also exist in true solution. This equilibrium is disturbed when vastly differing molecules are introduced into the mixture. Normal alkane liquids (such as pentane or hexane) are often added to crude oils in an attempt to reduce heavy oil viscosities. The result of this introduction is an alteration in the overall characteristics of the crude oil making it lighter. In response, resin molecules desorb from the surface of the asphaltenes in an attempt to re-establish the thermodynamic equilibrium that existed in the oil. This desorption of peptizing resins forces the asphaltene micelles to agglomerate in order to reduce their overall surface free energy. If sufficient quantities of the particular solvent are added to the oils, the asphaltene molecules aggregate to such an extent that the particles overcome the Brownian forces of suspension and begin to precipitate. It is obvious from this description that the quantity and type of solvent added to the crude oil is crucial to the amount and characteristics of the asphaltenes deposited.

In general, any chemical, mechanical or electrical disturbance which depeptizes the asphaltene micelles can lead to the precipitation of asphaltenes from the crude oil-asphaltene suspension.

Pure Dense Thermodynamic Model

The precipitated asphaltene is represented as a pure dense phase in this model. This phase is the asphalt phase. Computer Modelling Group (CMG) has a program named WinProp. WinProp is CMG's equation of state multiphase equilibrium and properties determination program, and one of its modules is asphaltene precipitation modelling

using the pure dense phase thermodynamic model. This program was used to study asphaltene precipitation with this model.

The fugacity of asphaltene in the asphalt phase is:

$$\ln f_a - \ln f_a^* = \frac{v_a (p - p^*)}{RT}$$

where f_a and f_a^* are the fugacities of pure asphaltene at pressures p and p* respectively, v_a is the molar volume of pure asphaltene, R is the universal gas constant and T is the temperature.

An important step in modeling asphaltene precipitation with this model is the characterization of the solid forming components, both in solution and in the solid phase. The heaviest component is split into two components: a non-precipitating component and a precipitating component. The non-precipitating component can be related to resins, asphaltene/resin micelles that will not dissociate, and heavy paraffins. The critical properties and acentric factors, are identical for both components but their interaction coefficients with the light components are different. The precipitating component has larger interaction coefficients with the light components. Larger interaction coefficients cause the precipitation of the asphalt phase when solvent is added (CMG, 1999).

A description of the equations, the multiphase flash calculation algorithm and stability test are presented by Nghiem et al. (1993). The calculation procedure using the pure dense model with the CMG program is shown in a block diagram in

Figure 4-1.

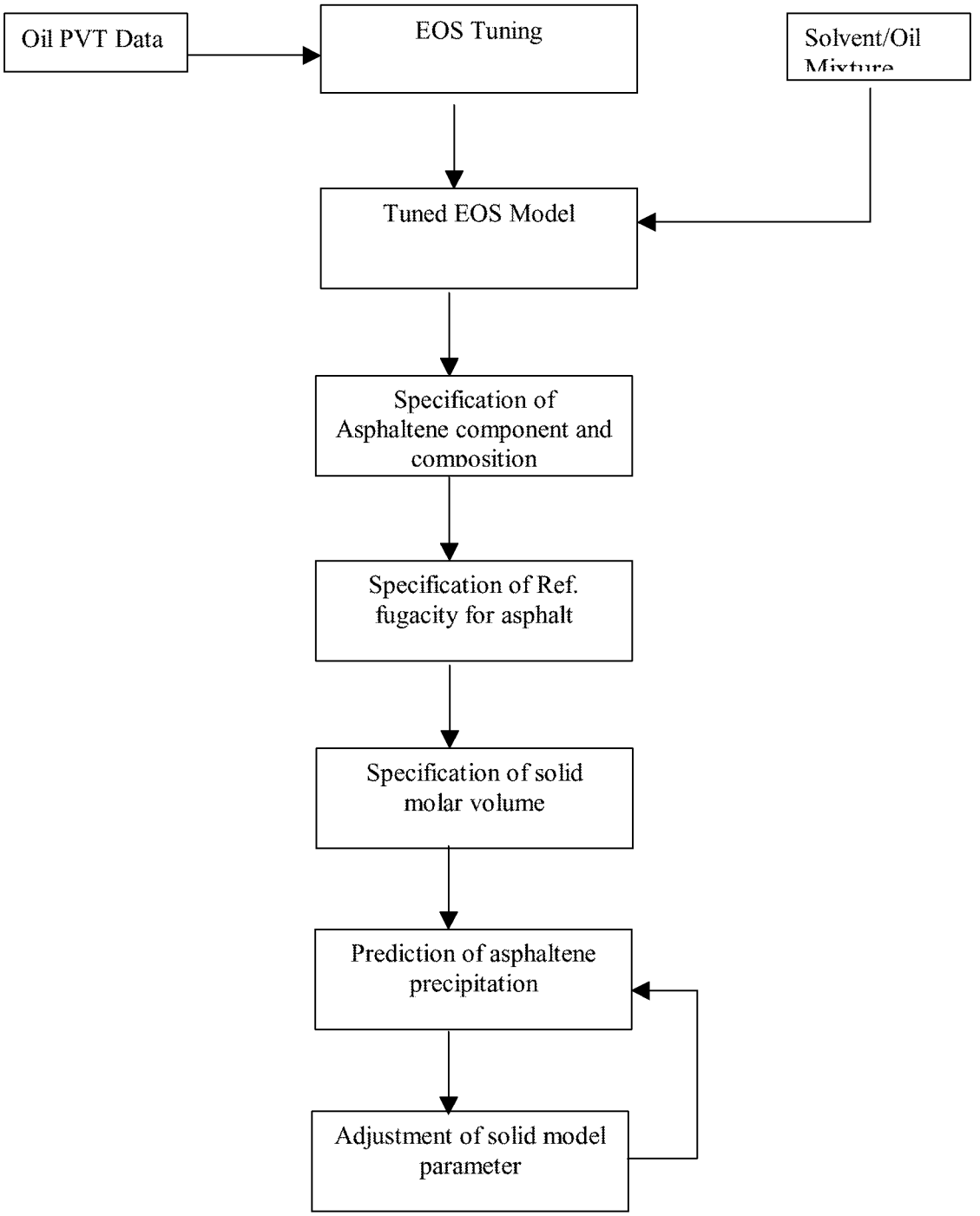

Figure 4-1 Calculation Flow Diagram for the Dense Phase Thermodynamic Model

Homogeneous Molecular Thermodynamic Model

This approach is based on the Flory-Huggins polymer solution theory. The crude oil is treated as a mixture of two liquid phases. The first phase is pure asphaltene liquid phase

$$?_A ? \exp\left[\frac{V_A}{V_L}\left(1 ? \frac{V_L}{V_A} ? \frac{V_L}{RT}\right)(?_A ? ?_L)^2\right]$$

that act as a solute and the second phase consists of the remaining components of the crude oil which acts as a solvent. The asphaltene volume fraction soluble in the crude is given by the following equation:

Therefore, the difference between the maximum amount (in weight fraction) of asphaltene W_m that is measured in an experiment and what is predicted by the above equation yields the amount of the precipitated solid.

$$W_A ? (W_m ? ?_A) ? 100\%$$

The molar volume (V_A) and solubility parameter ($?_A$) of the asphaltene are evaluated by fitting the model with the experimental data. The molar volume (V_L) and solubility parameter of liquid phase ($?_L$) are calculated from Peng-Robinson EOS.

The polynomial form of Peng-Robinson EOS is given by the following equation (in terms of compressibility factor):

$$Z^3 ? (1 ? B)Z^2 ? (A ? 3B^2 ? B)Z ? (AB ? B^2 ? B^3) ? 0$$

Where

$$A ? \frac{a_L P}{(RT)^2} \qquad B ? \frac{b_L P}{RT}$$

$$a_L ? ? ? x_i x_j a_{ij}$$

$$a_{ij} ? (1 ? ?_{ij})\sqrt{a_i a_j}$$

$$a_i ? 0.45724\frac{R^2 {Tc_i}^2}{{Pc_i}^2} ?_i$$

$$?_i ? 1 ? (0.37464 ? 1.54226?_i ? 0.26992?_i^2)(1 ? \sqrt{\frac{Tc_i}{T}})$$

Parameters a_L and b_L are determined as follows:

And

$$b_L ? ? ? x_i b_i$$

$$b_i ? 0.0778\frac{RTc_i}{Pc_i}$$

Z_L is first calculated by solving the cubic equation; then V_L is calculated by:

$$V_L = \frac{Z_L RT}{P}$$

In regular solution theory, the solubility parameter is defined as:

$$\delta_L = \left(\frac{\Delta U_L^V}{V_L} \right)^{1/2}$$

In order to develop an expression for this parameter we start with the expression for the internal energy of a fluid.

$$dU = TdS - PdV$$

Dividing each term by dV and substituting the Maxwell relation $(\partial S/\partial V)_T=(\partial P/\partial T)_V$ yields:

$$\left.\frac{\partial U}{\partial V}\right|_T = T\left.\frac{\partial P}{\partial T}\right|_V - P$$

Taking the pressure derivative of the Peng-Robinson equation with respect to temperature at constant volume,

$$\left.\frac{\partial U}{\partial V}\right|_T = \frac{a_L - T\frac{da_L}{dT}}{V_L(V_L + b_L\sqrt{2} - 1)(V_L - b_L\sqrt{2} - 1)}$$

Integrating the above equation by parts,

$$\Delta U_L^V = \left(\frac{a_L - T\frac{da_L}{dT}}{2\sqrt{2}b_L} \right) \ln\left(\frac{V_L - (1 - \sqrt{2})b_L}{V_L - (1 + \sqrt{2})b_L} \right)$$

Then

$$\delta_L^2 = \left(\frac{a_L - T\frac{da_L}{dT}}{2\sqrt{2}b_L V_L} \right) \ln\left(\frac{V_L - (1 - \sqrt{2})b_L}{V_L - (1 + \sqrt{2})b_L} \right)$$

Where

$$\frac{da_L}{dT} = \sum_i \sum_j \left[x_i x_j \left[1 - k_{ij} \right] \left[a_i a_j Tc_i Tc_j \right]^{1/2} \left[1 + K_j \left[1 + \sqrt{Tr_j} \right] - 0.5 K_i \sqrt{Tr_i} \right] \right.$$

$$\left. \left[1 + K_i \left[1 + \sqrt{Tr_i} \right] - 0.5 K_j \sqrt{Tr_j} \right] \right]$$

$$Tr_i = \frac{T}{Tc_i}$$

$$K_i = 0.37464 + 1.54226 \omega_i - 0.26992 \omega_i^2$$

The calculation procedure using the homogeneous thermodynamic model is shown in a block diagram in

Figure 4-2.

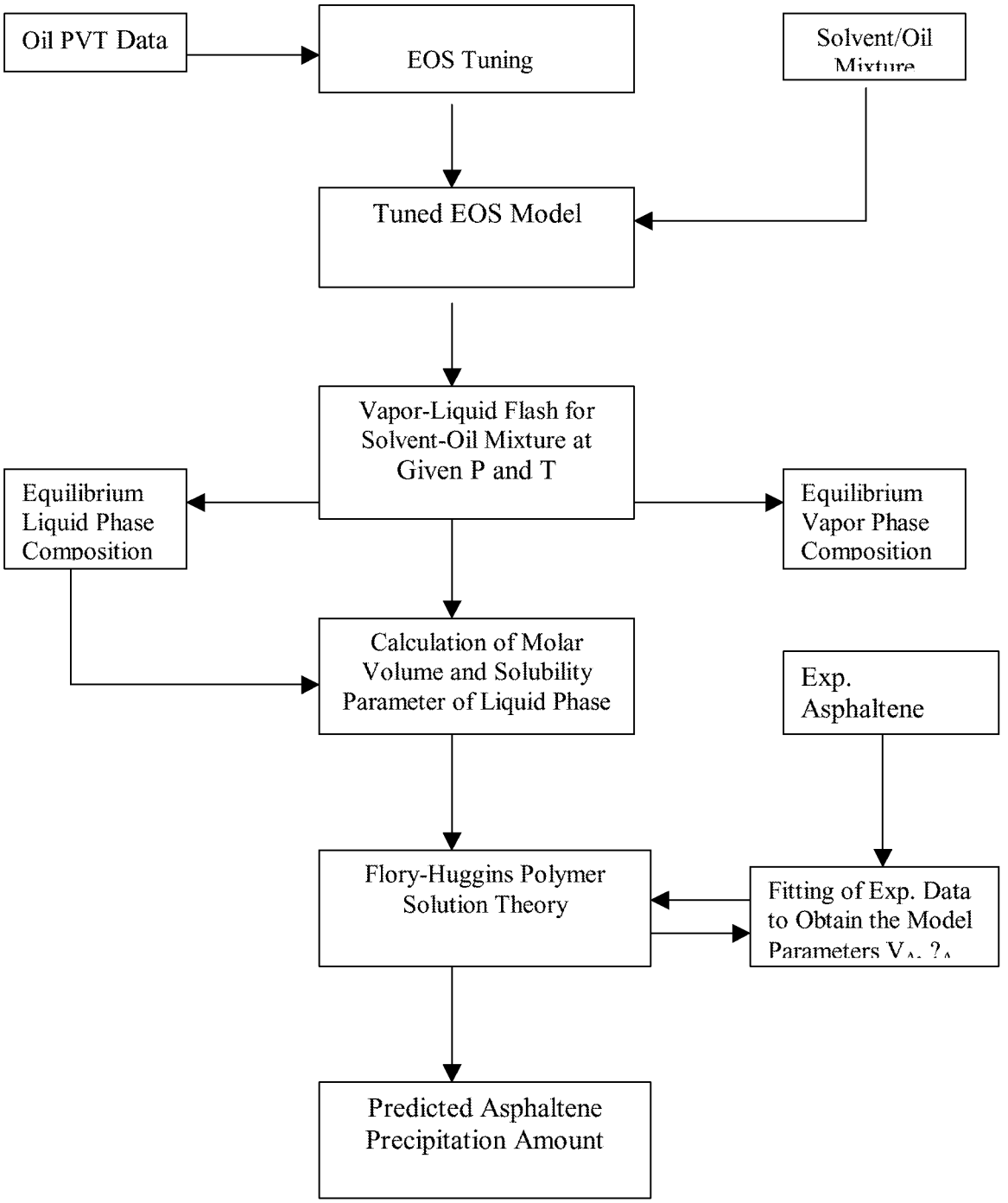

Figure 4-2 Flow Diagram of homogeneous molecular thermodynamic model

Results and Discussion

The Rangely crude oil was described using a large number of components. It was necessary to lump the components into pseudo-components before an equation of state could be used efficiently. Table 4-1 and Table 4-2 show the composition and properties of the pseudocomponents of the dead oil, and the live oil respectively. Table 4-3 shows the composition of the simulated multiple contact crude, which is a mixture of the live oil and a specially prepared light cut (out of the Rangely crude oil). Eighty-five percent of the light cut was below C15. Dead oil was lumped from 43 components into 8 hypothetical components and live oil was lumped from 46 components into 12 pseudocomponents, with the lighter components remaining unchanged. The pseudocomponents were determined using the CMG WinProp Program.

Table 4-1 Composition and Properties of Rangely dead oil

Pseudocomponents	Composition Mole%	Tc °K	Pc Atm	Acentric factor
HYPO 1	19.599	500.6	32.47	0.27288
HYPO 2	27.541	616.7	25.39	0.42768
HYPO 3	20.280	703.9	19.10	0.61113
HYPO 4	13.924	776.6	14.76	0.80232
HYPO 5	8.999	839.5	11.59	0.98706
HYPO 6	5.467	895.8	9.27	1.14787
HYPO 7	3.350	966.4	7.71	1.2847
HYPO 8	0.840	1065.7	6.15	1.42353

Rangely live oil was lumped from 43 components into 11 hypothetical components.

Table 4-2 Composition and Properties of Rangely live oil

Pseudocomponents	Composition Mole%	Tc °K	Pc Atm	Acentric factor
C1	23.110	190.6	45.4	0.225
C2	0.941	305.4	48.2	0.098
C3	1.317	369.8	41.9	0.152
C5	6.224	469.6	33.3	0.251
C6	5.233	507.5	32.46	0.275
C7	2.879	543.3	30.97	0.3083
FC8-FC12	22.701	620.28	25.09	0.4344
FC13-FC17	15.200	714.433	18.45	0.6368
FC18-FC25	11.680	794.19	13.82	0.8525
FC26-FC30	4.064	856.18	10.83	1.036
FC31-FC40	4.141	904.11	8.98	1.1716
FC41+	2.5115	1067.85	4.09	1.6191

Table 4-4and Table 4-5 gives the interaction coefficients among the components for dead oil and live oil respectively.

Table 4-3 Simulated multiple contact crude composition

Psedocomponents	Composition Mole%
C1	15.418
C2	0.631
C3	0.896
C5	4.069
C6	9.770
C7	3.490
FC8-FC12	31.379
FC13-FC17	17.801
FC18-FC25	9.094
FC26-FC30	2.771
FC31-FC40	2.762
FC41+	1.919

Table 4-4 Interaction coefficients for dead oil

	CO_2	Hypo1	hypo2	hypo3	hypo4	Hypo5	Hypo6	hypo7	hypo8
CO_2	zero								
hypo1	0.15	Zero							
hypo2	0.15	0.002924	zero						
hypo3	0.15	0.010142	0.002203	zero					
hypo4	0.15	0.019482	0.007441	0.001561	zero				
hypo5	0.15	0.027884	0.013022	0.00457	0.000794	zero			
hypo6	0.15	0.037277	0.019799	0.00893	0.00305	0.000735	Zero		
hypo7	0.15	0.046419	0.026763	0.013855	0.006181	0.002558	0.000553	zero	
hypo8	0.15	0.055337	0.033812	0.019136	0.009891	0.005114	0.001981	0.000442	zero

Table 4-5 Interaction coefficients for live oil

	CO_2	C_1	C_2	C_3	C_5	C_6	C_7	C_8-C_{12}	C_{13}-C_{17}	C_{18}-C_{25}	C_{26}-C_{30}	C_{31}-C_{40}	C_{41}+
CO_2	Zero												
C_1	0.103	zero											
C_2	0.13	0.0027	Zero										
C_3	0.135	0.0085	0.0017	zero									
C_5	0.125	0.0206	0.0086	0.0027	zero								
C_6	0.15	0.0253	0.0117	0.0046	0.0003	Zero							
C_7	0.15	0.0296	0.0147	0.0066	0.0008	0.0002	zero						
C_8-C_{12}	0.15	0.0441	0.0256	0.0145	0.0047	0.0028	0.0016	zero					
C_{13}-C_{17}	0.15	0.0662	0.0435	0.0287	0.0141	0.0106	0.0081	0.0025	zero				
C_{18}-C_{25}	0.15	0.0876	0.0617	0.0442	0.0256	0.0209	0.0173	0.0086	0.0018	zero			
C_{26}-C_{30}	0.15	0.1025	0.0748	0.0556	0.0348	0.0293	0.0251	0.0143	0.0048	0.0007	zero		
C_{31}-C_{40}	0.15	0.1162	0.0870	0.0665	0.0437	0.0376	0.0328	0.0204	0.0087	0.0026	0.0006	zero	
C_{41}+	0.15	0.1760	0.1421	0.1172	0.0878	0.0795	0.0728	0.0543	0.0343	0.0208	0.0138	0.009	zero

Pure Dense Phase Model Results

The steps required to develop a precipitation model are: fluid characterization, regression on fluid PVT, specification of solid model parameters, and prediction of precipitation behavior.

The parameters that control the behavior in the solid model are the solid molar volume and the interaction parameter between the precipitating component and the light ends of the oil. Increasing the solid molar volume increases the maximum amount of precipitation at the saturation pressure. Increasing the interaction parameter with the light ends will force the asphaltene to redissolve at lower pressures. Higher intereaction coefficients make the precipitating component more incompatible with the light components.

The two parameters are optimized for each system and are the same for the different solvent-oil mixtures. The optimized parameters for live oil and simulated multiple contact mixture are compared in Table 4-6. Figure 4-3 and Figure 4-4 give the comparison of experimental and calculated amount of precipitated asphaltene for both cases.

Table 4-6 Pure Dense Phase Model –Optimized Parameters

Parameters	Live Oil	Simulated Multiple Contact
Molar Volume (L/mol)	0.89	0.88
Interaction Coeff. CO_2	0.5	0.5
Interaction Coeff. C_1 –C_7	0.2	

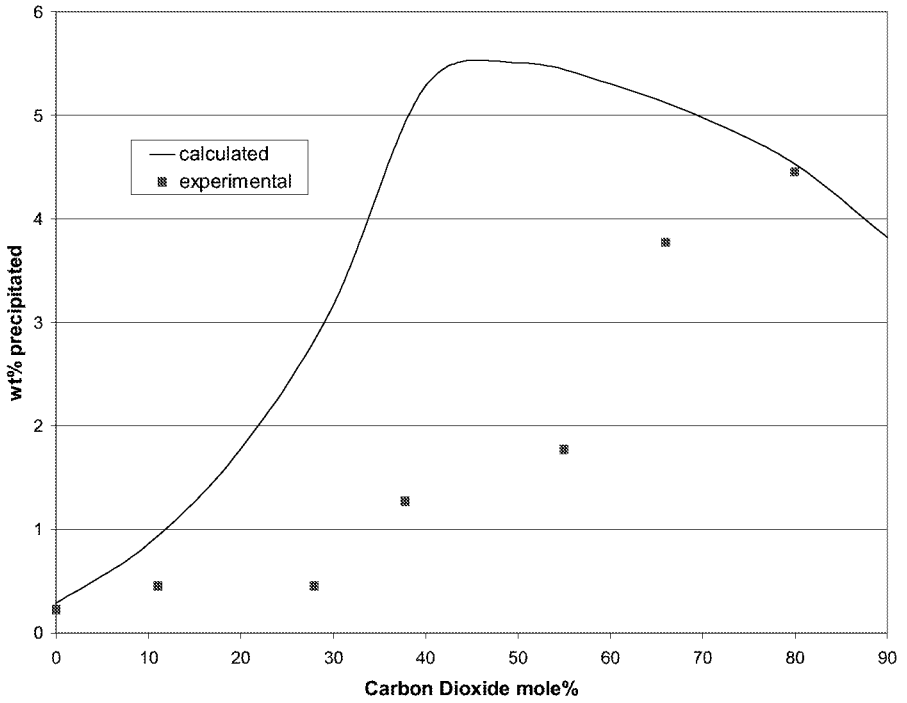

Figure 4-3 Pure Dense Phase Model – Live Oil

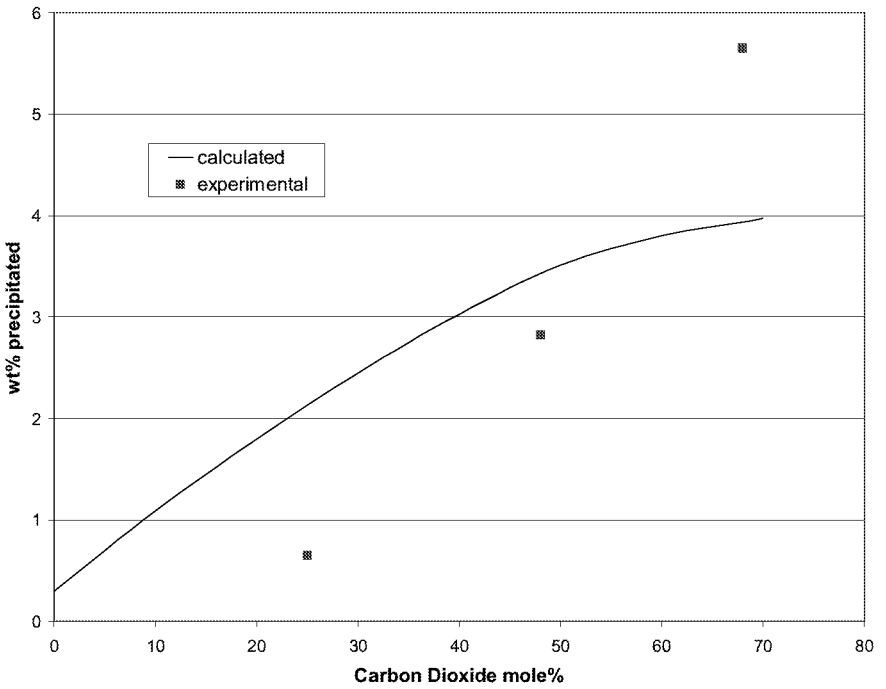

Figure 4-4 Pure Dense Phase Model – Simulated Multiple Contact

The calculated values do not match with the experimental data. The results from this model do not present an onset of precipitation, that is fact found in the experimental part.

Homogeneous Molecular Thermodynamic Model Results

This model has two parameters, molar volume and solubility parameter of asphaltene. After model parameters are fitted by experimental data, it can be used to predict the precipitation amount of asphaltene from the solvent-oil mixture.

The two parameters were optimized for each system: dead oil, live oil, and simulated multiple contact. The optimized values of these parameters are shown in Table 4-7. Figure 4-5 gives the comparison of experimental and calculated amount of precipitated asphaltene for dead oil. This model gives good agreement between the calculated and experimental results for dead oil. Figure 4-6 shows the results for live oil. A good agreement is also found for live oil. However, for simulated multiple contact system the predicted values are low at intermediate and high carbon dioxide concentrations (Figure 4-7).

Table 4-7 Optimized parameters for different systems

System	$?_A$ $(psia)^{0.5}$	V_A $(ft^3/mole)$
Dead oil	450.0	0.10
Live oil	302.0	0.4258
Simulated Multiple Contact	264.8	0.9802

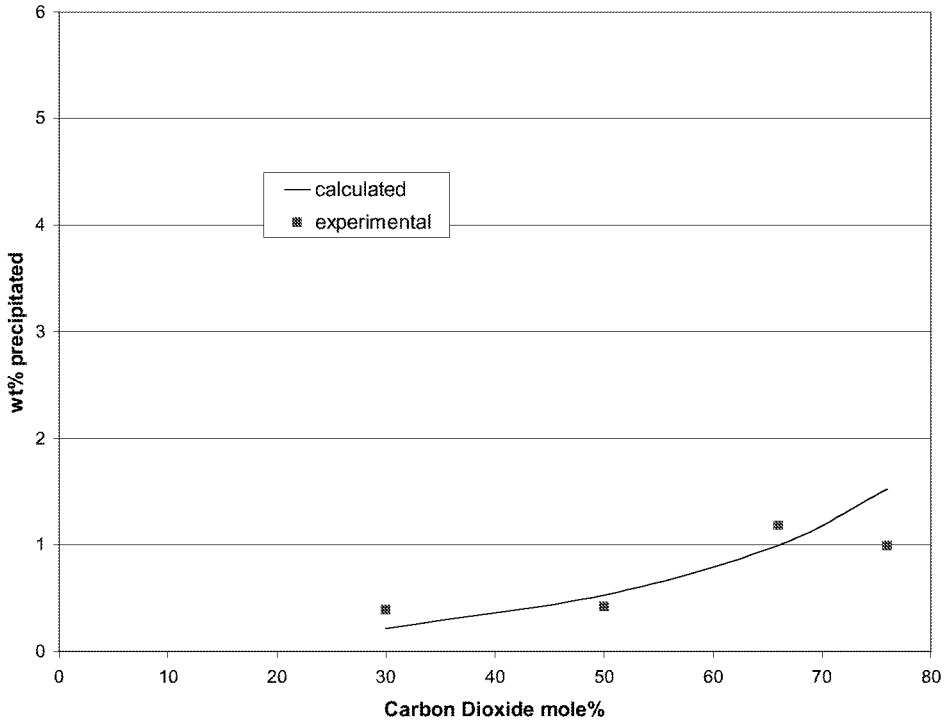

Figure 4-5 Homogeneous Molecular Thermodynamic Model – Dead Oil

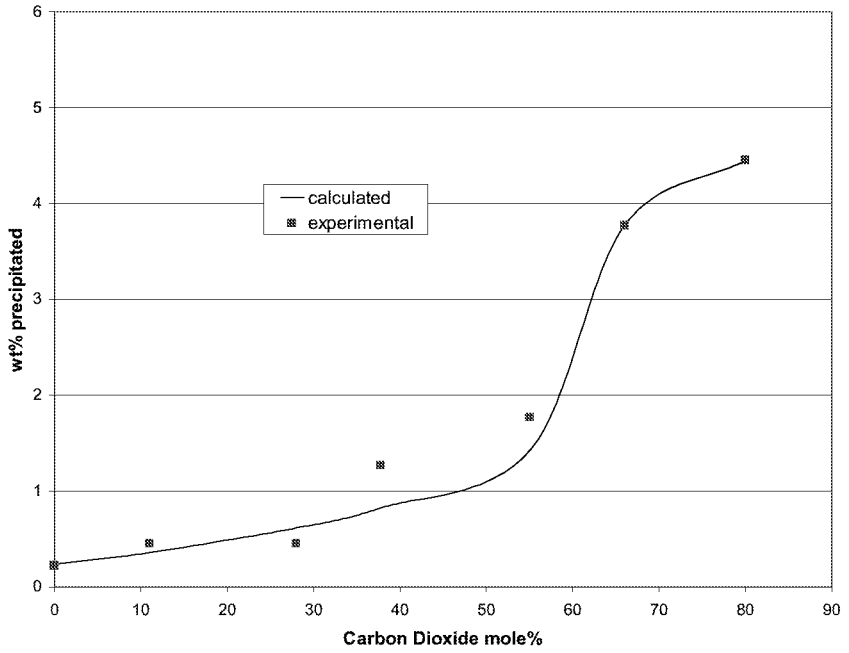

Figure 4-6 Homogeneous Molecular Thermodynamic Model – Live Oil

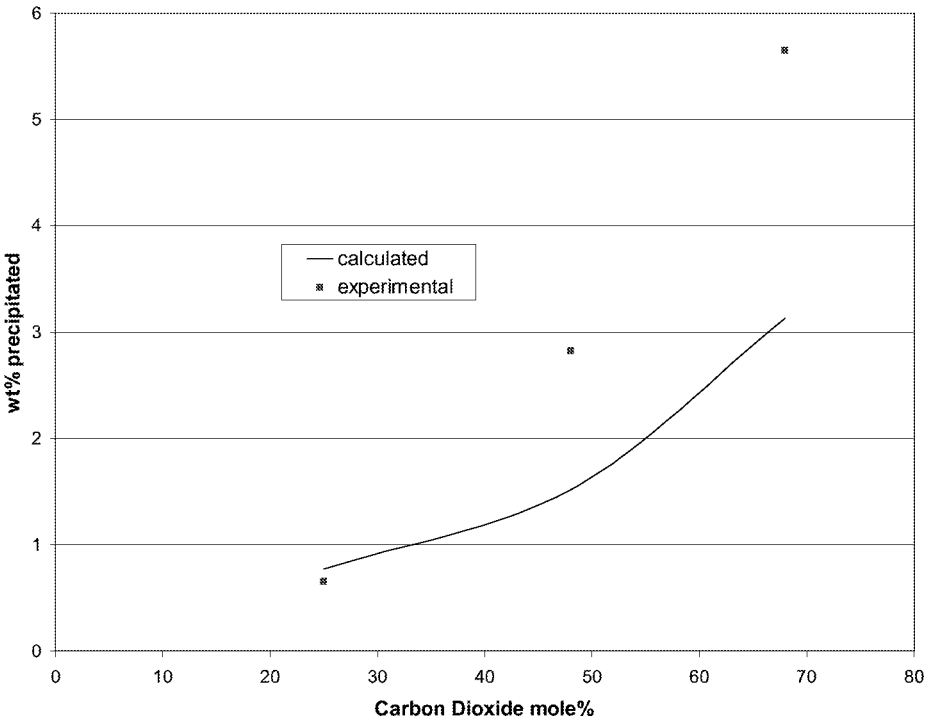

Figure 4-7 Homogeneous Molecular Thermodynamic Model – Simulated Multiple Contact Experiments

Homogeneous Molecular Thermodynamic Model gives a better representation of the precipitation of solids, especially for dead and live oils. The model prediction shows close agreement with the experimental data after regression of asphaltene properties such as molar volume, solubility parameter and molecular weight.

In addition, a new extended polydispersed molecular thermodynamic model was developed and applied to asphaltene precipitation data from liquid solvents. The model development and results have been discussed in detail in the second annual report (Deo, 2000).

Nomenclature

a Peng Robinson EOS Constant
a' Model Parameter
a_L Peng Robinson EOS Constant
A Peng Robinson EOS Constant
b Peng Robinson EOS Constant
b' Model Parameter
b_L Peng Robinson EOS Constant
B Peng Robinson EOS Constant
C_p Molar Heat Capacity
f Parameter Defined in Polydispersed Model
f_i Fugacity
F Objective Function
$F(M_A)$ Normal Distribution Function
G Gibbs Free Energy
H Enthalpy
K_i Solid-Liquid Equilibrium Constant in Wax Model
K_{AB} Interaction Parameter between Asphaltene and Asphaltene-free Liquid
K_{Ai} Solid-Liquid Equilibrium Constant in Polydispersed Model
M Molecular Weight
N Number of Components
NF Number of Asphaltene Free Components
R Gas Constant
P Pressure
P_c Critical Pressure
S Entropy
SG Specific Gravity
T Temperature
T_c Critical Temperature
T_r Reduced Temperature
U Internal Energy
V Molar Volume
W Weight Percent
x Molar Fraction
X Molar Fraction

Z Compressibility Factor

Greek Letters

? Peng Robinson EOS Constant
?? Model Parameter
? Model Parameter
? Solubility Parameter
? Volume Fraction
? Chemical Potential
? Density
? Standard Deviation of Normal Distribution Function
$?_{ij}$ Binary Interaction Parameters in EOS
? Accentric Factor
? Variable Defined in Normal Distribution Function
? Activity Coefficient

Subscripts and Superscripts

A Asphaltene
AD Deposited Asphaltene
Ai ith Fraction of Asphaltene
AT Total Asphaltene
B Asphaltene-free Liquid
F Fusion
i ith Fraction or Component
j jth Fraction or Component
L Liquid

5. Core Flooding Experiments

The objective of the core floods is to examine the link between development of miscibility and precipitation. It was important to determine if multiple contact miscibility was attained in the core and if it did, the type of compositional variations that it caused. The key question would be if the compositional changes leading to multiple contact miscibility also cause precipitation.

Experimental System

The experimental system shown in Figure 5-1 was also used for core floods. A triaxial core holder designed and built and the University of Utah was used. A six-inch long, 1.5 inch diameter berea core was used in all experiments.

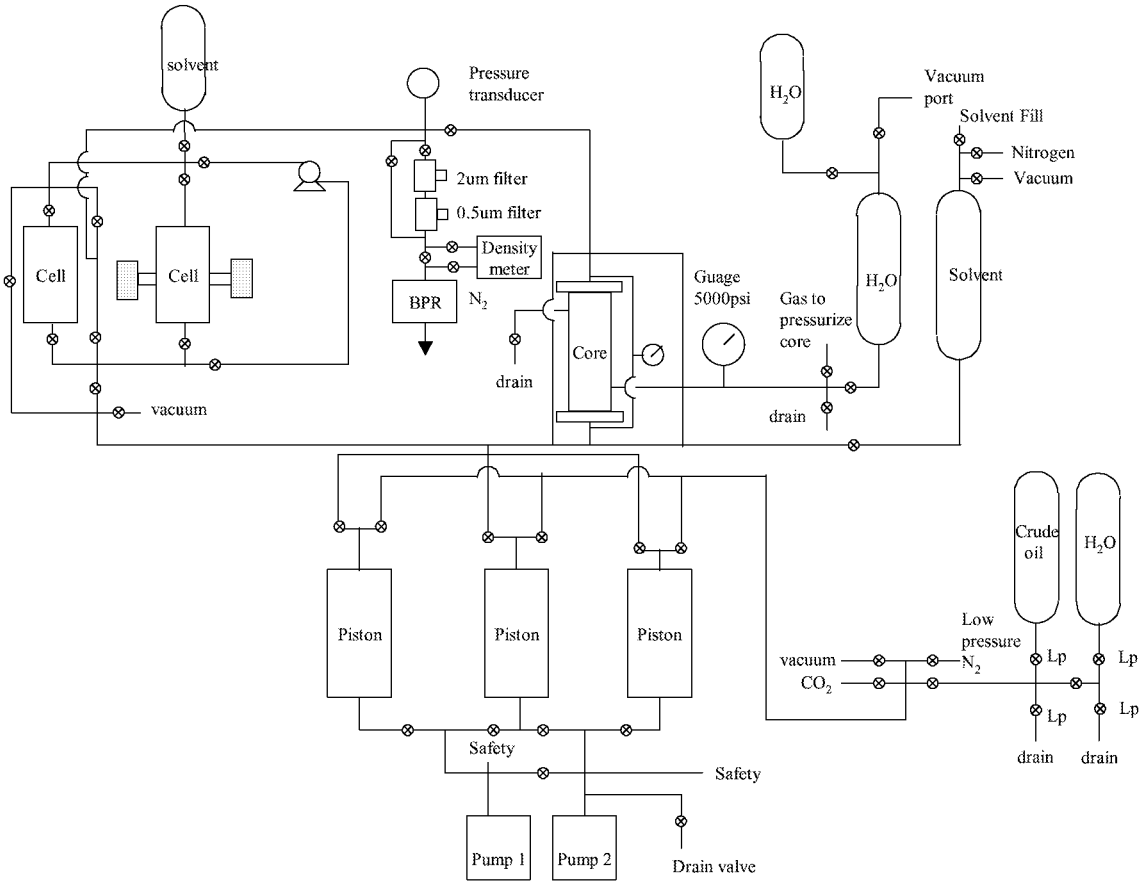

Figure 5-1 Experimental system used for the corefloods

Experimental Procedure

The core was dried and mounted. An overburden of 3000 psia was applied and the core was brought to the system temperature of 160^0F. The core was then saturated with CO_2 at about 50 psia. Brine (2% KCL) was injected from the bottom of the core. After brine breakthrough, the fluids in the core were pressurized to the system pressure of 2000 psia to dissolve residual CO_2. The resultant carbonated brine was displaced by four pore volumes brine from the top of the core. This was followed by an oil flood from the top and a secondary carbon dioxide flood from the top . Oil samples out of the back pressure regulator were collected. Six samples were collected over a run time of about four pore volumes.

Experimental Results

The porosity of the core was determined by performing gas filling and displacement experiments, and was determined to be 19 ? 2%. A value of 20% was used in all calculations. The core was 1.5 inches in diameter and 6 inches in length. Thus, the core had a pore volume of 35 cc.

The core was first saturated with carbon dioxide at about 50 psia and was flooded with 2% KCL brine. After water breakthrough, the core was pressurized to 2000 psia. The brine flood was continued for 2 more pore volumes to fully saturate the core with brine.

The core was then flooded with Rangely oil from the top for about 4 pore volumes. Oil saturation of about 85% was attained in the core (a total of 29 cc in the core). The core was then flooded with carbon dioxide at 2000 psia from the top. Six oil samples were collected over the course of a 4 PV flood. Compositions of these oil samples were measured using simulated distillation on a gas chromatograph. Results are shown in Figure 5-2. The samples that came out of the core at the start of the flood had compositions similar to the original oil. The samples collected in the middle of the run were substantially enriched in the intermediates. The samples at the end of the run were heavier. Thus, the compositional variations observed in the run were consistent with those reported by earlier investigators (Orr, et al, 1981).

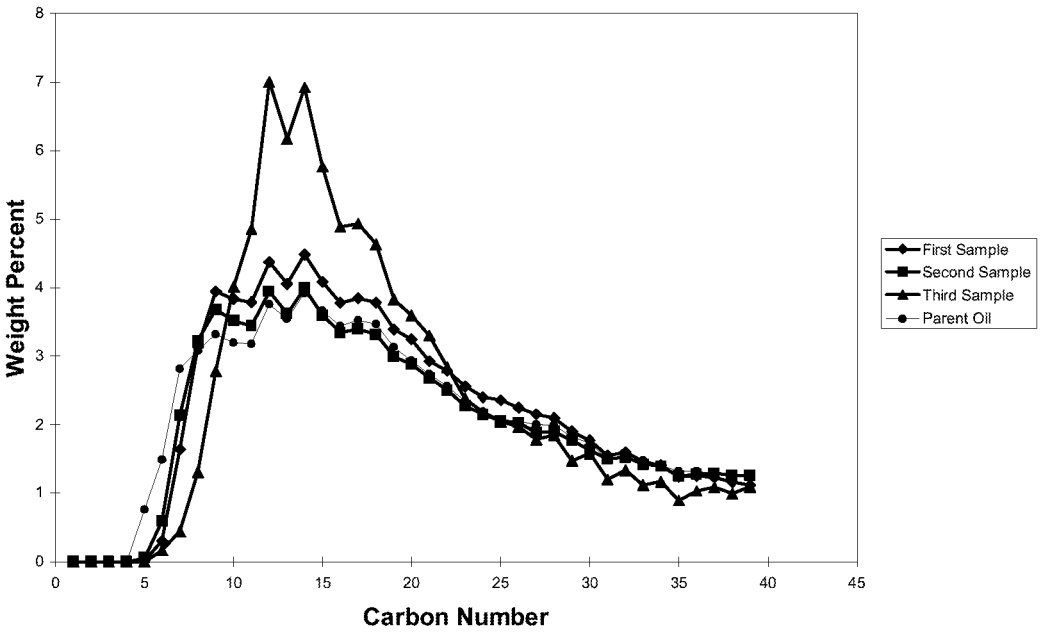

Figure 5-2: Carbon number distributions of the oil samples collected as the flood progressed; analyses were performed using simulated distillation

Thin sections of the core at both ends did not show any sign of precipitation in the core.

A Simulated Well-bore Flash Experiment

The previous core flood confirmed the compositional changes taking place in a carbon dioxide flood. The core flood performed during this period was essentially to see if these compositional changes were causing added precipitation in the core. One additional objective was to examine the behavior of fluids exiting from the core when subjected to a "wellbore" flash.

The high-pressure, core flooding experimental setup described earlier was used with some modifications. The core outlet was connected to two visual (PVT) cells. These cells were filled with carbonated brine at system conditions prior to the carbon dioxide core flood.

The sequence of operations and results were as follows. The core was mounted in a triaxial core holder and was pressurized to about 3000 psia. The pore volume of the core was recorded using volume expansion measurements. Approximately 12 different pressure cycles were used and the pore volume was averaged. The pore volume was 39 cc. The core was six inches long and was 1.5 inches in diameter for a total volume of 174 cc. The porosity of the rock was thus 22 %. The core was saturated with CO_2 at about 100 psia and was flooded with brine. After brine breakthrough, the fluids were pressurized to 2000 psia; the brine flood continued for about four PV.

The Rangely crude was introduced into the core. A total of about 4 PV of oil was sent through the core. The oil exited the core through 2 filters, a 2 micron filter and a 0.5 micron filter. This was basically to obtain a baseline for solids movement and deposition on filters without any compositional changes. The solids collected amounted to 0.1562 g or about 0.13% of the oil flowed through the filters. The core was sealed, the filters were returned online.

CO_2 was flooded through the core at 2000 psia. The oil exiting the core was filtered and collected in two high-pressure PVT cells. The PVT cells originally contained carbonated brine and thus simulated production wells. The amount of solids collected were 0.55 g for a total of 26 g of oil exiting the core. If the baseline solid value is subtracted (0.13%), this amounts to 2% solids from the oil exiting the core. The first contact precipitation amounts were all less than 1% (with the exception of one experiment, which is being repeated). Thus, the multiple contact mixture generated in the core has a tendency to precipitate twice the amount of solids as single-contact mixtures at any CO_2 concentration.

The high-pressure, oil-CO_2 mixtures collected in the PVT cells were flashed and sampled to assess the tendency of these mixtures to form solids. As a gas bubbles form and leave the flash chamber, they appeared to deposit some solid material on fittings and tubing.

This was estimated to be only about 0.06% of the oil in the chamber. The oil in both the chambers was filtered and the solids collected and weighed. The total amount of solids collected amounted to 0.11% which, given the margin of error in the measurements was close to the baseline solids amount in the oil. Thus, almost all of the solids precipitated in the multiple contact mixture were trapped at the core outlet.

A Comprehensive Coreflood on Live Oil

A 1.5 –inch diameter Berea core, 6.88 inches long was used for the experiment. The core was mounted in a heat shrink Teflon sleeve, which was shrunk in place. The ends of the core along with the sleeve were clamped onto two specially designed end pieces of a triaxial core holder. Several measurements were made of the core pore volume. The average from all the measurements was 51 mL.

The coreflood was performed with live oil. The gas oil ratio was 155 scf/stb and the temperature was 160^0F. The core was first evacuated and charged with oil. The coreflood was performed without any water in the core. Two pore volumes of carbon dioxide was sent through the core at about 3000 psi. Twenty two (22) samples were collected as a function of time. Detailed compositional analyses were performed on each of the samples. The data was analyzed by simulated distillation (SIMDIS). Figure 5-2shows the compositions of different samples as they eluted from the core. As is seen from the figure, until about CO_2 breakthrough, the compositions of the mixtures remain unchanged. At and after CO_2 breakthrough, intermediate compounds go through a high and this high shifts to heavier and heavier compounds as more oil eluted from the sample. Compositions of the some of the key hydrocarbon constituents are shown in Figure 2, as a function of time. Lighter components (up to about C20) are produced at their original composition until CO_2 breakthrough. Thereafter, they go through an increase before declining in concentration. The intermediate compounds have the biggest increase after CO_2 breakthrough The heaviest of hydrocarbons are lower in concentration more or less throughout the run and their amounts are significantly higher in the oil left behind and obtained using a solvent flood (dichloromethane was the solvent used).

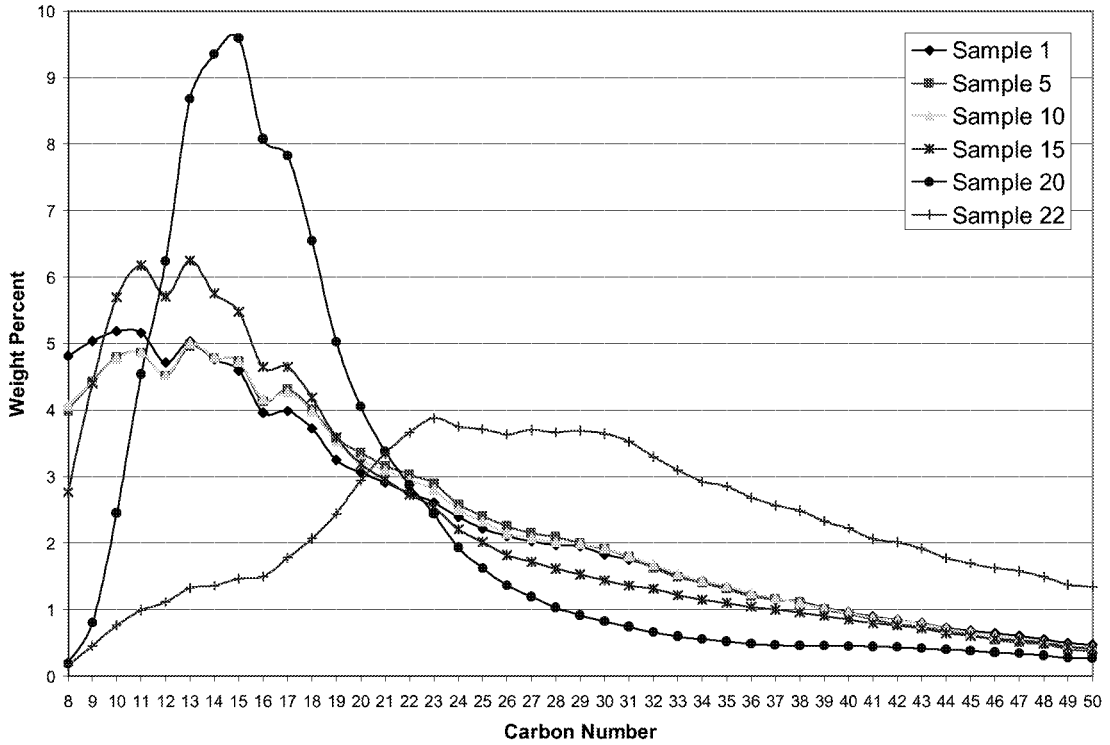

Figure 5-3 Coreflood results from the live-oil experiment. Compositions of the oil samples were obtained using simulated distillation. The sample numbers indicate when they were collected. Higher numbers indicate later times. The CO2 breakthrough was at 15.

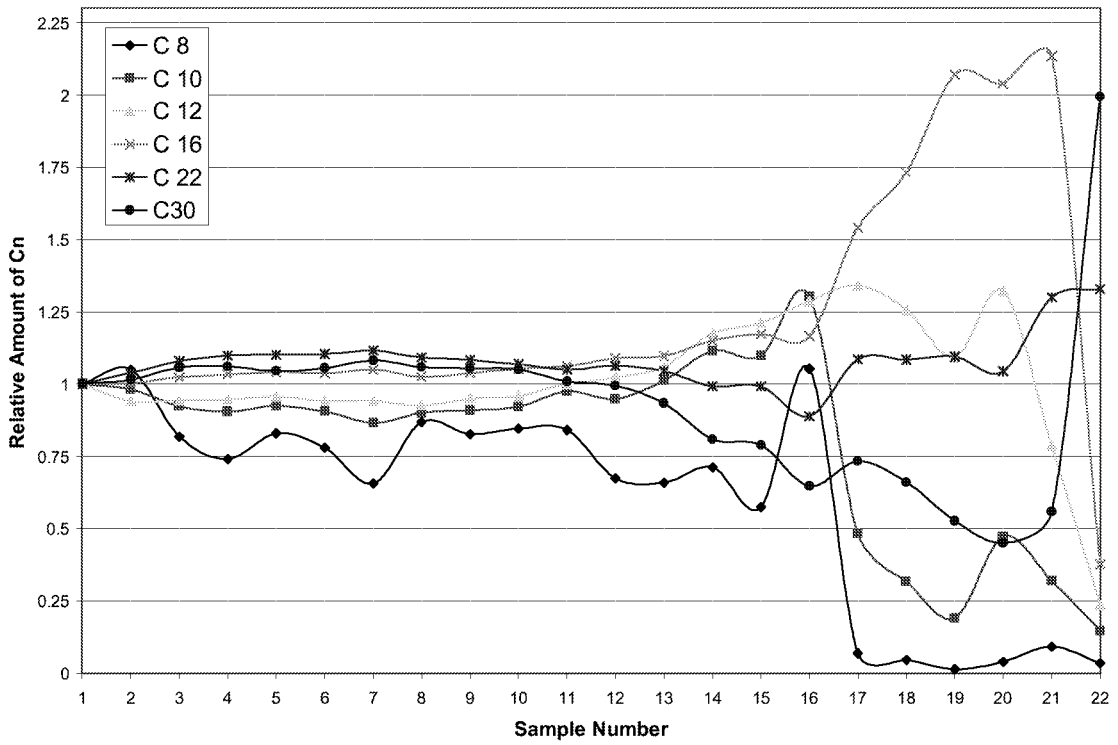

Figure 5-4 Plots of different carbon numbers in the samples as they eluted from the core with respect their original concentration in the oil.

6. Kinetic Measurements

Preliminary Approach

There is no reported data on kinetics of CO_2 induced precipitation. Rate effects such as heat and mass transfer rates are becoming important considerations in determining wax precipitation and may be important in asphaltene precipitation as well. There has been a great deal of work on crystallization kinetics, particularly with inorganic mixtures (Ring and Dirksen, 1997), and one of the original project goals was to use the same approach in determining kinetics of asphaltene precipitation. The idea was to see if temperature programmed cooling and measurements of oil-solvent mixtures could be used to detect onset and rate of precipitation of asphaltenes. The basic method is calorimetric. The mixture is placed in a bath and the bath is cooled at a pre-determined rate. Temperature response is measured and compared to the expected baseline temperature response. Crystallization (or precipitation) causes a deviation of the measured response in comparison to the baseline response. This deviation is used to quantify onset, rate, etc.

Since precipitation occurs as solvent is added, a titration-type experimental system was developed. This system is shown in Figure 6-1. The intent was to develop a titration protocol and the idea was to develop the protocol using solvents that would precipitate solids from the oil at room pressure. The system was simple; the oil solvent mixture temperatures were recorded continuously as solvent was added to oil.

Cooling Experiments

The following cooling cycle experiments were performed: 25 ml of the two Rangely crudes (one from the CO_2 region and the other from the non-CO_2) area were held in an oil bath at 50^0C for about 12 hours. The oils were cooled to 30^0C in 30 minutes followed by cooling to -15^0C at 20^0C/hour. The oils were held at this temperature for 30 minutes. The temperature of the bulk mixture was monitored precisely (two decimal points). These experiments were performed to establish a precipitation baseline from parent oils.

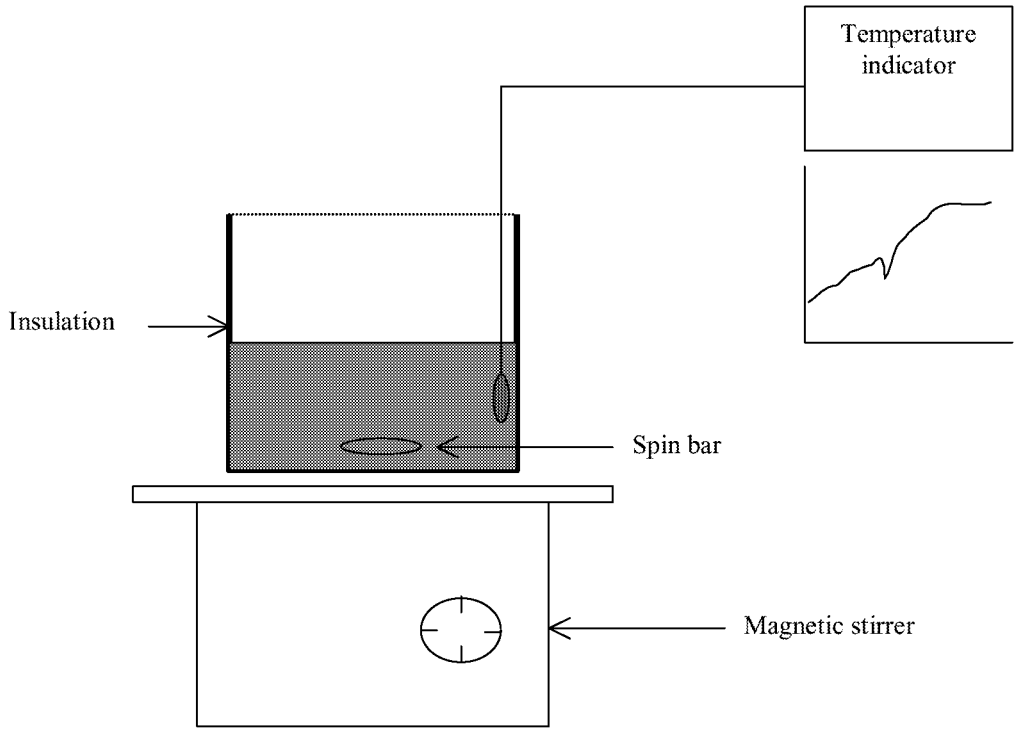

Figure 6-1: Experimental system developed to determine composition induced precipitation

Precipitation of any solid material would have been detected via a burst of heat release at the point of precipitation. As can be seen in Figure 6-2, the mixture essentially follows

the temperature ramp, indicating no solids formation. These experiments were repeated with varying amounts of light hydrocarbons (1-10% pentane and heptane). These experiments were also inconclusive as to the formation of solids.

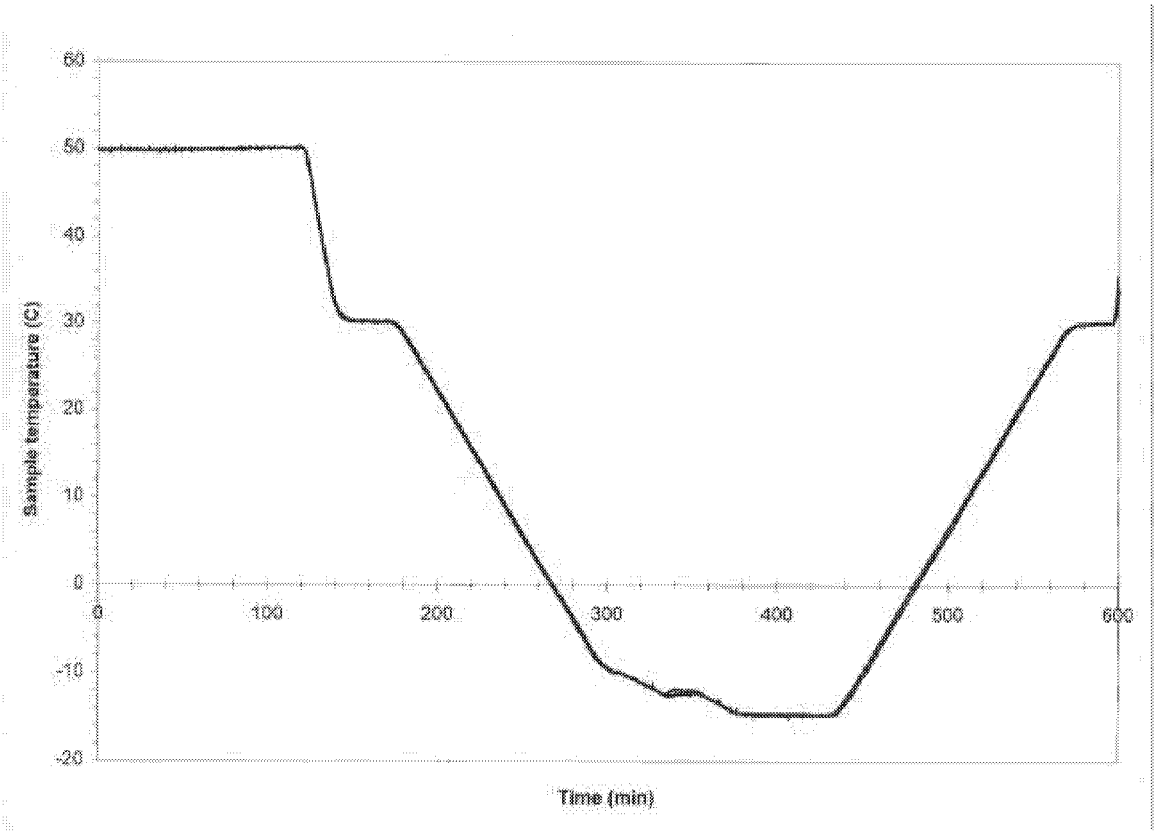

Figure 6-2: Temperature of the oil placed in a bath cooled at a predefined rate

Titration Experiments

Results of one of the titration experiments are presented in Figure 6-3. Temperature changes at the onset of precipitation are seen clearly in all the figures. The precipitation is most intense with pentane at low rates, since it is not mixing limited. The data was analyzed to determine kinetics of precipitation.

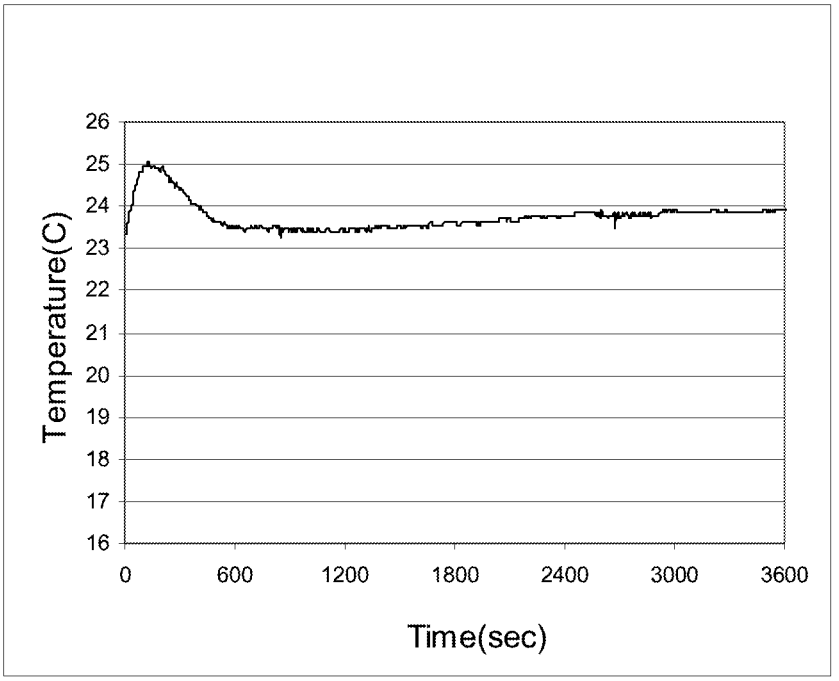

Figure 6-3: Temperature of the Rangely oil as pentane is added at a rate of 1 ml/min

Modeling

Experiments were performed in which 10 ml of Rangely oil was placed in an insulated vessel. In the vessel is a magnetic stirrer and a thermocouple to record the temperature. The temperature is recorded as a solvent (either pentane, hexane or heptane) was added at a constant flow rate of either 1 ml/min or 2.5 ml/min. An example of the experimental results was shown in Figure 6-3, where pentane at a flow rate of 1 ml/min is mixed with oil. It is seen that the temperature initially rises and then decreases, then finally increases. This curve appears to be the result of the superposition of two curves: 1) the initial quick rise and 2) a slowly increasing temperature profile. The initial quick rise is over by 600 sec corresponding to the point where the mole fraction solvent has reached 0.5. In this sample, some asphaltenes were precipitated by the pentane addition. Analysis of this type of curve was performed by considering the energy of mixing, heat of mixing two liquids and heat of precipitation of the asphaltene fraction.

Consider mixing of oil with a solvent when asphaltene precipitation does not takes place. When the solvent feed temperature and the initial temperature of oil in the vessel are the same, T_0, then the overall energy balance is given by:

$$(V_o ? Qt)\frac{C_v}{?}\frac{d(T ? T_o)}{dt} ? E_{mix} ? (V_o ? Qt)\frac{?(? H_m)}{d? _1}\frac{?? _1}{?t}$$

As written, this equation assumes that the heat capacity, C_v, and the molar volume, ?, are constant, however, this can be changed if necessary. This assumption is reasonable, if the heat capacity and molar volume of the solvent and oil are similar or more precisely if their ratio does not vary as the solvent mole fraction is increased from zero to 0.5 and beyond. Other quantities in the equation are given by:
Mixing Energy per unit time = E_{mix}
Heat of mixing per unit volume, $? H_m = ? _1(1-? _1)(?_1 -?_o)^2$.
where $? _1$ is the volume fraction solvent and ? is the solubility parameter for the solvent, subscript 1, and for the oil, subscript o.

When oil is modeled as a true multicomponent mixture, a method to evaluate mixture molar volume and equivalent solubility parameter will have to be developed.
In the above, Scatchard and Hildebrand regular solution theory is used for the formulation of the heat of mixing. Upon integration the temperature difference, $? T=T-T_o$, is given by:

$$? T(t) ? T(t) ? T_o ? \frac{?}{C_v}\left[\frac{\ln(1 ? \frac{Q t}{V_o})}{Q}\right] V_o E_{mix} ? ? \frac{?}{C_v}\left[\frac{Qt}{V_o ? Qt}(1 ? \frac{Qt}{V_o ? Qt})(?_1 ? ?_o)^2\right]$$

In this equation, there are two terms; the first corresponding to mixing which slowly grows with time and the second which first increases then decreases due to the effects of the $? _1(1-? _1)$ term as the volume fraction of solvent increases shows the separate effects of various values of E_{mix} and $(?_1 -?_o)$ on ?T(t). Increasing the value of o increases the height of the peak observed at 10 min. At 10 minutes, the mole fraction of solvent is 0.5 corresponding to a maximum in the $? _1(1-? _1)$ term. Since the precipitation takes place when the mole fraction of the solvent is changing the most, i.e. in the first 10 minutes, we can use this equation for the long time effects on the temperature and by curve fitting determine the unknowns, E_{mix} and $(?_1 -?_o)^2$.

Since the maximum in the experimental data occurs at a time of approximately 100 seconds, and not 10 minutes, we can be assured that the initial quick rise is not due to solvent mixing but to precipitation of asphaltenes. Thus, we can use the best fit of the temperature difference equation for the long time data, t>30 min, and extrapolating back to shorter times we can clearly identify the differences that must be due to precipitation. The difference between the fit and the data at short times corresponds to the enthalpy due to precipitation of asphaltenes. is a plot of the temperature effect of this precipitation. The point of deviation of the experimental data from the fit curve in Figure 6-5, indicates the mole fraction at which asphaltene is supersaturated in the system. In this case, it is essentially immediately. Precipitation appears to stop after 10 minutes. Calculations are being continued at the present time to determine the enthalpy of precipitation (mass of asphaltenes precipitated and molecular weight of asphaltenes are necessary for this exercise).

Regular solution theory can also be used to identify the asphaltene solubility, $X_{a,eq}$.

$$? RT \ln X_{a,eq} ? ? H_{F,a} ? ? _a ? _s^2 (? _s ? ? _a)^2$$

$$? ? H_{F,a} ? ? _a (\frac{? _1 X_1 ? ? _o X_o}{? _1 X_1 ? ? _o X_o ? ? _a X_a})^2 ((? _1 X_1 ? ? _o X_o ? ? _a X_a) ? ? _a)^2$$

where R is the gas constant, T is the temperature, $? H_{F,a}$ is the heat of fusion of asphaltene at a reference temperature ,T_R, $? _a$ is the molar volume of asphaltene, $? _a$ is the solubility parameter of asphaltene, $? _s$ is the volume fraction of the solvent system (oil plus solvent at any time) and $? _s$ is the solubility of the solvent system. The heat of fusion for asphaltene can be measured by differential scanning calorimetry of the precipitated solid. As the volume fraction of solvent (subscript, 1) is increased the volume fraction of the system approaches 1.0 and the value of the solubility parameter decreases to a value near that of the solvent. The result of both of these effects is to decrease the solubility of asphaltene as solvent is added as shown in Figure 6-6. Also shown is an assumed concentration of asphaltene. Initially the solution is undersaturated. At the intersection of the two curves, the solution is saturated. At higher mole fractions of solvent, X_1, the solution is supersaturated. The supersaturation ratio, Xa/Xeq, is the driving force for precipitation.

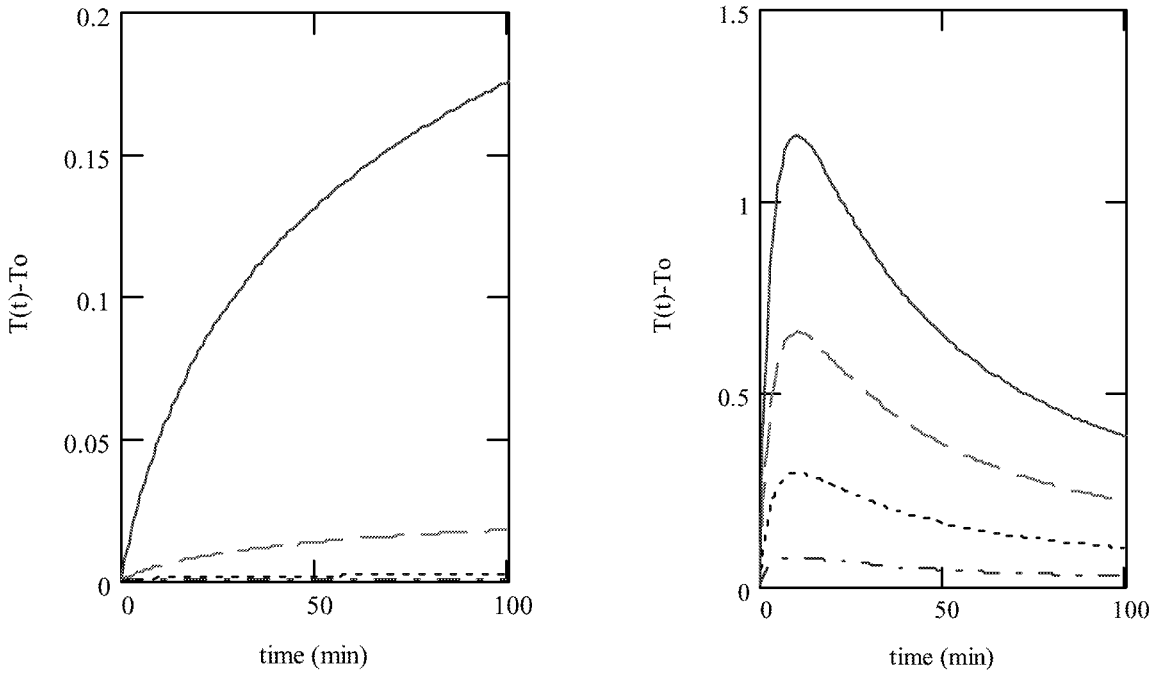

Figure 6-4: Effect of Emix and (d1 -do) on DT(t) (°C). (a) Effect of various values of (d1 -do) on DT(t) assuming Emix is zero, for curves from bottom to top (d1 -do) = 7.3, 7.5, 7.7, 7.9, (b) Effect of various values of Emix on DT(t) assuming (d1 -do) is zer

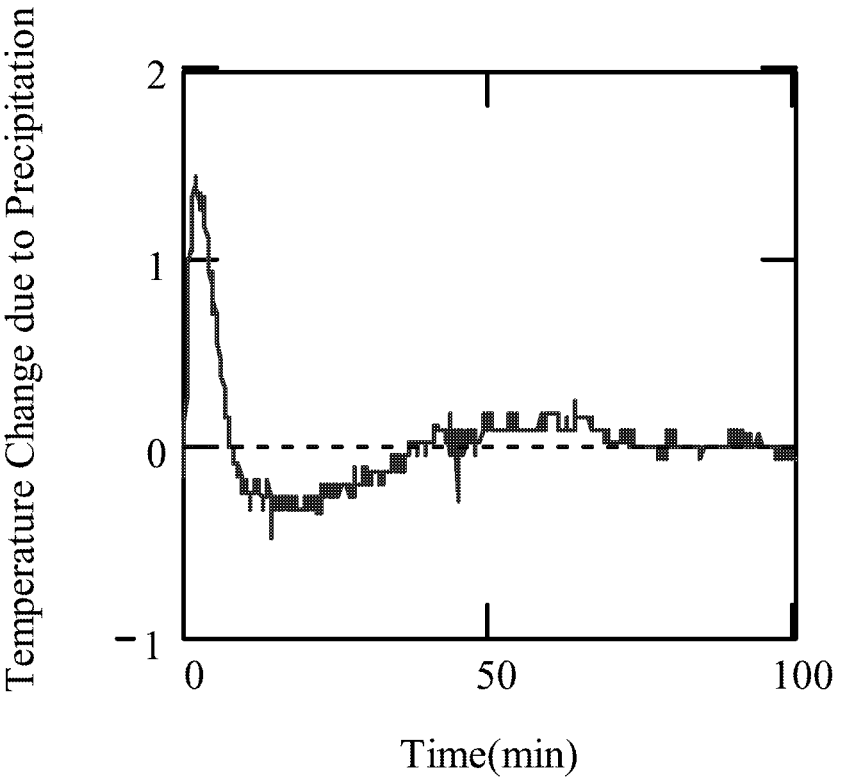

Figure 6-5: Difference in the experimental and curve fit of long time data identifying the temperature change due to the enthalpy of asphaltene precipitation

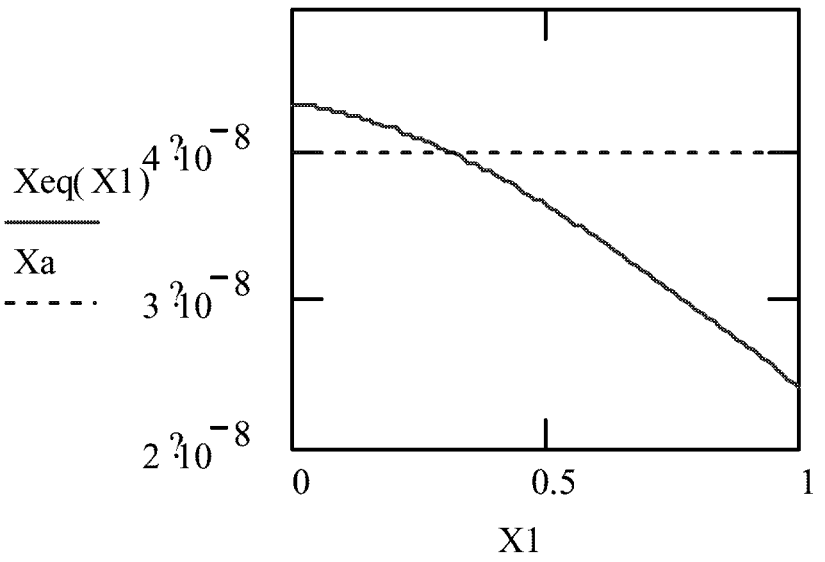

Figure 6-6: Solubility of asphaltene, Xeq, (solid line) and asphaltene, Xa, (dashed line), in solution assumed to be 4x10-8 as the solvent mole fraction, X1 is increased. Depending upon the amount of asphaltene in the oil, the point at which the solution is satur

Titration Kinetics Based on Titration

Kinetics of precipitation of asphaltenes with liquid solvents were measured. The data used in the analysis is shown in Figure 6-7. A simple kinetic model was used to fit the data.

$$1 - \frac{W}{W_{max}} = \exp(-kt)$$

W: Weight of the precipitate as a function of time (as a percentage of the original oil)
W_{max}: Maximum weight percent precipitated
k: rate constant
t: time(hours)
k values for a number of solvents are listed in Table 16. The rate constant decreases as the solvent carbon number increases.

Table 6-1:Rates of asphaltene precipitation with liquid solvents

Solvent	**K-value (1/hour)**
Pentane	1.90
Hexane	1.35
Heptane	1.16

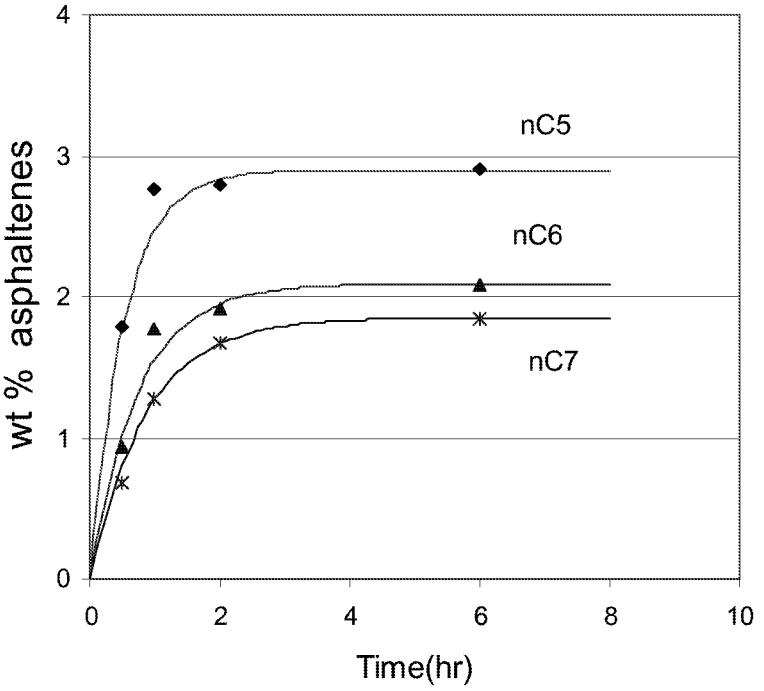

Figure 6-7: Precipitation of asphaltenes as a function of time

Onset Measurements Using Near Infrared Spectroscopy

Introduction

Crude oil asphaltenes are compounds classified by their solubilities in n-alkanes. The asphaltene precipitation problems are common both in the upstream (production and transportation) and the downstream (processing, refining) segments of the oil industry. Deposition problems are known to occur even when the amount of asphaltenes in the original mixture is relatively low. Conversely, in some instances, oils with relatively higher amounts of asphaltenes show no signs of precipitation/deposition (Kokal and Sayegh, 1995). For instance, oil from the Boscan field in Venezuela showed no asphaltene precipitation problems even with an initial asphaltene content of 17.2 wt.%, while, the Ula field in North Sea was plagued with solids precipitation problems with an oil containing relatively small amount of asphaltenes (0.57wt%).

The reason is the complexity of asphaltene compound class. This class of compounds is not easily characterized because of the high molecular weight and polarity of compounds. All aspects of asphaltenes have been extensively studied. Researchers have attributed the formation of solids to solubility related phenomena as wells as colloidal particle agglomeration. This paper examines changes in the solubility of asphaltenic compounds in oil as a result of induced compositional variations.

In terms of controlling or providing solutions to the precipitation problem, it is important to know when the precipitation is initiated and the quantity of asphaltenes which can be deposited during oil production, transportation or processing. Accurate determination of the onset of precipitation is therefore important. Onset is defined as the minimum amount of precipitant necessary to induce the precipitation of solids, believed to be asphaltenes. A number of methods have been developed to measure the onset of precipitation or flocculation of asphaltenes. Precipitation onset data have been reported with conductivity (Fotland, et al., 1993), refractive index (Buckley, 1999) and viscosity (Escobedo and Mansoori, 1995) measurements.

Spectroscopy has been a popular tool for the determination of the onset of precipitation. UV spectrometer has often been used to determine the onset of solids precipitation. Andersen (1999) chose a wavelength of 740nm for measuring the onset while Reichert and coworkers (1986) used 900nm. They both used toluene as a dispersant. Direct measurements on precipitation onset with UV spectroscopy are difficult due to the dark nature of the original oil. Near-Infrared (IR) spectroscopy is ideal for determining the onset directly. Effectiveness of the use of Near-IR spectroscopy to accurately measure precipitation onset has been demonstrated (Fuhr, 1991). Typically, onset as a function of precipitant concentration is measured by titration of the oil with the appropriate solvent.

A number of investigators have studied precipitation of solids as a function of the carbon number of the alkane precipitant (Speight, 1999). It is well known that as the alkane carbon number increases, the amount of precipitated material decreases. The molecular weight distribution of the precipitated material shifts to the left (indicating that relatively

smaller compounds become part of the asphaltene class) as the n-alkane carbon number decreases. It was also known that the oil phase becomes more stable with the addition of light aromatic compounds, such as toluene and xylene and it is comparatively more difficult to precipitate asphaltenes from these mixtures.

Clarke and Pruden (1998) reported the effect of additives on the onset of asphaltene precipitation from Canadian bitumens by the heat transfer technique. They used aromatics, heteroatomic compounds, hydrogen donor chemicals and surfactants as additives. The results showed that the addition of aromatic compounds delayed the onset of precipitation from highly asphaltic oils (bitumens). Phenanthrene addition (20 wt.%) to Cold Lake bitumen delayed the onset, and appeared to be more effective than the additions of toluene, xylene or naphthalene. They hypothesized that phenanthrene's high aromaticity and molecular weight gave it resin like features. The effects of the additions of heteroatomic compounds and hydrogen donor chemicals (tetralin, decalin) were relatively small. Addition of the surfactant, nonyl-phenol was most effective in delaying the onset while dodecylbenzene sulfonic acid was ineffective. Chang and Fogler (1993) suggested that the asphaltene stabilizing effects were dependent on the length of the alkyl tail and the polarity of the head group in the surfactants added. They found that the additives were most effective in delaying precipitation when the compound consisted of more than six alkyl chains with a sufficiently polar head, such as a hydroxyl or a sulfonate.

One of the objectives of this study was to examine the effects of solid organic additives on the onset of the precipitation of asphaltenic solids. The objective was also to explore solubility related solids precipitation in a broad context. Apart from significant inorganic solids precipitation issues and problems related to gas hydrates, there are two organic solids precipitation phenomena of significance in the oil industry; precipitation of waxes, which is primarily temperature induced and precipitation of asphaltenes, which is driven by changes in oil composition. Under some circumstances, coprecipitation of these compounds may be important. Asphaltene precipitation is observed during primary depletion and in the course of miscible gas injection processes. The primary depletion is carried out at high pressures, and pressure is an important parameter. The quality of asphaltenes collected during miscible injection processes is different from the quality of laboratory asphaltenes (n-heptane insolubles), possibly due to the presence of higher molecular weight waxes. If asphaltene precipitation occurs at high temperatures (over 60^0C), co-precipitation of waxes is usually not an issue. In wax precipitation, there are questions about the quantity of asphaltenes that co-precipitate. In this study, that aspect was examined by measuring asphaltene precipitation onset on addition of n-alkane solid compounds. For comparison, addition of aromatic solid compounds was also investigated. The Near-IR Spectroscopy provided a quick, accurate and direct measurement of the onset points. Oil with a relatively low amount of initial asphaltene content was employed. The first few experiments were performed with different precipitants and with liquid additives to streamline and validate the experimental procedures.

Experimental Procedure

A single crude oil was used in all the experiments. The crude oil was from the Rangely field in western Colorado. The initial asphaltene content (heptane insolubles) of the oil was 1.7 wt%. Fractions of saturates, aromatics and resins, as determined by column chromatography were approximately 49%, 23% and 3% respectively (the remainder is accounted for by lights and the unrecovered portion of oil).

Phenanthrene, eicosane and tetracosane were used without purification from Aldrich Chemicals. Naphthalene was used from Mallinckrodt, also without further purification. Toluene and n-heptane were HPLC grade and were more than 99% pure.

Near-IR spectra were collected over the 1200 to 2400nm spectral region with Quantum-1200 (from LT Industries, Inc.) spectrometer consisting of a fiber optic detector. The spectra were collected through a probe equipped with a sapphire lens. The path length was 6 mm. Scans were collected every 30 seconds.

A known amount (40g) of the crude oil was charged to a flask and a normal paraffin solvent was added to the oil at a controlled, constant rate (titration). The oil-solvent mixture was mixed continuously with a magnetic stirring device. Schematic diagram of the experimental system is shown in Figure 6-8. To study the effect of the addition of different organic solids, the solid compounds were added until they dissolved completely in the crude oil (with an initial mixing period of several hours). In most experiments, about 2 grams of solids dissolved in the oil completely. The flow of alkanes (precipitants) was controlled by peristaltic pump. The Near-IR spectra were obtained with the probe directly placed inside the mixture. After 300mL titration with the precipitant, the mixture was filtered with a 2.7-micrometer filter. The weighing was continued until the weight was constant.

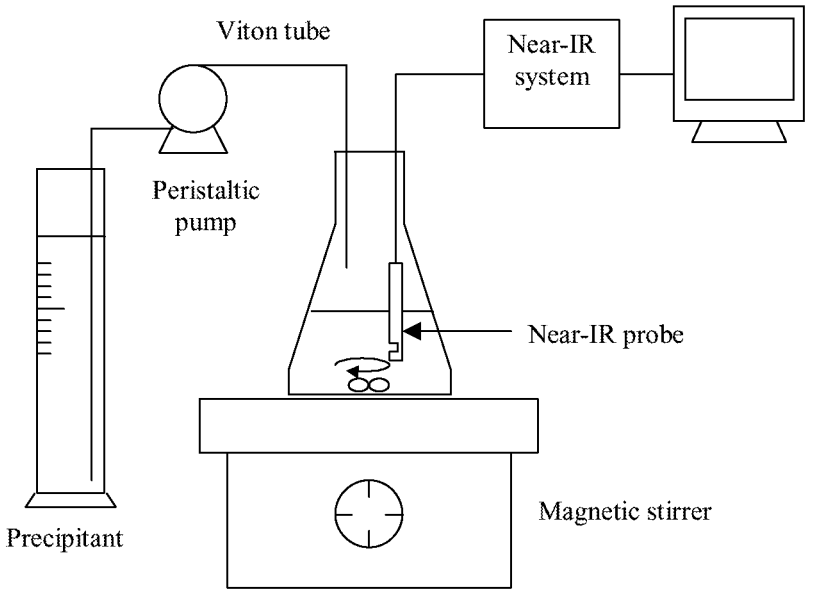

Figure 6-8 Schematic diagram of the experimental system used.

Results and Discussion

A series of spectra at different precipitant concentrations for a typical experiment are shown in **Figure 6-9**. The precipitant used in this experiment was n-heptane. The n-heptane spectrum is also shown for comparison. Most significant information is obtained by studying the absorbance values of the mixtures at around 1600 nm. Fuhr et al.[9] used this wavelength for their diagnostics. Typical absorbance curve at a wavelength of 1600nm is shown in **Figure 6-10**. This curve was obtained by the addition of n-heptane to 40g of the crude oil at a flow rate of 1mL/min. Absorbance data were collected every 30 seconds when n-heptane was added to the oil. The initial decrease in absorbance is due to dilution. The Near-IR signal is affected by a number of factors and it does not decrease linearly as solvent is added. It has been argued that the absorbing molecules in the oil undergo changes that affect the Near-IR absorbance. During asphaltene precipitation, new (larger) particles that absorb/scatter light are formed and this event is adequate to turn the signal upward. The minimum in absorbance corresponds to the onset. As the particles grow and agglomerate, they tend to settle leading to a slight decrease in absorbance as the titration continues. Thus, the mild maximum in the absorbance curve may correspond to the beginning of the settling process. In these types of measurements, the emphasis is only on identifying the starting point of precipitation. These methods (titration type) are a faster alternative to static measurements, and are more suitable for high-pressure/blind cell measurements. The error in these measurements was 0.0125 mL/g of oil.

First few experiments were performed to study the effect of the n-alkane solvent carbon number on the onset and the effect of the addition of toluene. There has been some controversy in the literature regarding the effect of the solvent chain length on precipitation onset. Visually determined onset data by Hirschberg et al. (1984) showed that onset accelerated with increased solvent carbon number. The onset in these experiments was determined by observations through a microscope, which magnified the image 200 fold. Recent measurements by light absorbance/scattering showed that increasing the solvent carbon number delayed the onset (Browarzik, et al., 1999). Precipitation onset points for the Rangely crude oil were measured using three solvents and the results are shown in Figure 6-11. In this figure, the absorbance at 1600 nm is plotted as the various solvents are added at 1 mL/min. In case of n-pentane, the onset is much faster (0.62 mL of precipitant per gram of oil) than with n-hexane (0.87 mL/g) or n-heptane (1 mL/g). Rassamdana et al. (1996) reported similar findings, even though their onset variations (with respect to alkane carbon number) were comparatively small. For the carbon number range studied, as the solvent carbon number increased, more of the solvent was necessary to initiate precipitation. The carbon number range studied was narrow and the trend may reverse for solvents with higher carbon number.

The weight percents of asphaltenes precipitated with the three different alkanes after six hours of titration at a flow rate of 1mL/min are shown in Figure 6-12. As is well known, the amount of asphaltenes increased with decreasing n-alkane carbon number. The weight percents of asphaltenes precipitated were 2.63, 2.02 and 1.68 for n-pentane, n-hexane and n-heptane, respectively. This means that compounds, which were not part of the solids

with n-heptane, were precipitating when n-pentane is used. The flow rate of 1 mL/min was chosen after a number of experiments at different flow rates. It was observed that

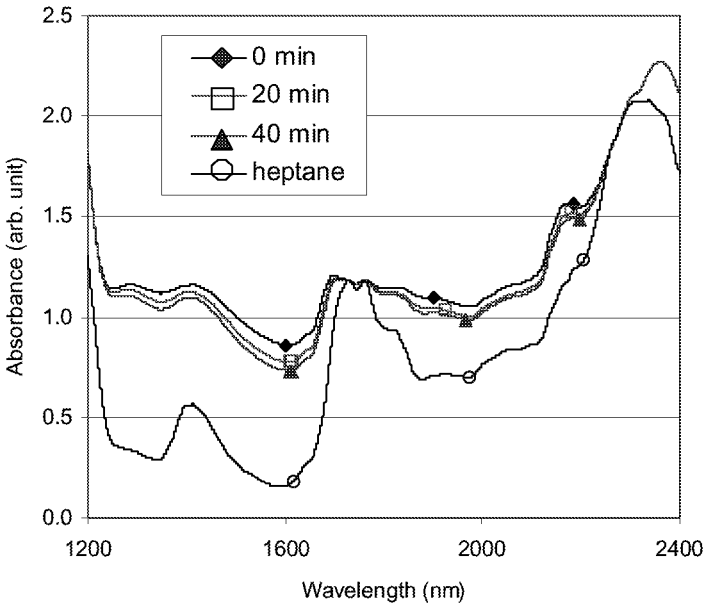

Figure 6-9 Near-IR spectra at various times as oil is titrated with normal heptane. Spectra over the 1200 nm – 2400 nm range are shown.

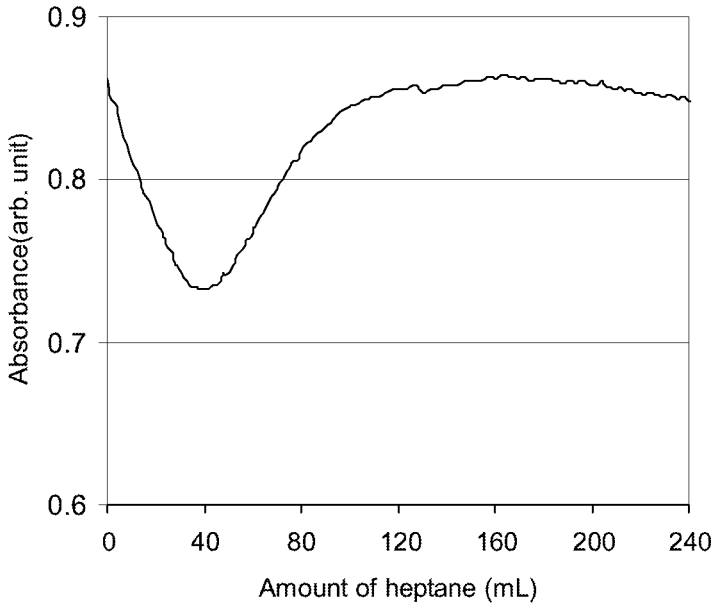

Figure 6-10 Near-IR absorbance at a wavelength of 1600nm for oil titration with heptane (Flow rate = 1mL/min).

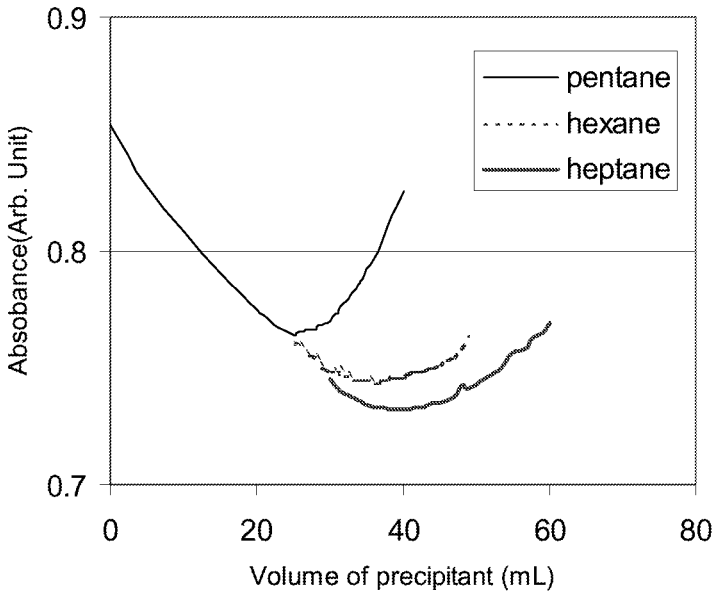

Figure 6-11 Near-IR absorbance curves at 1600 nm when three different precipitants are employed

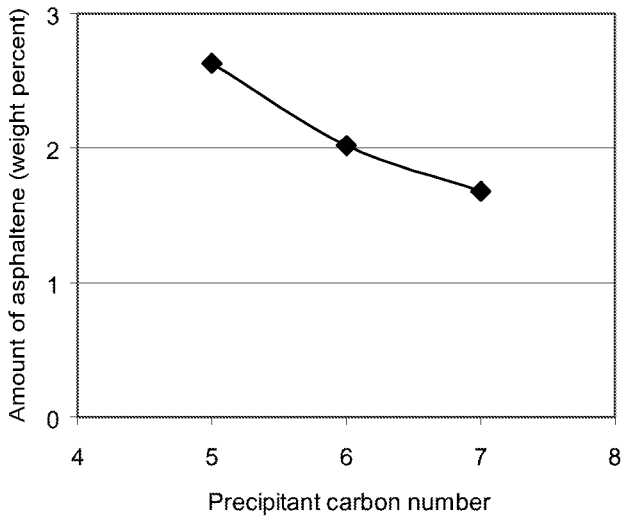

Figure 6-12 Asphaltene amounts versus n-alkane precipitant carbon number after 300 minutes of titration at 1mL/min.

the onset was delayed at higher flow rates. The onset value stabilized at or below 1 mL/min and the differences were within the experimental error in onset determination (0.0125 mL/g of oil). This is to be expected since there are mixing and mass transfer limitations at higher flow rates.

To study the effect of the addition of toluene on precipitation, the Rangely crude oil was initially mixed with different amounts of toluene and the resulting mixtures were titrated using the procedure described. In this experiment, 40g of the crude oil and 5~20 mL of toluene were separately mixed before titration. As the amount of toluene added increased, the precipitation onset was delayed more or less in a linear manner. The data is presented in Figure 6-13. Toluene is a polar compound that acts as a stabilizer in the oil. The toluene onset data (plotted later for comparison with other additives) showed that the oil was undersaturated with respect to asphaltenes.

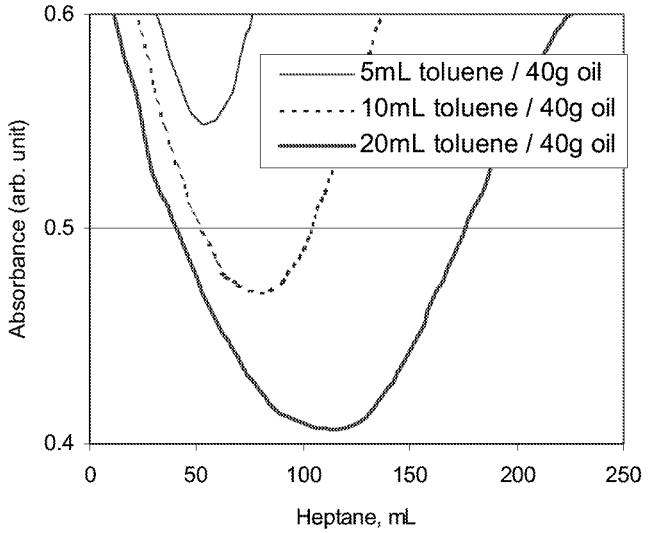

Figure 6-13 Near-IR spectra at 1600 nm for titrations of oil-toluene mixtures with heptane. As more toluene is added, precipitation is delayed.

Effect of addition of n-heptane insoluble asphaltenes on asphaltene precipitation from the oil was examined. In these experiments, asphaltenes were first separated from the oil using a procedure described by Speight et al. (1984) In this method, the oil and the solvent (n-heptane) are mixed at a ratio of 1:40 and equilibrated for 16 hours. The asphaltenes were filtered, washed with n-heptane, and were dried. The asphaltenes so obtained were stored in the laboratory at normal conditions. Dissolution of small amounts of heptane-insoluble asphaltenes in the oil accelerated the precipitation onset from the oil. The Near-IR absorbance values for three solutions of asphaltenes and oil are provided in Figure 6-14. The onset declines from a value of 1.0 mL/g to about 0.75 mL/g by adding 0.5 weight percent n-heptane insolubles to the oil.

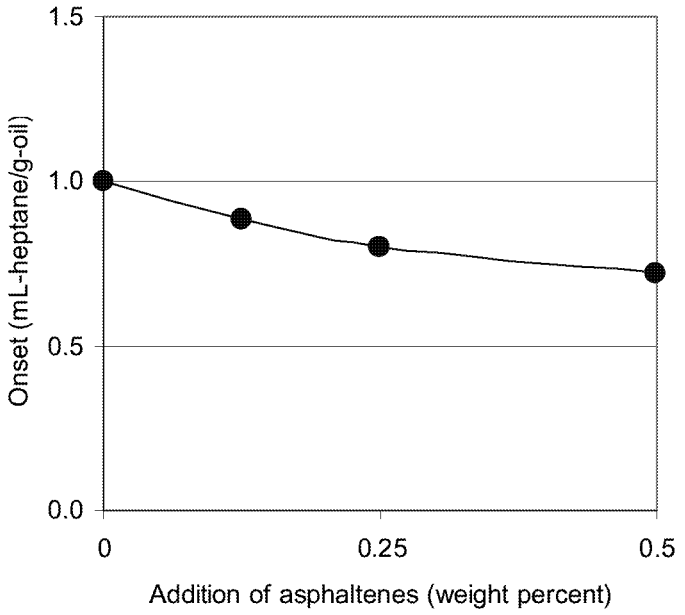

Figure 6-14 Plot indicating accelerated onset when additional n-heptane insoluble asphaltenes are dissolved in oil.

Effect of the addition of hydrocarbon solids

The effect of the addition of solid pure hydrocarbon compounds on the onset is shown in Figure 6-15. Onset data for toluene has also been shown on this plot for comparison. The addition of eicosane and tetracosane accelerated the onset of solid precipitation, while, the addition of phenanthrene, naphthalene and toluene led to delayed solid precipitation from the oil. Onset trend with toluene addition can be viewed to evaluate if the oil is undersaturated with respect to asphaltenes. The positive value of the y-intercept for the toluene line in Figure 6-15can be interpreted to mean that that asphaltenes phase in oil is stable and undersaturated. The effect of the addition of naphthalene and toluene on the onset appears more or less equivalent. Phenanthrene delays precipitation; but, not to the same extent as toluene or naphthalene. Molecular weight of the additive also influences precipitation (apart from its solubility parameter). Rapid accelerations of precipitation observed with small additions of eicosane and tetracosane indicate that seemingly minor changes to the solubility character of the solvent holding asphaltenes in solution has a profound impact on asphaltene precipitation. The finding that naphthalene was more effective than phenanthrene in keeping asphaltenes in solution was contrary to results reported by Clarke and Pruden (1998) for precipitation from Cold Lake bitumen. It appears that the effectiveness of an additive in delaying precipitation depends on the initial composition of the oil. In this study, the measurements were direct and light oil with relatively low amount of asphaltene was used.

Experiments were also performed with mixtures of polar and nonpolar solids. These experiments were performed with the total weight of solid additive fixed at 2 grams. Each solid mixture was initially mixed with 40g of oil. The onset data for these experiments is plotted in Figure 6-16. The x-axis on this figure shows the grams of naphthalene or phenanthrene added (y grams). Since the total weight of solid additive was constant at 2 grams, the weight of eicosane added was equal to 2-y grams. It should be noted that when no solids are added, the precipitation with heptane occurs at 1 mL/g. If the effect of adding mixtures of polyaromatic compounds (naphthalene or phenanthrene) and eicosane on asphaltene precipitation onset was linear, then the onset data for mixtures would lie on straight lines connecting the onset point for the addition of pure eicosane (y = 0) and onset points for the additions of pure naphthalene or phenanthrene (y = 2). These lines are shown in Figure 6-16. Since most of the onset points for the mixtures lie below these straight-lines, it is clear that eicosane has a more dominant effect on onset than either naphthalene or phenanthrene.

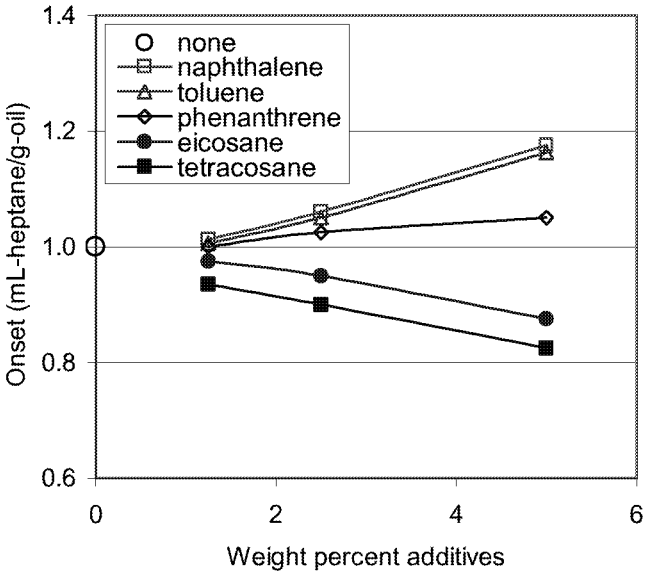

Figure 6-15 Effect of the initial dissolution of n-alkane-solids and polyaromatic compounds (weight percent) in the oil on the onset of asphaltene precipitation from the oil.

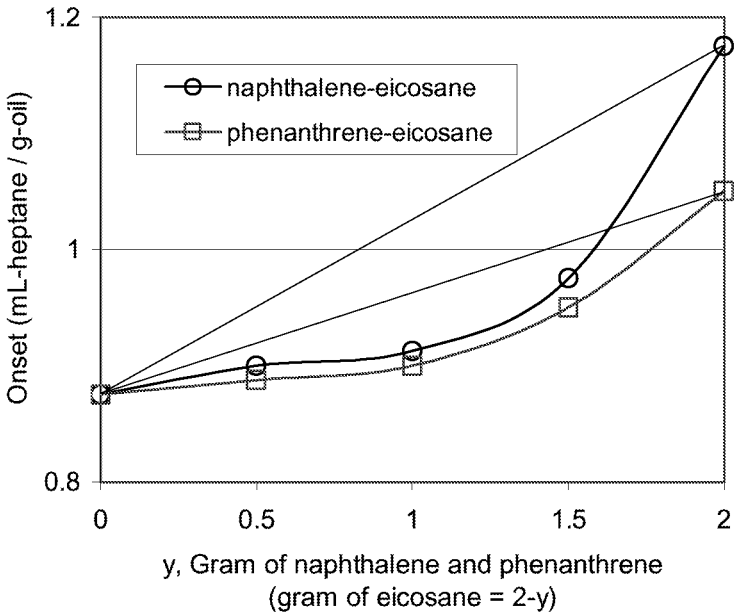

Figure 6-16 Asphaltene precipitation onset changes when combinations of n-alkane and polyaromatic solid compounds are used as additives.

The experiments were repeated using asphaltenes dissolved in toluene. In these experiments, asphaltenic solids from the Rangely field were dissolved in toluene and a 2 weight percent mixture was prepared. The asphaltenic solids were formed in the course of a carbon dioxide flood in the field. The effects of the addition of n-alkane and polyaromatic solids were examined with this mixture. Eicosane or phenanthrene (0.5 grams to 2 grams) was added to the mixture (40 grams) and the precipitation onset was measured using n-heptane as the precipitant. The data is presented in Figure 6-17. The trend in precipitation initiation with additions n-alkane and polyaromatic solids is observed to be similar to the oil data. These experiments show that it is possible to dissolve asphaltenes in appropriate solvents and reprecipitate them using n-alkane additives. The type of compositional changes that cause either delayed or accelerated precipitation are observed in oils and in asphaltene-solvent mixtures.

This study is an examination of the onset of asphaltene precipitation and how it is affected by solid organic additives to the whole oil. As lighter n-alkanes are used, the amounts of solids precipitating increase indicating that some compounds which remained in solution with higher n-alkanes, become part of the class. It is logical also that precipitation occurs sooner with lighter alkanes than with the heavier ones. Whatever changes the quality of the solution changes the solution dynamics of the compounds in solution. Addition of small quantities of straight-chain, n-alkane solid compounds decreases the relative solubility of the asphaltenic compounds and expedites their precipitation. Addition of polyaromatic compounds increases the overall solubility of the solution and delays precipitation of asphaltenic material.

The data reported in this paper underscores the nature of asphaltenes as a solubility class. Basic compound properties of the additives used in this study (including the solubility parameters) are listed in Table 1. The solubility parameters of naphthalene and phenanthrene are about 9.9 $(cal/mol)^{0.5}$, which are in the same range as the solubilities of the asphaltenic compounds. The solubility parameters of eicosane and tetracosane are 8.06 $(cal/mol)^{0.5}$ and 7.42 $(cal/mol)^{0.5}$ respectively. Based on several studies in the literature, asphaltene solubility parameter is approximately between 9.0$(cal/mol)^{0.5}$ and 10 $(cal/mol)^{0.5}$. Higher the contrast between the solubility parameters of the asphaltenic compounds and the additives, easier and quicker it is to bring them out of solution. When adding multiple additives, the low solubility parameter compounds govern the behavior of the solution and it is not possible to offset the effect by adding compounds with higher solubility. However, solubility parameter is not the sole determinant of the effect of the additive. The molecular weight and other properties of the additives become important. The delay in precipitation becomes more gradual as the solid additive is changed from naphthalene to phenanthrene. Addition of asphaltenes to the oil, expedited the precipitation of the dissolved asphaltenic compounds from the oil.

The data can also be examined with respect to the co-precipitation implications. Since adding solid n-alkanes brings about a quicker onset of asphaltene precipitation, it can be assumed that taking them out of the oil, selectively, helps keep asphaltenes in solution. It is quite clear that the precipitation of n-alkanes from the oil on cooling (wax precipitation) is governed by the solubilities of these alkanes in oil. As the alkanes come

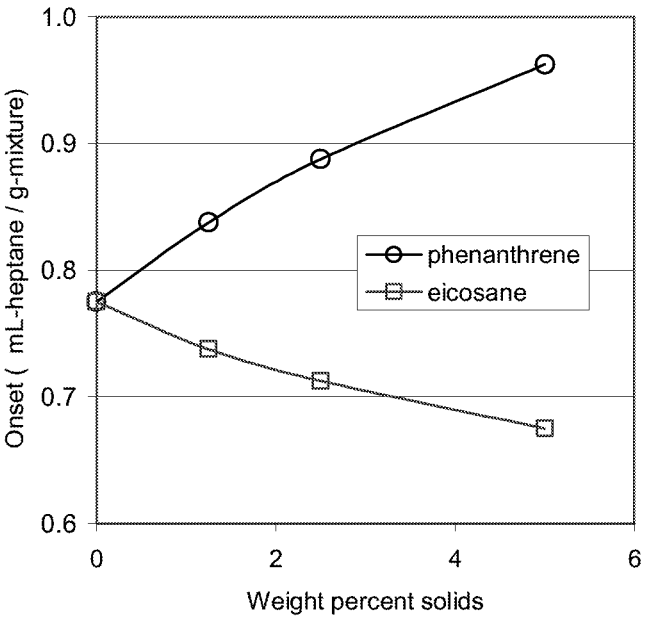

Figure 6-17 Asphaltene precipitation onset from asphaltene-toluene mixtures with the addition of n-alkane solid or polyaromatic compounds

Table 6-2 Solubility parameters and melting temperature of solids in this study

	Molecular Weight	Solubility Parameter $(cal/mol)^{0.5}$	Melting Point (°C)
Toluene	92.14	8.93	-95
Naphthalene	128.17	9.9	80.5
Phenanthrene	178.23	9.92	100
Eicosane	282.55	8.06	36.8
Tetracosane*	338.66	7.42	54

*at 374K from reference 25

out of solution, the polar components that have higher solubility in the oil to begin with, have even greater solubility in the remaining oil (liquid) mixture making their precipitation unlikely. It should be noted that from an overall compound classification viewpoint, the oil that was examined contained close to 50% saturated compounds.

Summary

The onset of asphaltene precipitation from a light crude oil was determined using Near-IR spectroscopy. In the carbon number range studied (5 to 7), more solvent was necessary to initiate precipitation onset as the carbon number of the solvent increased. The onset was faster when the n-alkane carbon number of the precipitant decreased resulting ultimately in higher amounts of asphaltenes precipitated. Addition of toluene delayed precipitation and also showed that the oil was undersaturated with respect to the asphaltenes. When aromatic solids (phenanthrene and naphthalene) were initially mixed with the oil, the onset of solid deposition was delayed. In case of the addition of solid n-alkane compounds (eicosane and tetracosane), the onset of solid precipitation was accelerated. Addition of separated asphaltenes to the oil, however, accelerated the precipitation onset. When mixtures of polar and nonpolar solids were added, the precipitation was governed by the nonpolar compound additive. These observations were true for the reprecipitation of dissolved/dispersed asphaltenes as well. The measurements show that the complex phenomenon of dissolved asphaltene precipitation is controlled to a significant extent by simple solubility rules.

7. Compositional Modeling

The experimental component of the project focused on thermodynamics and kinetics of precipitation. Traditionally this static data has been interpreted in the context of one-dimensional displacements in rocks. The compositional simulations performed in this project were aimed at understanding the mechanisms of displacements in two-dimensional setting and how they differed from the one-dimensional displacements.

Pure-Component Preliminary Simulations

Simulations with a model oil were performed with a three-component system containing methane, decane and carbon dioxide. In the one-dimensional simulations, the 60-foot domain was divided into 20 equal sized blocks. The grid size in the y and z directions was 0.025 foot. All the simulations were performed at 160^0F. The porosity was 30% and the permeability was 1 Darcy. In order to minimize or eliminate the effects of relative permeabilities, straight-line relative permeabilities were employed. Initial concentrations were 25% methane, 30% butane and 45% decane. Simulations were conducted by injecting pure CO_2 at different pressures. The saturation plots and compositional profiles at three different pressures were presented in an earlier report (Deo, 2000).

The displacement at 1500 psia was immiscible as evidenced by the number of pore volumes required to recover all of the heavier component. It was also seen that the oil bank was not formed. The displacement at 1800 psia was multiple-contact miscible, as seen from the oil bank and recovery profiles. The displacement at 1900 psia was first contact miscible because in about one pore volume injection, all of the components were recovered. This was a simple, well researched three-component system and the minimum miscibility pressure could be established to be about 1725 psia at 160^0F.

Identical compositional system was simulated in two dimensions. The two dimensional model was 20X1X5. It was a interwell-scale model, 2000 feet in the x direction and 150 feet in the z-direction. The model was one foot in thickness. At 1800 psia, there is multiple-contact displacement in a one-dimensional setting. In the two-dimensional setting, in the top layer, the displacement is more efficient. This is due to the "drainage" of some of the oil to the lower layers and due to the fact that the CO2 overrides and provides more efficient contact in the top layer. The gravity override creates a scenario wherein CO2 does not contact the oil in the bottom layer, extracting it less efficiently. The displacement and recovery in the middle layer is multiple-contact miscible and is similar to that in one-dimensional model. Thus, the compositional paths in different sections of the reservoirs are different. This implies that for a reservoir undergoing multiple-contact displacement, the middle and the bottom layer would be susceptible for solids deposition. For a reservoir undergoing immiscible displacement, the top layer would have MCM-type displacement, making it also more susceptible to precipitation.

Similar results were obtained with four and six component systems.

Simulations with the Rangely Crude

The composition of the Rangely Crude oil used in all the simulations is shown Table 4-2. The composition is identical to the live-oil composition used in thermodynamic modeling of the precipitation results (Section 5). One and two dimensional studies were conducted using the same geometrical systems described in the pure-component simulations. One-dimensional results at three different pressures (1900 psia, 3500 psia and 4000 psia) are shown in Figure 7-1 to Figure 7-6.

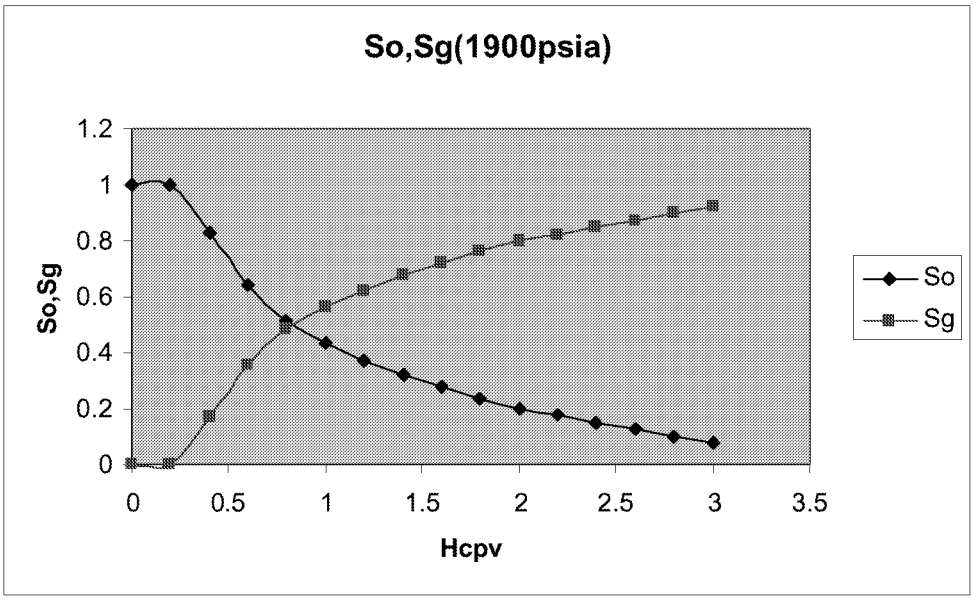

Figure 7-1 Oil and gas saturations for the Rangely crude oil system at 1900 psia

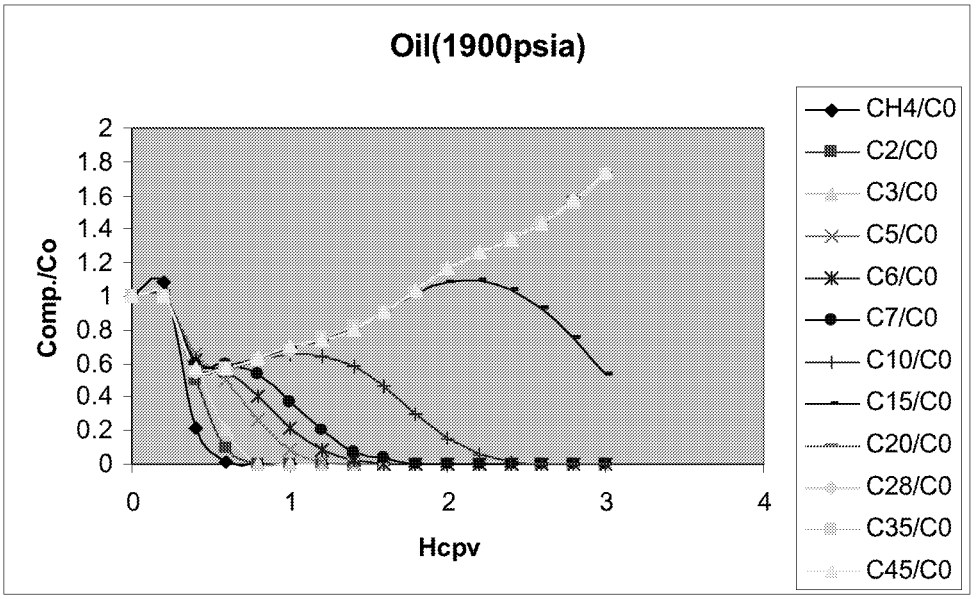

Figure 7-2 Individual component concentrations versus pore volumes of carbon dioxide injected - 1900 psia

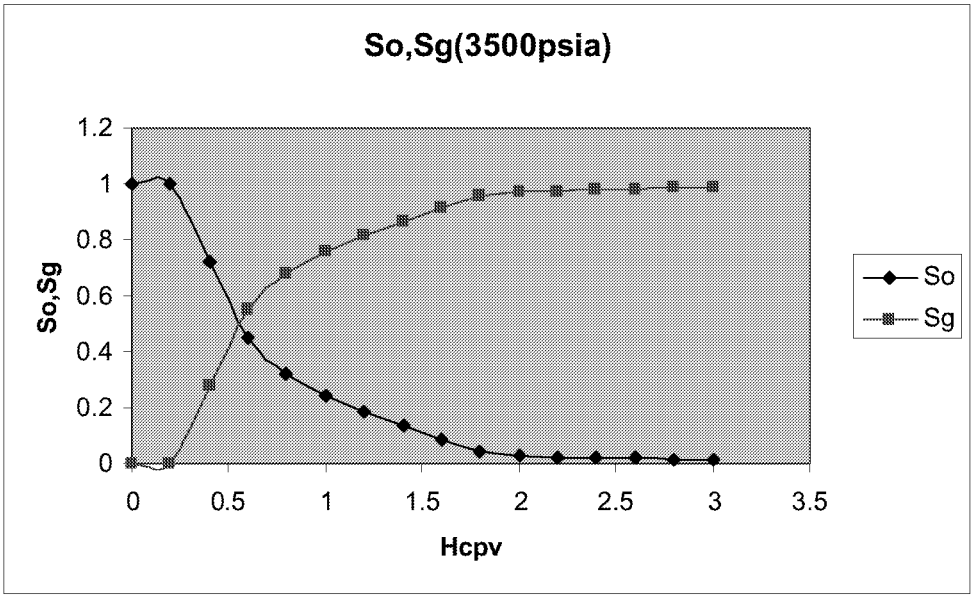

Figure 7-3 Oil and gas saturations for the Rangely crude oil system at 3500 psia

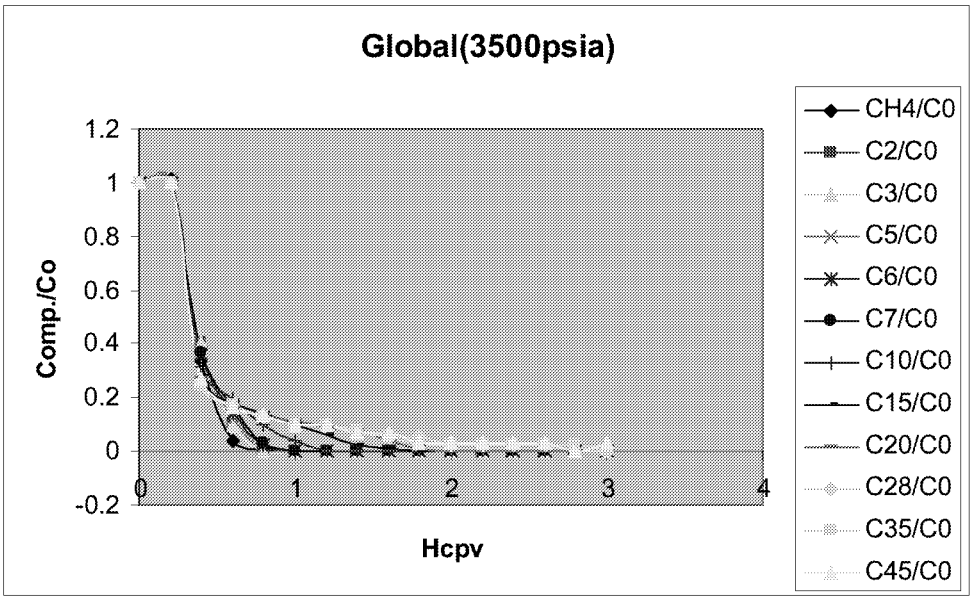

Figure 7-4 Individual component concentrations versus pore volumes of carbon dioxide injected - 3500 psia

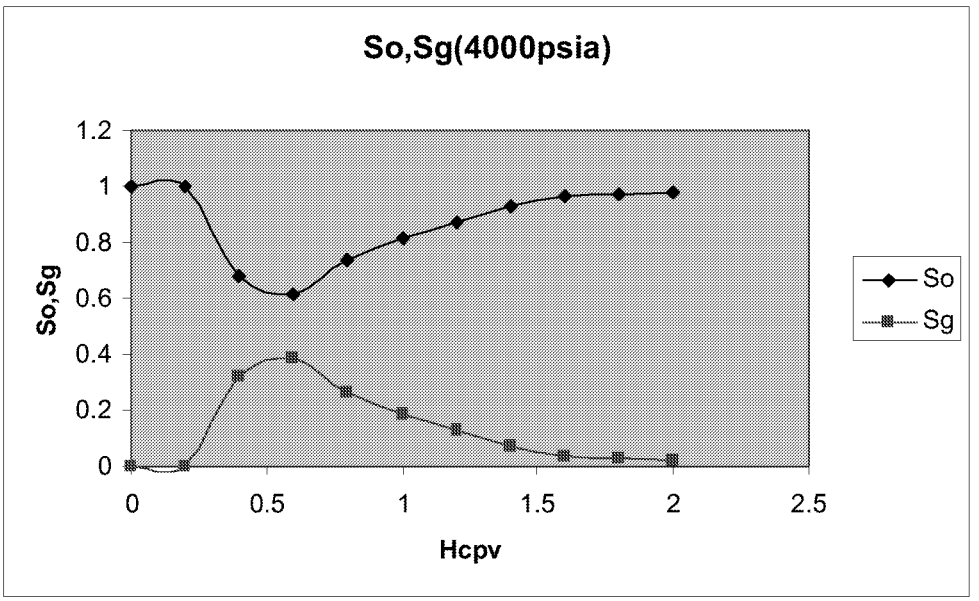

Figure 7-5 Oil and gas saturations for the Rangely crude oil system at 4000 psia

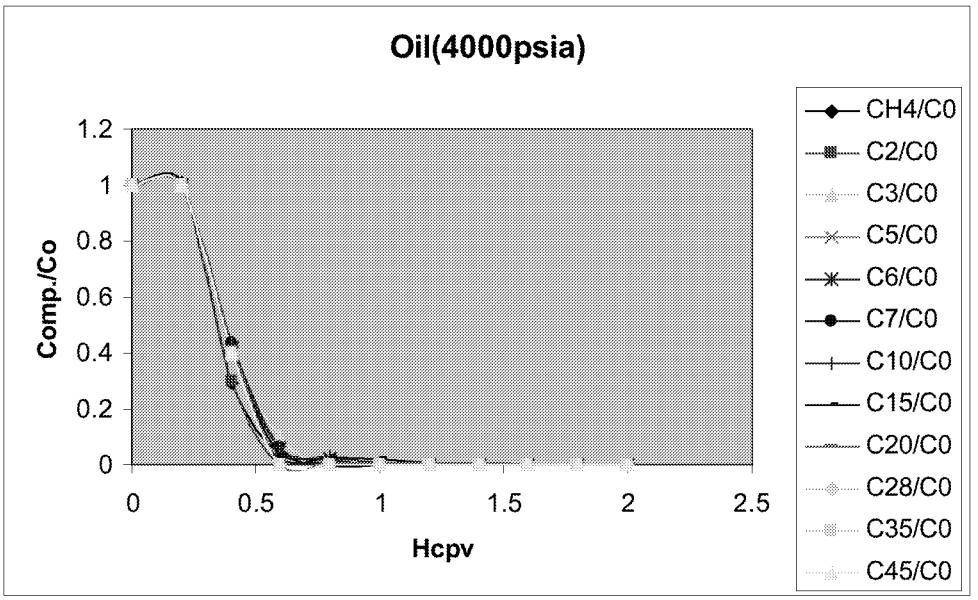

Figure 7-6 Individual component concentrations versus pore volumes of carbon dioxide injected - 4000 psia

It is clear from the figures that at 1900 psia, the oil undergoes immiscible displacement, while at 3500 psia, an MCM type displacement occurs. First-contact displacement takes place at 4000 psia. This is the only pressure at which two saturation shocks are seen. At 3500 psia, it takes between 1.5 to 2 PV injection to recover 95% of the heavier components.

Figure 7-7to Figure 7-13 show saturation and composition profiles for the same system in a two-dimensional setting. At 3500 psia, the upper portion of the reservoir is depleted in less than one pore volume. The saturation shocks are fast. This is related to the carbon dioxide override and drainage of oil into the middle and bottom layers. The middle layer, where oil is recovered in about 1.5 PV, behaves more like a multiple-contact displacement. The oil and gas saturation shocks are slower than in the upper portion of the reservoir. The recovery from the bottom layer is slower and thus it is exposed to a different compositional environment. Overall, the reservoir behaves like it is being displaced through the multiple-contact displacement process. This exercise showed that multiple contact displacement is being effected at Rangely; however, different portions of the reservoir are being subjected to different compositional history. As a result, the bottom portions of the reservoir, are more susceptible to the formation of solids. These simulations did not consider viscous fingering or reservoir heterogeneities.

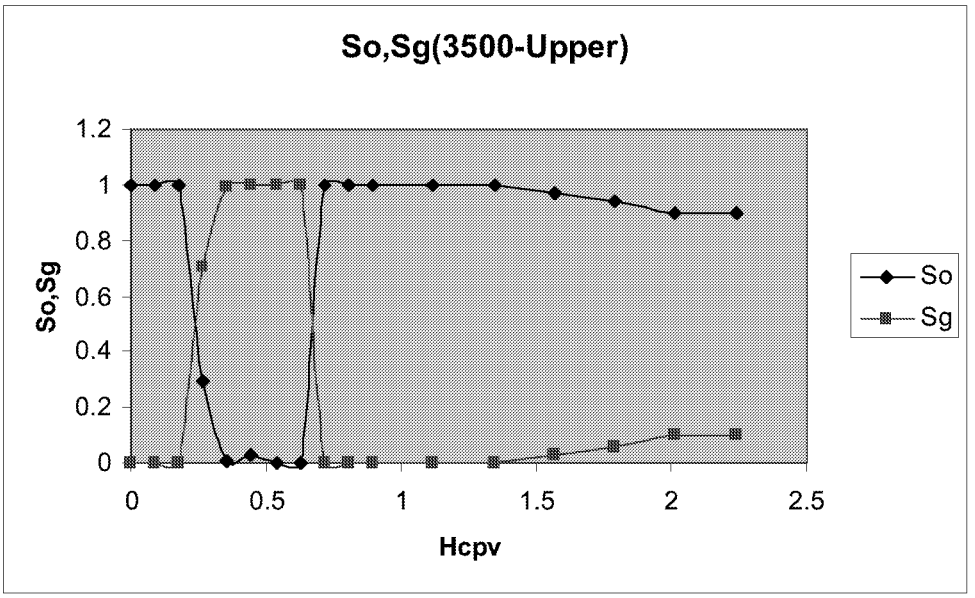

Figure 7-7 Oil and gas saturations in the upper portion of the reservoir (top two layers) at 3500 psia

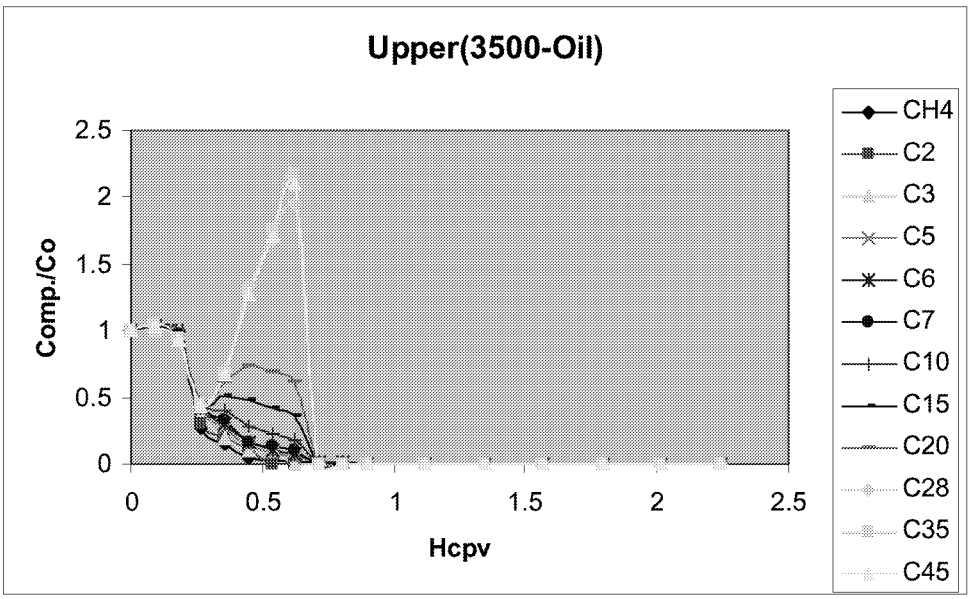

Figure 7-8 Compositions of all the components in the upper two layers at 3500 psia. Most of the components are recovered/drained prior to 1 PV injection with displacement resembling first-contact

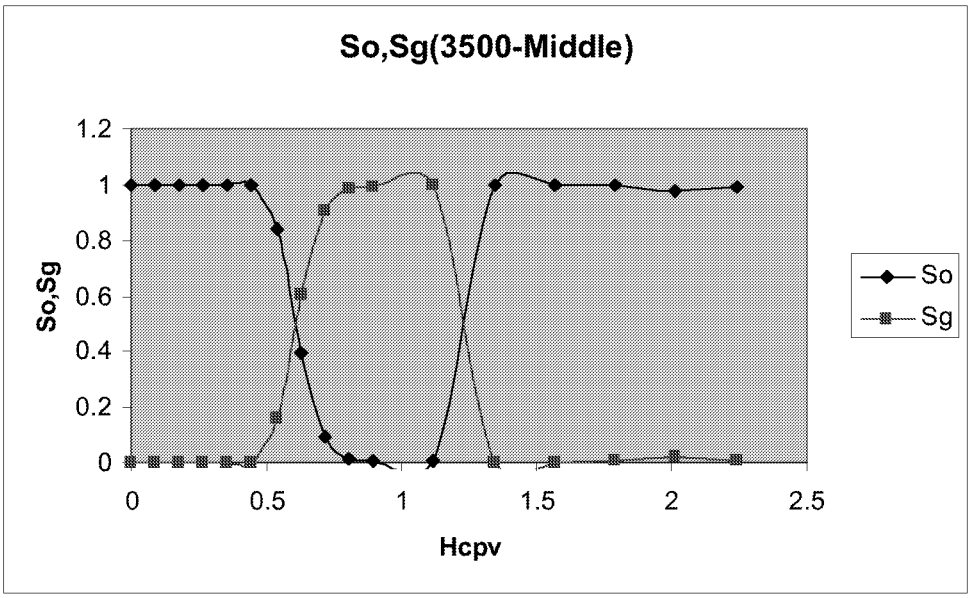

Figure 7-9 Oil and gas saturations in the middle portion of the reservoir (middle layers) at 3500 psia. The saturation shocks travel slower than in the upper portion of the reservoir.

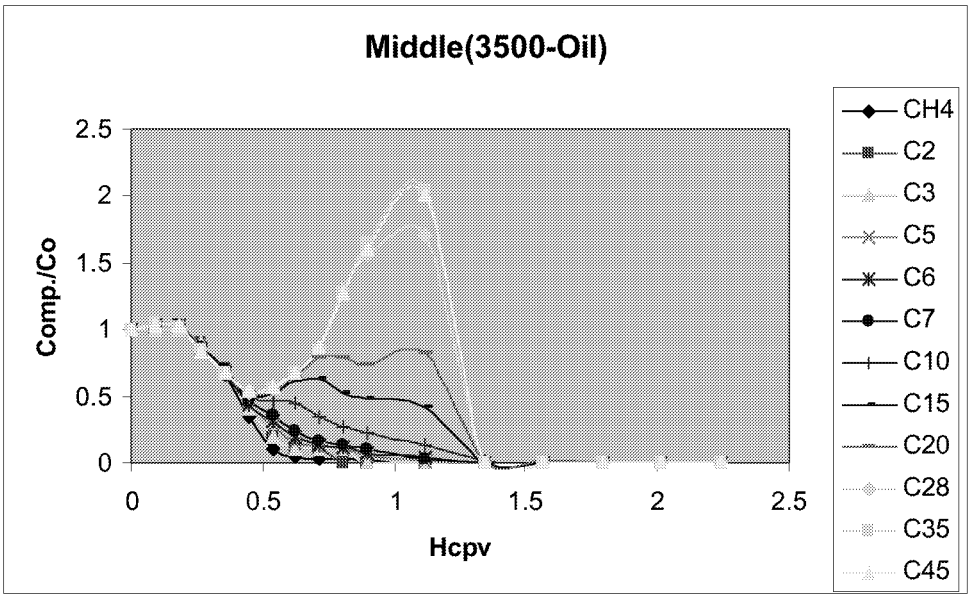

Figure 7-10 Compositions of all the components in the middle layers at 3500 psia. Most of the components are recovered/drained at about 1.5-2 PV injection with displacement resembling multiple-contact miscible

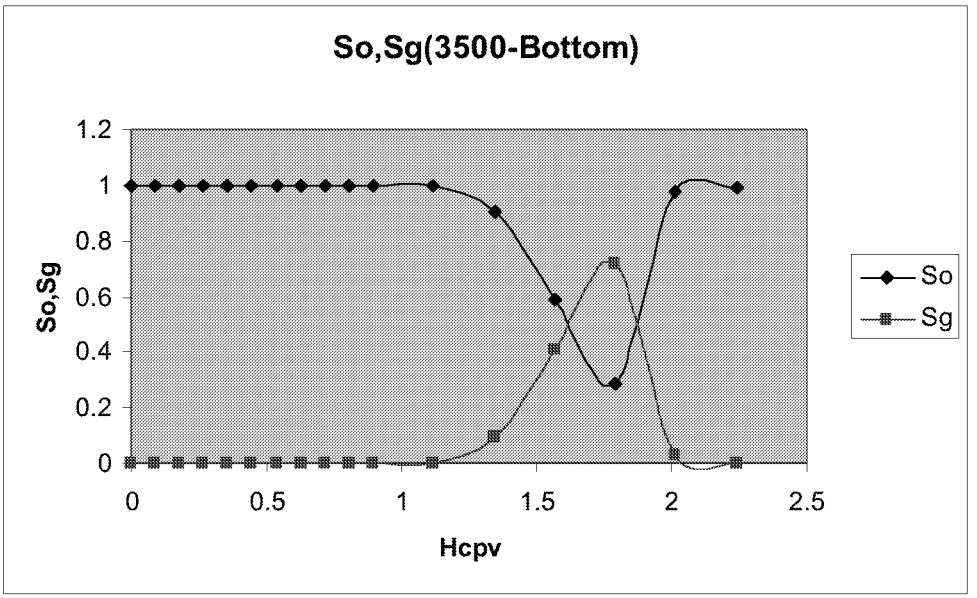

Figure 7-11 Figure 7-12 Oil and gas saturations in the bottom portion of the reservoir (bottom two layers) at 3500 psia. The saturation shocks travel the slowest.

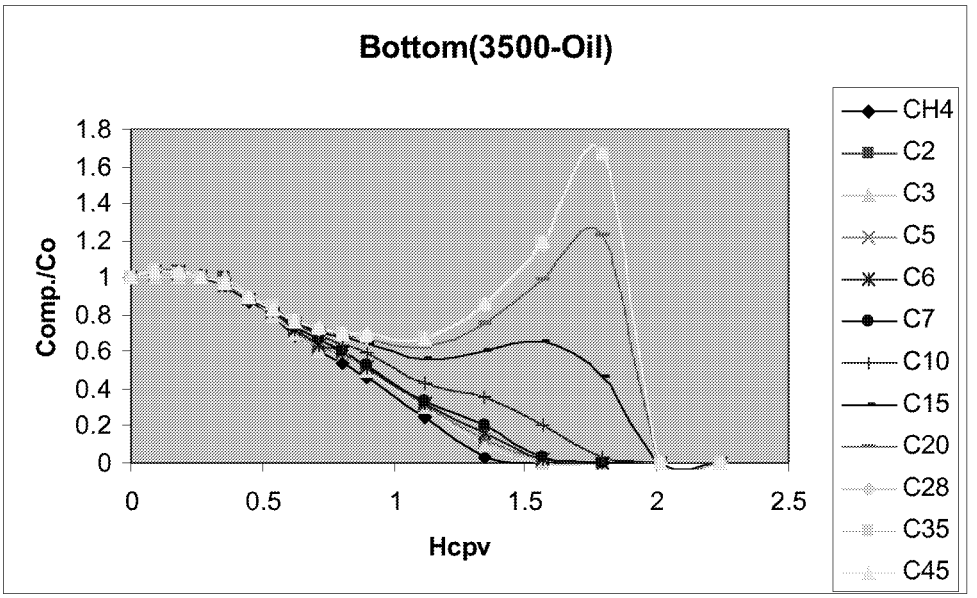

Figure 7-13Compositions of all the components in the bottom two at 3500 psia. Most of the components are recovered/drained at about 2 PV injection with displacement resembling multiple-contact to immiscible

8. Summary and Conclusions

The objective of this project was to establish conditions that lead to carbon dioxide induced solids precipitation in carbon dioxide enhanced recovery floods. The primary purpose was to determine thermodynamic conditions at which precipitation occurs. Measurement of kinetics of precipitation, thermodynamic and compositional models of precipitation were also project goals.

A high-pressure thermodynamic system was designed and fabricated, and a number of thermodynamic experiments were performed with dead oils (oils with no initially dissolved gas) and with live oils (oils with a predetermined quantity of dissolved gas). The success of the carbon dioxide miscible floods (over 90% of the carbon dioxide floods fall into this category) depends on the development of miscibility. Therefore, one of the logical questions that arose in the course of this research was how the process of miscibility development affected the solids formation from oils. To answer this, two types of experiments were conducted; one where a light-to-intermediate cut (C_{15}-) was added to the crude oil; the second was a true multiple contact miscibility experiment. Most of the experiments were performed using the crude oil from the Rangely field, where Chevron, Inc. is conducting one of the largest carbon dioxide floods in the world. The Rangely crude oil is a high-API oil with low asphaltene content. A few experiments were also performed using a high asphaltene crude oil provided by Phillips.

The liquids were analyzed primarily via SARA fractionation, gas chromatography, gas chromatography-mass spectrometry and by FTIR. The solids were analyzed by a variety of methods; SARA fractionation, FTIR, chemical ionization – mass spectrometry, time of flight mass spectrometry, etc.

Comparison of results with the dead and live oils showed that the precipitate amounts were three to four times higher from live oils compared with equivalent dead oil solid deposits. The results also showed that precipitation starts between 20 –30 mole% CO_2. To simulate the effect of enrichment with intermediate components to attain miscibility, a light cut (85% below C_{15}) from the crude oil itself was added to the live oil. With the addition of the "light-intermediate" fraction, the amount of precipitation was approximately twice the amount for equivalent CO_2 concentration without the cut (compared to live oil precipitates). The precipitation was also more sensitive to CO_2 concentrations and increased more rapidly as CO_2 concentrations went up. The concentrations of pentane insolubles in the precipitates were about 44% for CO_2 concentration of at least 48 mole%. Therefore, these CO_2 induced precipitates were heavier solids. Pentane insolubles in the liquid fractions were reduced more significantly than in the case of live oil experiments, without the addition of the specially distilled cut.

True multiple contact experiments were performed with dead oils. The multiple contact precipitate amounts were about two to three times the first contact precipitate amounts for the same CO_2 concentrations. First contact experiments with live oils gave three to four times more precipitation than first contact experiments with dead oils.

The analysis of precipitates from thermodynamic experiments and solids obtained from the field revealed that the CO_2 induced precipitates are not all asphaltenes (defined as either pentane or heptane insoluble solids). The laboratory sample contained significant fractions of saturates. The asphaltenes in the field solid sample, in comparison to the laboratory sample, were higher. On GC-MS analyses, a number of five ring aromatic compounds were identified among the polyaromatics.

Chemical structures of asphaltenes and resins are complex and similar. However, from their infrared spectra, it became evident that the polar groups in the asphaltene fractions are appreciably lower in intensity than those existing in the resins. It was also found that there were differences between CO_2 induced precipitates and paraffinic insoluble precipitates (asphaltenes); the former contained more polar functionalities and shorter substituted alkyl chains. According to chemical ionization spectra, molecular weights of CO_2 induced precipitates and asphaltenes were determined to be below 1000 amu. For the resins, masses from 60 to 1000 amu were examined, and the fragments registered intensities from 200 to 850 amu, with a mean molecular weight of about 600 amu. Time of flight mass spectrometry (TOF-SIMS) and chemical ionization results consistently suggested that the asphaltenes molecular weights were below 1000, which is in agreement with previously published data Asphaltene molecular weight values of several thousand amu must be due to the high aggregation of asphaltenes in solution. Most compounds, from TOF-SIMS, even with complex structures had only 5-7 rings.

An attempt was made to explain the thermodynamic data by using two thermodynamic models; a homogeneous molecular model and a dense solid phase model. Homogeneous Molecular Thermodynamic Model gave a better representation of the precipitation of solids, especially for dead and live oils. The model prediction was in close agreement with the experimental data after regression of asphaltene properties such as molar volume, solubility parameter and molecular weight.

Corefloods confirmed that most of the precipitation in carbon dioxide floods is associated with the generation of multiple-contact miscibility. No additional precipitation was observed in simulated wellbore experiments, where the multiple-contact mixture was flashed.

Kinetic experiments showed that addition of simple polyaromatic compounds delays precipitation. These experiments also showed that co-precipitation of wax was likely with asphaltene precipitation, but significant co-precipitation of asphaltenes with wax was unlikely.

Compositional simulations showed that, even though multiple-contact displacement may be occurring , overall, in the reservoir, different portions of the reservoir may experience different compositional environments. This would be true even in homogeneous reservoirs, where carbon dioxide override and thus gravity drainage is possible.

9. Acknowledgements

We would like to thank my faculty colleagues, Dr. Terry Ring, Dr. Francis hanson and Dr. Dave Wavrek for their contribution during the project and to this report.

Most of the project work was undertaken by graduate students working toward their degree programs and our thanks to all of them. The following graduate students worked on the project over the last three years.

Martha Parra Ramirez
Kyeongseok Oh
Duan Schici
Sangeetha Pasala
Robab Emami

Martha Parra developed the results for the thermodynamic portion of the report in her Ph.D dissertation (University of Utah, 2001). K. Oh provided the results for the kinetic portion of the report and S. Pasala for the compostional simulations. The homogeneous thermodynamic model, which Martha Parra used subsequently was developed by D. Schici.

The following undergraduate students worked on different aspects of the project.
Brett Peterson
Jessica Moffitt
Susan Bowman

We would also like to acknowledge support from the Chevron Field Office in Rangely Colorado. They provided oil and asphaltene samples and provided technical details at meetings. We would like to thank Mr. Wackowski, and Mr. Cramer for their help from that office. The Chevron LaHabra Research center donated a back pressure regulator without which core floods and sampling in thermodynamic experiments would have been very difficult, if not impossible. We would like to thank Mr. Jayram Kamath and Mr. Russ Boyer from the Los Angeles office.

We would also like to thank project managers from NPTO who helped with suggestions and comments during the project. Our thanks to Mr. Bobby Harris, Mr. Dan Ferguson and Mr. Jerry Casteel.

10.References

Andersen, S. I., 1999, Flocculation Onset Titration of Petroleum Asphaltenes, *Energy & Fuels*, 13, 315-322.

Andersen, S.I., Lindeloff, N. and Stenby, E.H., 1997, Investigation on asphaltene precipitation at elevated temperature. Petroleum Science and Technology 16 (3 –4): 323-334.

Andersen, S.I. and Speight, J.G., 1993, Observations on the critical micelle concentration of asphaltenes. Fuel 72(9): 1343- 1344.

Brock, W. R. and Bryan, L. A., 1990, Summary Results of CO_2 EOR Field Tests, 1972-1987, Paper SPE 18977 presented at the Seventh SPE/DOE EOR Symposium, Tulsa, OK, April, 11.

Buckley, J.S., 1999, Predicting the Onset of Asphaltene Precipitation from Refractive Index Measurements, *Energy Fuels* , 13, 328-332.

Bukka, K.; Hanson, F.V.; Miller, J.D. and Oblad A.G., 1992, Fractionation and Characterization of Whiterocks Tar sands Bitumen. Energy and Fuels 6(2):160-165.

Burke, N. E., Hobbs, R. D. and Kashou, S. F., 1990, Measurement and Modeling of Asphaltene Precipitation, JPT, Volume 42, No. 11, 1440-1446.

Bryant, D. W. and Monger, T. G., 1988, Multiple-Contact Phase Behavior Measurement and Application With Mixtures of CO_2 and Highly Asphaltic Crude, *SPE Reservoir Engineering*, May, 701-710.

Chang, C. L.; Fogler, H. S., 1993, Asphaltene Stabilization in Alkyl Solvents Using Oil-Soluble Amphiphiles, Paper SPE 25185 presented at the SPE International Symposium on Oilfield Chemistry, New Orleans, LA, March, 1993.

Christy, A.A.; Dahl, B.; and Kvalheim, O.M., 1989, Structural features of resins, asphaltenes and kerogen studied by diffuse reflectance infrared spectroscopy. Fuel 68 (4): 430 – 435.

Clarke, P. F.; Pruden, B. B., 1998, Asphaltene Precipitation from Cold Lake and Athabasca Bitumens, *Petr. Sci. Technol.*, 16(3&4), 287-305.

CMG Ltd. User's guide WinProp. Version 1999.

Darmstadt, H, Chaala, A., Roy, C. and Kaliaguine, S. SIMS and ESCA characterization of bitumen reinforced with pyrolytic carbon black. Fuel 75 (2): 125 - 132, 1996.

Deo, M. D., 2000, Enhancing the Effectiveness of Carbon Dioxide Flooding by Managing Asphaltene Precipitation, Annual Report, U.S. DOE Project, Contract Number: DE-AC26-98BC15107.

Deo, M. D. and Hanson, F.V., 1994, Asphaltene Rejection Via Supercritical Fluid Extraction, *Fuel*, **73**, #9, 1493.

Deo, M. D., and Hanson, F. V., 1993, Asphaltene Precipitation: Experimental Observations and Modeling, SPE 25193, *Proc. 1993 SPE Intl. Symp. Oil Field Chemistry*, SPE, Dallas, 429-434.

Deo, M. D., Hwang, J. and Hanson, F. V.,1993, The Effect of Cosolubilizing Lighter Components on the Asphaltene Content of Heavy Oils, *Fuel. Proc. Tech.*, **34**, 217-228.

Escobedo, J.; Mansoori, G.A., 1995, Viscometric Determination of the Onset of Asphaltene Flocculation: A Novel Method, *SPE Production and Facilities*, May, 115-118.

Fotland, P., 1993, Detection of Asphaltene Precipitation and Amounts Precipitated by Measurement of Electrical Conductivity", *Fluid Phase Equilibria*, 82, 157-164.

Fuhr, B.J., Cathrea, C., Coates, L, Kalra, H and Majeed, A.I., 1991, Properties of Asphaltenes from A Waxy Crude, *Fuel*, 70,1293-1297.

Graue, D. J. and Zana, E. T., 1981, Study of a Possible CO_2 Flood in Rangely Field, Journal of Petroleum Technology, July, 1312-1318.

Groenzin, H; and Mullins, O.C., 2000, Asphaltene Molecular Size and Structure of asphaltenes from various sources. Energy and Fuels 14 (3): 677 – 684.

Hervey, J. R. and Iakovakis, A. C., 1991, Performance Review of a Miscible CO_2 Tertiary Project: Rangely Weber Sand Unit, Colorado, *SPE Reservoir Engineering*, May, 163-168.

Hirschberg, A., deJong, L. N. J., Schipper, B. A. and Meijer, J. G., 1984, Influence of Temperature and Pressure on Asphaltene Flocculation, Society of Petroleum Engineers Journal, Volume 24, 283-293.

Huang, E. T. S., 1992, The Effect of Oil Composition and Asphaltene Content on CO_2 Displacement, SPE 24131, Paper Presented at the Eighth Symposium on Enhanced Oil Recovery of the SPE/DOE held in Tulsa, OK, April.

Hwang, R.J. and Ortiz, J., 1998, Effect of CO_2 flood on geochemistry of McElroy oil. Organic Geochemistry 29 (1 - 3) part 1: 485 – 503.

Kawanaka, S., Park, S. J. and Mansoori, G. A., 1991, Organic Deposition from Reservoir Fluids: A Thermodynamic Predictive Technique, SPERE, May, 185.

Kokal, S. L.; Sayegh, S. G., 1995, Asphaltenes: The Cholesterol of Petroleum, Paper SPE 29787 presented at the SPE Middle East Oil Show, Society of Petroleum Engineers, Barain, March.

Masoner, L. O. and Wackowski, R. K., 1994, Rangely Weber Sand Unit CO_2 Project Update: Decisions and Issues Facing a Maturing EOR Project, SPE 27756 Presented at the SPE/DOE Ninth Symposium on Improved Oil Recovery held in Tulsa, Oklahoma, April.

Miller, J.T., Fisher, R.B., Thiyaganarajan, P., Winans, R.E. and Hunt, J.E. Subfractionation and characterization of Mayan asphaltene. Energy and Fuels 12 (6): 1290 - 1298, 1998.

Monger, T. G. and Trujillo, D. E., 1991, Organic Deposition During CO_2 and Rich-Gas Flooding, SPERE, February, 17.

Monger, T. G. and Fu, J. C., 1987, The Nature of CO_2-Induced Organic Deposition, SPE 16713, Paper presented at the 62nd Annual Meeting of the SPE, Dallas, TX.

Nghiem, I.X., Hassam, M.S. and Nutakki, R., 1993, Efficient Modelling of Asphaltene Precipitation. Paper SPE 26642, 275-384, 1993.

Novosad, Z. and Costain, T. G., 1990, Experimental and Modeling Studies of Asphaltene Equilibria for a Reservoir Under CO_2 Injection, Paper SPE 20530 Presented at the 66th Annual Technical Conference and Exhibition of the SPE held in New Orleans, LA September.

Orr, F. M., Jr., and Taber, J. J., 1981, Displacement of Oil by Carbon Dioxide, DOE/ET/12082-9, U. S. Department of Energy.

Parra-Ramirez, M., 2002, Precipitation and Characterization of Asphaltenes, Ph. D. Dissertation, University of Utah, Salt lake City, UT.

Payzant, J.D.; Lown E.M. and Strausz, O.P.,1991, Structural Units of Athabasca asphaltene: The aromatics with a linear carbon framework, Energy and Fuels 5(3):445-453.

Rassamdana, H.; Dabir, B.; Nematy, M.; Farhani, M.; Sahimi, M., 1996, Asphalt Flocculation and Depostion: I. The Onset of Precipitation, *AIChE J.*, 42, 10-22.

Ring, T. A. and Dirksen, J. A., 1997, LiBr Crystallization Inhibitors, Second Annual Report to the Gas Research Institute, January.

Speight, J.G. The chemistry and technology of petroleum, 3rd. edition, Dekker, 1999.

Speight, J. G., Long, R.B. and Trowbridge, T.D., 1984, Factors Influencing the Separation of Asphaltenes from Heavy Petroleum Feedstocks, *Fuel* 63, 616-620.

Walas, S. M., 1985, Phase Equilibria in Chemical Engineering, Butterworth-Heinemann.

Wilt, B.K., Welch, W.T. and Rankin, J.G., 1998, Determination of Asphaltenes in Petroleum crude oils by Fourier Transform Infrared Spectroscopy. Energy and Fuels 12(5): 1008 – 1012.